

NOTE TO USERS

This reproduction is the best copy available.

UMI[®]

RICE UNIVERSITY

**METABOLIC BIOTINYLATION OF THE ADENOVIRAL CAPSID: AVIDIN-BASED
APPLICATIONS AND STUDIES OF LIGAND-TARGETED GENE DELIVERY**

by


Samuel Knox Campos

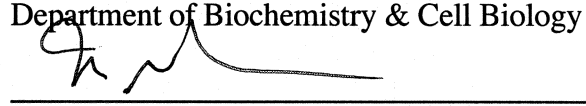
A THESIS SUBMITTED IN PARTIAL FULFILLMENT
OF THE REQUIREMENTS FOR THE DEGREE

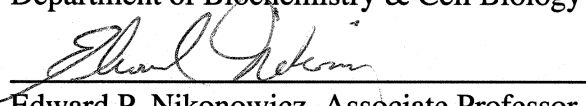
DOCTOR OF PHILOSOPHY

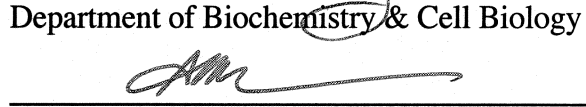
APPROVED, THESIS COMMITTEE:


Michael A. Barry, Chair, Associate Professor
Department of Bioengineering


Kathleen M. Beckingham, Professor
Department of Biochemistry & Cell Biology


Michael C. Gustin, Associate Professor
Department of Biochemistry & Cell Biology


Edward P. Nikonowicz, Associate Professor
Department of Biochemistry & Cell Biology


Antonios G. Mikos, John W. Cox Professor
Department of Bioengineering

HOUSTON, TEXAS
APRIL, 2005

UMI Number: 3168064

INFORMATION TO USERS

The quality of this reproduction is dependent upon the quality of the copy submitted. Broken or indistinct print, colored or poor quality illustrations and photographs, print bleed-through, substandard margins, and improper alignment can adversely affect reproduction.

In the unlikely event that the author did not send a complete manuscript and there are missing pages, these will be noted. Also, if unauthorized copyright material had to be removed, a note will indicate the deletion.



UMI Microform 3168064

Copyright 2005 by ProQuest Information and Learning Company.

All rights reserved. This microform edition is protected against unauthorized copying under Title 17, United States Code.

ProQuest Information and Learning Company
300 North Zeeb Road
P.O. Box 1346
Ann Arbor, MI 48106-1346

Abstract

Metabolic Biotinylation of the Adenoviral Capsid: Avidin-Based Applications and Studies of Ligand-Targeted Gene Delivery

by

Samuel Knox Campos

Adenoviral vectors have great potential for use in gene therapy and genetic immunization. The targeting of Ad vectors to the relevant tissue and cell types *in vivo* could greatly improve their safety and performance by lowering the effective dosage required for therapeutic levels of gene expression. Redirection of Ad vector tropism will require physical modifications of the adenoviral capsid but direct genetic modification of the Ad capsid has so far been limited to small peptides.

A novel system for the attachment of targeting ligands to the Ad capsid, based on the extremely strong avidin-biotin interaction, is described herein. The genetic insertion of a biotin acceptor peptide (BAP) into the fiber, protein IX, or hexon components of the Ad capsid has resulted in vectors that are metabolically biotinylated upon production in host cells. Avidin-dependent redirection of transduction through a variety of biotinylated ligands is greatly dependent on the nature of the biotinylated capsid protein. While targeted transduction via the fiber was efficient through a broad array of ligand-receptor interactions, redirection of binding and uptake through the more abundant protein IX and

hexon resulted in poor transduction. Although the basis of these differences has not been determined, it most likely reflects functional differences between the capsomeres during the process of vector uptake and trafficking. This study represents the first direct comparison of transduction through the various capsomeres and strongly suggests that future targeting efforts should be focused on fiber modification.

In addition to the functional studies on Ad-IX-BAP, structural analysis by cryoelectron microscopy and particle reconstruction is presented. The C-terminal BAP fusion was used as a structural tag to visualize the position of IX within the capsid. Results contradict all previous reports on the location of IX and suggest the surface accessible density currently assigned as IIIa is actually attributable to protein IX. These studies highlight the need for a more thorough analysis of adenoviral structure and the complex interactions between its components.

Acknowledgements

First and foremost, I would like to thank my advisor, Dr. Mike Barry for the opportunity of pursuing my doctoral work in his laboratory. I thank Mike not only for the guidance and encouragement he has provided me during my time in the lab, but also for the intellectual freedom he afforded me. I greatly appreciate the fact that I was able to work rather independently on the campus of Rice University rather than in the hectic environment of the Texas medical center, a place where my efforts were not productive. Mike, thanks for always being there when I needed you.

I would like to thank my thesis committee: Dr. Kate Beckingham, Dr. Mike Gustin, Dr. Ed Nikonowicz, and Dr. Tony Mikos. I am grateful for all their support and advice during my time at Rice. I appreciate all the time and effort they put forth towards helping me better my scientific thinking, writing, and presentation skills.

I am deeply indebted to the late Dr. Fred Rudolph, Mrs. Dolores Schwartz, Mrs. Jo Gerla, and the rest of the administration of both the biochemistry and bioengineering departments. I thank them for all their support and assistance throughout my time at Rice University.

I want to thank all the past and present members of the Barry lab for all their help along the way. I thank Mary Barry for all her help in getting me the supplies I needed for my experiments and for all the work she does as the lab manager. I thank Dr. Brandon Parrott, Dr. Jeremy Blum, Dr. Hoyin Mok, Debadyuti, Kristen, Skip, Marco, Julien, Sean, and Jared for all the great lab meetings and all the other good times. Best of luck to all of you, and for those still working towards their degree, you can do it!!! I would like to

thank all my friends here at Rice and those from VA Tech and Episcopal High School. Miles, Raf, Michelle, Beth, Jeff Moore, Ziad Kanna, Keith Messenger, and Yusuke Koyama, thanks for all the good times. Special thanks to Mr. Buck for being such a wonderful high school biology teacher and inspiring me to pursue this course of study.

I want to thank the Corral family, Emilio, Olga, and Jessica. Thank you for welcoming me into your family and for all your support in the past few years. I am fortunate to have married into such a wonderful family.

I am especially thankful for my wonderful grandparents, Sue and Buddy Horton. You both have always been so good to me and I could never have done this without all your love and support. Having you nearby during my time as a graduate student has been great, I will always be grateful for all the good times we had together. I want to thank my dad, Raoul Campos, who has always encouraged me to “use the Force” in everything I pursue. Dad, thanks for always believing in me. I am so fortunate to have Kate Campos as my sister. Kate, you are a wonderful person and I am grateful for all the love and support you have always given me. I am so proud of you, keep up the great work and always believe in yourself. Special thanks goes to my mom, Melissa Horton. Mom, thank you for nurturing my creativities when I was a young boy. Thank you for all your love and encouragement, I would not be where I am without you.

Finally I would like to thank my wife Erica. Honey, I was lost until we found one another. I could never have accomplished this without your love and support. I am so fortunate to have such a wonderful woman as my wife and partner in life. I look forward to spending the rest of our lives together and raising a family of our own. One last thanks goes to Wee. You are the best doggie in the world and I will never forget you.

Table of Contents

	<u>page</u>
Abstract	i
Acknowledgements	iii
List of Figures and Tables	vii
 Chapter I: Thesis Overview and Specific Aims	 1
 Chapter II: Background	 7
2.1 Gene Therapy and Gene Transfer Vectors	8
2.2 Adenoviral Vectors	12
2.3 Adenoviral Capsid Structure and Genome Organization	16
2.4 Adenoviral Biology and Life Cycle	25
2.5 Adenoviral Vector Targeting	35
2.6 Metabolic Biotinylation and the Biotin Acceptor Peptide (BAP)	40
 Chapter III: Construction of BAP-Modified Adenoviral Vectors Through Bacteriophage λ Red Recombination	 44
3.1 Introduction	45
3.2 Materials and Methods	50
3.3 Results and Discussion	55
3.4 Conclusions	60

Chapter IV: Characterization and Avidin-Based Applications of Metabolically Biotinylated Adenoviral Vectors	61
4.1 Introduction	62
4.2 Materials and Methods	64
4.3 Results and Discussion	70
4.4 Conclusions	86
Chapter V: Ligand-Targeted Transduction of Metabolically Biotinylated Adenoviral Vectors	88
5.1 Introduction	89
5.2 Materials and Methods	91
5.3 Results and Discussion	98
5.4 Conclusions	115
Chapter VI: Cryo-Electron Microscopy of IX-Modified Vectors Reveals the True Position of IX Within The Adenoviral Icosahedron	117
6.1 Introduction	118
6.2 Materials and Methods	124
6.3 Results and Discussion	125
6.4 Conclusions	132
Chapter VII: Conclusions and Future Directions	133
References	138

List of Tables and Figures

Chapter I	<u>page</u>
Fig 1.1 Diagram of avidin-based targeting of metabolically biotinylated Ad vectors.	4
Chapter II	
Table 2.1 Properties of viral gene transfer vectors.	10
Fig 2.1 Vector usage in current gene therapy clinical trials	15
Fig 2.2 Current model of the Ad5 virion	16
Fig 2.3 Backbone trace of the Ad5 hexon trimer	18
Fig 2.4 Organization of the minor capsid proteins within one facet of the adenoviral icosahedron	21
Fig 2.5 Organization of the Ad5 genome	23
Fig 2.6 Timecourse of adenovirus binding, entry, and cytoplasmic translocation	27
Fig 2.7 Nuclear accumulation of progeny virions	33
Fig 2.8 Schematic of Ad vector targeting strategies	38
Fig 2.9 Ribbon diagram of the BAP from <i>P. shermanii</i>	42
Chapter III	
Fig 3.1 Diagram of the AdEasy system	47
Fig 3.2 Modification of the fiber gene with the λ Red system	56
Fig 3.3 Plasmid maps of pIX-display and pHVR5-display	58

Chapter VI

Table 4.1	Plaque assays of BAP-modified vectors	70
Fig 4.1	CAR-mediated transduction of BAP-modified vectors	71
Fig 4.2	Virion thermostability assay	72
Fig 4.3	Negative stain TEM micrograph of Ad-wt	73
Fig 4.4	Western blot showing metabolic biotinylation of BAP-modified vectors	74
Fig 4.5	Biotin quantification by ELISA	76
Fig 4.6	Avidin-dependent neutralization	77
Fig 4.7	Physical targeting of metabolically biotinylated vectors	79
Fig 4.8	Purification of metabolically biotinylated vectors with monomeric avidin resin	81
Fig 4.9	SDS-PAGE analysis of input and elution fractions	83
Fig 4.10	Coomassie stain of concentrated elutions	84

Chapter V

Fig 5.1	Targeted transduction of K562 cells	99
Fig 5.2	Quantification of A431 cell targeting	100
Fig 5.3	C2C12 myotube targeting	102
Table 5.1	Summary of BAP vector targeting results	103
Fig 5.4	Tracking of 555-labeled vector targeting in C2C12 cells	105
Fig 5.5	Analysis of the fate of IX during vector uptake	110
Fig 5.6	Complexing of BAP-modified vectors to targeting ligands	111
Fig 5.7	Targeted transduction of C2C12 myotubes with Ad-fiber-BAP/Ctx-B complex	112

Fig 5.8 Reduced transduction of HeLa cells with Ad-IX-BAP/Transferrin complex	114
Chapter VI	
Fig 6.1 Structural organization and spatial relationships between hexon trimers and protein IX	120
Fig 6.2 Cryo-EM reconstruction and difference imaging of Ad-IX-BAP	126
Fig 6.3 Cryo-EM micrograph of Ad-IX-45-EGFP	127
Chapter VII	
Fig 7.1 Design of Ad-FT-BAP vectors	136

Chapter I

Thesis Overview and Specific Aims

Gene therapy has great potential for the treatment of both inherited disorders as well as acquired disease. The development of safe and effective gene transfer vectors is an extremely important prerequisite to the successful delivery of therapeutic genes [36]. Viruses are naturally evolved to efficiently deliver their genetic material into host cells for their own replication, and vectors derived from replication-deficient viruses, engineered to carry therapeutic genes, hold great promise for the effective delivery of these therapeutic genes to human cells.

Adenovirus type 5, a member of the *Adenoviridae* family of non-enveloped viruses, has received much attention as a gene transfer vector because of its efficient delivery of genes into a variety of both dividing and non-dividing cell types, as well as the relative ease in which high titer stocks of replication deficient virions can be produced. Adenoviral (Ad) vectors can be engineered to carry large ~35 kb fragments of foreign genetic material, another added benefit enabling the simultaneous expression of multiple genes or the potential for expression of actual human genomic sequences, complete with introns and other regulatory elements.

One major drawback to the use of Ad vectors for clinical gene therapy is the potent immune response directed towards the capsid. Both the host acquired and innate

immune responses against Ad vectors limit their potential as gene delivery vectors. The intravenous administration of high amounts of Ad vector can result in rapid inflammatory and cytokine responses, potentially leading to intravascular coagulation, acute respiratory distress, and multiorgan failure. The unfortunate death of 18-year old Jesse Gelsinger was caused by such a response against the large bolus (3.8×10^{13} viral particles) of vector he received during a University of Pennsylvania clinical trial designed to test the safety of Ad vectors [88].

The broad tropism of Ad vectors, while useful for *in vitro* transduction applications, can limit the *in vivo* efficacy of Ad vectors. The treatment of many diseases will require the expression of therapeutic genes within specific cells and tissues of the host. Cystic fibrosis and Duchenne's muscular dystrophy will require expression of the cystic fibrosis transmembrane regulator (CFTR) and dystrophin in the columnar airway epithelial cells and musculature of the host, respectively. Likewise, the treatment of cancers by delivery of tumor-suppressor, proapoptotic, proinflammatory, or toxic suicide genes requires that their expression be limited to the cancerous tissue avoiding deleterious expression in normal tissues. Much effort is currently focused on strategies aimed towards improving the safety and efficacy of Ad vectors by modification of the capsid. The specific targeting of Ad vector transduction to the sites of disease could result in improved safety and efficacy by lowering the therapeutic dosage of vector required, thereby minimizing the dangers involved with immune response against larger quantities of vector. One general strategy involves the alteration of Ad tropism by genetic ablation of natural capsid-receptor interactions, combined with the physical

targeting of the vector to the site of disease through introduction of new target cell-specific ligands.

While much research is focused on the biology of Ad-host interactions and ways to ablate natural Ad tropism, the focus of this work is on the introduction of new tropism into Ad vectors by the addition of ligands to the Ad capsid. Incorporation of targeting ligands by genetic manipulation of the Ad capsid genes is the most direct method of altering tropism. Several sites within the adenoviral capsid tolerant to genetic manipulation and amenable to ligand display have been identified, yet only limited success has been reported, and so far targeting ligands have been restricted to small peptide sequences. The successful insertion of foreign peptides and proteins into adenoviral capsomeres is very unpredictable in nature and often results in the inactivation of either the capsomere or the ligand function upon fusion of the two species [114, 171]. Moreover, the incorporation of larger, more complex ligands like single chain antibodies and secreted growth factors/signaling molecules is restricted by incompatibilities between their requirements for the secretory pathway for proper folding and the fact that Ad virions are assembled in the nucleus and all capsid proteins are transported into the nucleus [86, 137].

One approach to circumvent the problems associated with the genetic incorporation of cell targeting ligands is the display of ligands through non-covalent interactions. Hybrid adaptor molecules, consisting of a capsid-binding portion fused to a cell-binding ligand, have been used to display a wide variety of ligands, from small molecules, peptides, and hormones to larger antibodies, and growth factors, reviewed in [7]. The major drawback to this approach is the relatively weak interactions that tether

the ligands to the virion. Capsid binding is typically mediated through anti-[Ad] antibody fragments or soluble adenovirus receptor, and these complexes are prone to dissociation in the relatively harsh *in vivo* environment.

This thesis explores a novel strategy for the modification of Ad tropism, combining the genetic modification of the Ad capsid with the extremely strong coupling activity of the avidin-biotin system (Fig 1.1). Covalent addition of the small molecule cofactor biotin to certain carboxylase enzymes is mediated by the natural protein biotinylation machinery present within all mammalian cells. The possibility of using this natural system for the production of metabolically biotinylated vectors displaying covalently attached biotin molecules on the surface of their capsids, is explored herein. The hypothesis is that the biotin molecules can function as adaptors, enabling the display of biotinylated ligands from the capsid through the extremely tight avidin-biotin interaction ($K_d \approx 10^{-15}$ M), the strongest non-covalent interaction in nature [174].

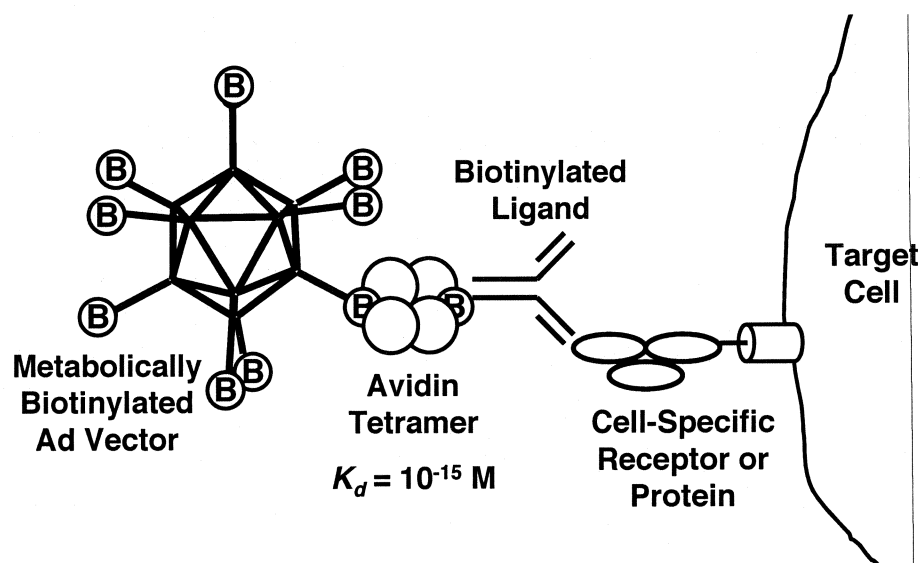


Fig 1.1 Diagram of avidin-based targeting of metabolically biotinylated Ad vectors.

Specific aims for this work are as follows:

1. The construction and characterization of metabolically biotinylated adenoviral vectors, made by the genetic fusion of a biotin acceptor peptide (BAP) into the fiber, protein IX, and hexon capsomeres of the Ad virion.
2. Investigation into the possible use of these vectors with avidin-based resins for affinity purification.
3. Evaluation of these vectors for avidin-based attachment of cell-targeting ligands and redirection of transduction through different capsomere-ligand-receptor interactions.

Chapter II of this thesis will provide an overview of gene therapy vectors, adenoviral vectors, adenovirus biology, genome and capsid structure, adenoviral vector targeting strategies, and metabolic biotinylation and the biotin acceptor peptide. Chapter III describes the use of bacteriophage λ Red recombination for the construction of these genetically modified vector genomes, containing BAP fusions. Chapter IV characterizes the properties of these vectors and explores their use in avidin-based purification and physical targeting applications. Chapter V explores the avidin-based cell targeting abilities of the metabolically biotinylated vectors and compares vector transduction

through fiber, protein IX, and hexon using a variety of ligands. Chapter VI focuses on the structural biology of the minor capsid protein IX within the icosahedral virion. Cryo-electron microscopy of the IX-modified vectors provides very interesting insights on the position of protein IX within the virion, and highlights the need for a more extensive analysis of the adenoviral capsid structure. Finally chapter VII provides the overall conclusions of this work and discusses future directions.

Chapter II

Background: Gene Therapy and Adenoviral Vectors, Structure, Biology, and Targeting Strategies

Abstract

This chapter begins with a brief overview of gene therapy and its enormous potential, reviewing the different types vectors used for gene transfer into humans. Adenoviral vectors will then become the focus with a short summary on the development of adenoviral vectors and their innate properties. Reviews on adenoviral structure, biology, and vector targeting strategies will then follow. The chapter ends with a brief background on metabolic biotinylation and the avidin-biotin interaction.

2.1 Gene Therapy and Gene Transfer Vectors

The completion of the human genome project, combined with the extensive research efforts towards the understanding of the molecular basis of disease and development has resulted in an abundance of information, opening possibilities for the use of genetic material as a drug for the treatment of disease. Hereditary genetic disorders like hemophilia, sickle cell anemia, cystic fibrosis, muscular dystrophy, diabetes, as well as the numerous inborn errors of metabolism and lysosomal storage diseases are all potentially amendable by gene therapy through the transfer of corrected versions of the underlying defective genes [161]. Cancers could be treated through the use of tumor-suppressor, proapoptotic, proinflammatory cytokine, or toxic suicide genes. Anti-microbial gene therapy may be used for the treatment or prevention of acquired infectious disease of viral, bacterial, or parasitic nature. Finally, genetic immunization through the transfer and expression of antigenic genes represents a valuable alternative to the traditional protein and pathogen-based vaccines for the establishment of cellular and humoral immunity [161].

Gene therapy holds great promise for human medicine, but technical challenges must be surmounted before the full potential can be realized. The development of safe and effective gene transfer vectors for the delivery and expression of these genes must be achieved if all the envisioned therapies are to become a reality. Much effort has been devoted to the development of these technologies, which fall into two broad categories: viral and non-viral vectors.

The simplest vectors include naked DNA, usually in the form of plasmids for the expression of therapeutic genes. Although the injection of naked DNA *in vivo* can lead to transgene expression [148], the efficiency of this delivery is very low and many non-viral vector formulations have been developed to interact with and enhance the cellular uptake of plasmid DNA. Polycationic molecules like poly(ethyleneimine) (PEI) or poly(lysine) can interact with negatively charged DNA to form compacted polyplexes, which function to both protect the DNA from degradation as well as to enhance the cellular uptake of the DNA through endocytic mechanisms. Another strategy involves the complexation of DNA with cationic lipids, thereby forming liposomes that can directly fuse with cell membranes to deliver the DNA into the cytoplasm [148].

Many intracellular barriers like endosomal escape, degradation by intracellular nucleases, and inefficient cytoplasmic transport, can prevent efficient delivery of the DNA to the nucleus. To overcome these hurdles non-viral formulations can include functional components (i.e. proteins or other chemical moieties) that mediate processes like cell binding and uptake, escape from endosomes, and nuclear import. Advancements in the field of non-viral vectors are geared towards the creation of “artificial viruses”, DNA containing complexes that functionally mimic viruses by efficiently binding, entering, and delivering their genetic payload to target cell nucleus [41].

Viruses have naturally evolved to efficiently deliver their genomes into host cells as part of their life cycle, and therefore viral-based vectors have received much attention for the delivery of therapeutic genes. Viral vectors are replication-deficient viruses that have been genetically engineered to express foreign genes upon infection of host cells. A wide variety of viruses have been successfully developed into vector systems including

enveloped RNA viruses like retroviruses and lentiviruses, enveloped DNA viruses like herpesviruses, and non-enveloped DNA viruses like adenoviruses and adeno-associated viruses (AAV). More recently many other viral vector systems based on a multitude of both enveloped and non-enveloped, RNA and DNA viruses have been described, although their use has not become widespread as of yet. The various viral vector systems all have their own unique properties, both beneficial and detrimental towards their use as gene delivery vectors. Table 2.1 provides a summary of the main viral vectors, highlighting their individual properties.

Table 2.1 Properties of Viral Gene Transfer Vectors.

Vector	Virion	Genome	Packaging Capacity	Tropism	Inflammatory Potential	Genome Maintenance
Retrovirus	Enveloped	ssRNA	~ 8 kb	Dividing Cells	Low	Integrated
Lentivirus	Enveloped	ssRNA	~8 kb	Broad	Low	Integrated
Herpesvirus	Enveloped	dsDNA	~150 kb	Neurons	High	Episomal
AAV	Naked	ssDNA	~4.5 kb	Broad	Low	Episomal/ Integrated
Adenovirus	Naked	dsDNA	~35 kb	Broad	High	Episomal

Retroviral and lentiviral vectors have the capacity to mediate stable, persistent gene expression through their ability to integrate into the host cell genome. Although this property makes these vectors particularly attractive for the long-term treatment of hereditary single-gene disorders, certain dangers are inherent to the chromosomal integration of retroviral and lentiviral genomes. These dangers became apparent recently when two patients of gene therapy for severe combined immunodeficiency disorder

(SCID), received *ex vivo* retroviral treatments for the re-establishment of their immune systems. The retroviral transduction of the patients hematopoietic stem cells had not only replaced the defective γ -c chain receptor gene, required for lymphocyte maturation and a functional immune system, but integration also resulted in the activation of an oncogene, leading to leukemia-like malignancies [62, 149]. In addition to the dangers involved with retroviral and lentiviral integration, these vectors have a small packaging capacity and are difficult to produce at high titers, thereby limiting their use for many *in vivo* gene therapy applications [162].

Herpesvirus vectors, based on herpes simplex virus-1 (HSV-1) have an enormous packaging capacity of ~150 kb, and thereby have the potential for gene transfer of human genomic sequences and entire genetic loci containing many cis-regulatory elements for proper gene expression. These vectors may be particularly useful for long-term gene expression in the nervous system and treatment of neurological disorders, although they can elicit immune responses that can limit the duration of gene expression [149, 162].

AAV-based vectors are attractive because of their potential to deliver genes into a wide variety of non-dividing cell types. Administration of AAV vectors is well tolerated and high doses can be injected without dangerous inflammatory responses and acute toxicity. The main limitations of AAV vectors are the extremely small packaging capacity and the production process, relying on the transfection of producer cells with multiple plasmids [149, 162].

2.2 Adenoviral Vectors

Adenoviruses (Ad) were first discovered in 1953, isolated from cultures of human adenoid tissues [126]. Since then, over 50 different serotypes of human adenoviruses have been isolated and characterized and the family *Adenoviridae* has been shown to be comprised of numerous non-human serotypes from a variety of mammalian, avian, reptilian, amphibian, and even fish species [42, 137]. Adenoviruses consist of a ~30-40 kb linear dsDNA genome encased within a non-enveloped icosahedral particle.

Adenoviruses were one of the first vector systems to be developed. The use of adenovirus for the expression of foreign genes (transgenes) was actually more of a discovery than an intentional development. Stocks of live adenovirus vaccines that had been propagated in monkey cell lines were found to be contaminated with simian virus 40 (SV40). The infection of tissue culture cells with the Ad vaccine resulted in the production of the SV40 T antigen, even after removal of the SV40 virions from the Ad stocks by immunodepletion. Analysis of the adenovirus revealed that the T-antigen gene from SV40 had been inserted into the E3 region of the Ad genome, thereby demonstrating the dispensability of the E3 genes for *in vitro* replication and creating the first Ad vectors [127]. The development of adenoviral vectors, particularly those based on adenovirus type 2 and 5 (Ad2/Ad5) has substantially progressed since this initial discovery.

Vectors based on Ad5 can mediate high levels of transduction in a wide variety of both quiescent and proliferating cells. Transgene expression from Ad5 vectors is typically transient because the Ad5 genome does not integrate into host cell

chromosomes. First-generation replication deficient ($\Delta E1/\Delta E3$) Ad5 vectors have been developed by the deletion of the E1 genes, necessary for Ad DNA synthesis and viral replication. Early work on the transformation of mammalian cells led to the creation of the 293 cell line, which was transfected with sheared adenovirus-type 5 (Ad5) genomic DNA and stably expresses the E1 genes [56]. The 293 cell line can trans-complement the E1 deletion of first generation vectors, allowing the efficient production of replication deficient Ad vectors. Ad vectors can be grown to extremely high titers in the 293 cell line, with burst sizes typically between 10^3 - 10^4 viral particles (VP) per cell and final concentrations reaching 10^{13} VP/ml, after banding by CsCl density gradient centrifugation [164]. The deletion of the E1 and E3 regions also allows ~8 kb of foreign DNA to be inserted into the Ad vector genome, permitting the expression of transgenes in mammalian cells infected with the Ad vector.

Although the first-generation vectors are generally considered replication defective, there is some low level expression of viral antigens that limits the duration of transgene expression *in vivo*, due to elimination of transduced cells by the immune system [92]. To avoid eliciting the unwanted cellular immune responses, helper-dependent Ad (HDAd) vectors, also called “gutless” vectors have been developed. These HDAd vectors are devoid of all viral coding sequences and consist of merely the *cis*-elements required for genome encapsidation. Since all viral sequences are deleted, helper adenoviruses must be used during HDAd production to provide all the necessary functions in *trans* [3]. The elimination of Ad antigen expression in HDAd vectors permits long-term episomal expression of genes in quiescent cells by avoiding problems associated with the cellular immune response [111, 151]. In addition, these vectors have

a much higher packaging capacity of ~35 kb of foreign DNA, enabling the expression of large transgenes or the inclusion of human genomic regulatory elements [111].

The major drawback to the use of Ad vectors for clinical gene therapy is the acute toxicity and inflammatory host response upon injection of large amounts of vector. These innate host responses mediated by increased production of pro-inflammatory cytokines is believed to result from the uptake of vector particles by Kupffer cells, resident macrophages in the liver [2, 101]. Complement proteins are also thought to play a role in the innate response, but the interactions between the Ad capsid and complement proteins have not been well characterized yet [101]. Studies with HDAd vectors have revealed that these innate responses are triggered by the actual Ad capsids, and are independent of the expression of any viral genes [102].

In addition to triggering the innate immune response, the uptake of Ad vectors by Kupffer cells has been shown to cause a non-linear dose response, requiring the administration of high levels of Ad vectors for therapeutic levels of transgene expression [147]. Injection of high amounts of Ad vectors can provoke severe acute inflammatory responses, compromising the safety of the patient. Targeting Ad vectors to the site of disease and reducing their native interactions with host cells and the innate immune system should therefore lead to safer and more efficacious vectors, reducing the dosage of vector required for an effective therapeutic response. The physical modification of Ad vectors with the goal of removing the native tropism and blocking natural capsid-host interactions, combined with the introduction of new ligands for the targeted transduction of specific host cells, is therefore a major objective in the field of Ad gene therapy.

The use of Ad vectors for clinical gene therapy is widespread, despite their inherent immunogenicity. As of January 2005, adenoviral vectors are used in 26% of the 1,020 current worldwide gene therapy clinical trials (Fig 2.1), making adenoviral and retroviral vectors the two most popular vectors. Of the 262 clinical trials involving the use of Ad vectors, 76% are for the treatment of cancer with vascular disease and monogenic disorders following at 14% and 7% respectively.

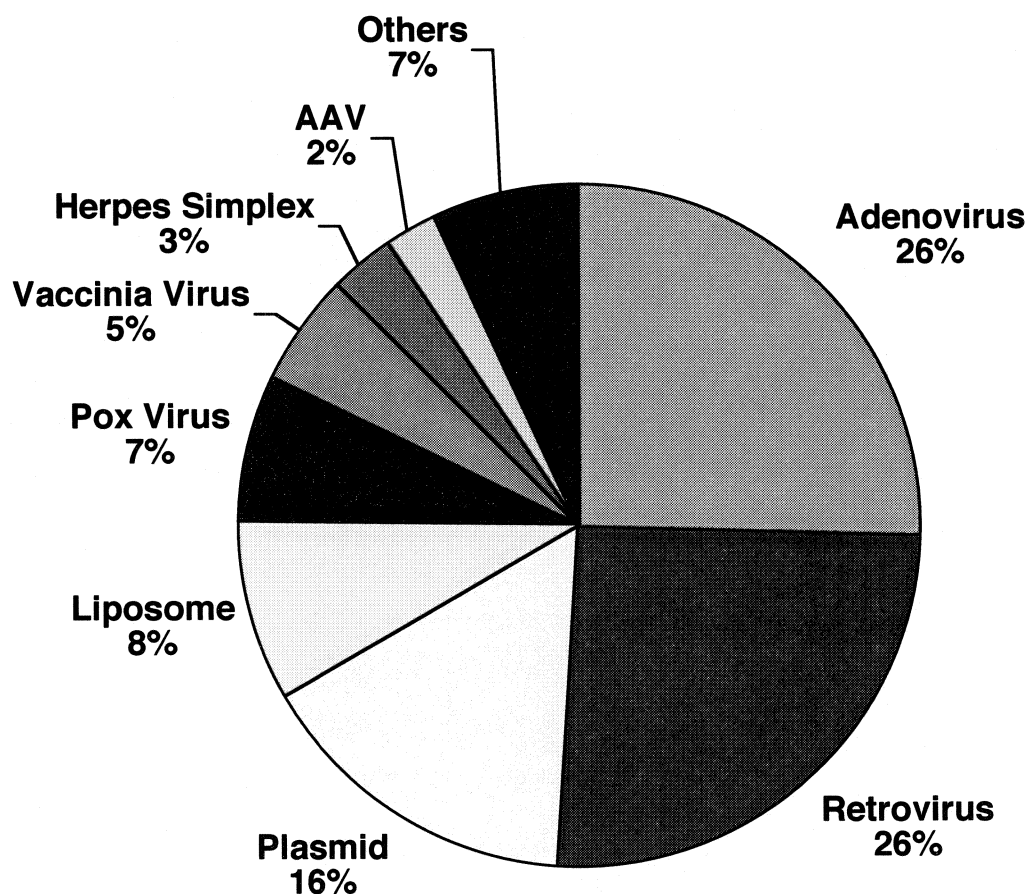


Fig 2.1 Vector usage in current gene therapy clinical trials. Data taken from the Journal of Gene Medicine Clinical Trial Database (<http://www.wiley.cp.uk/genetherapy/clinical>).

2.3 Adenoviral Capsid Structure and Genome Organization

The adenoviral virion is a non-enveloped icosahedral particle composed of 12 distinct polypeptides and a ~36 kilobase double stranded linear DNA. Electron microscopy provided the first visual picture of the icosahedral capsid architecture, revealing 252 distinct capsomeres and the presence of long fibers protruding from each of the twelve vertices [68, 153]. The bulk of the particles are ~900 Å in diameter with a molecular mass on the order of 150 MDa [155]. Detailed analyses of the structure and composition of the adenovirus virion [143, 155], and the interactions between its components [49, 120] has resulted in a detailed model of the virion structure (Fig 2.2). The seven polypeptides comprising the capsid are hexon (II), penton base (III), IIIa, fiber (IV), VI, VIII and IX. Four additional proteins, V, VII, X (mu), and the terminal protein (TP) are associated with the DNA genome to form the core [19]. The adenoviral protease is also present within the virion [4].

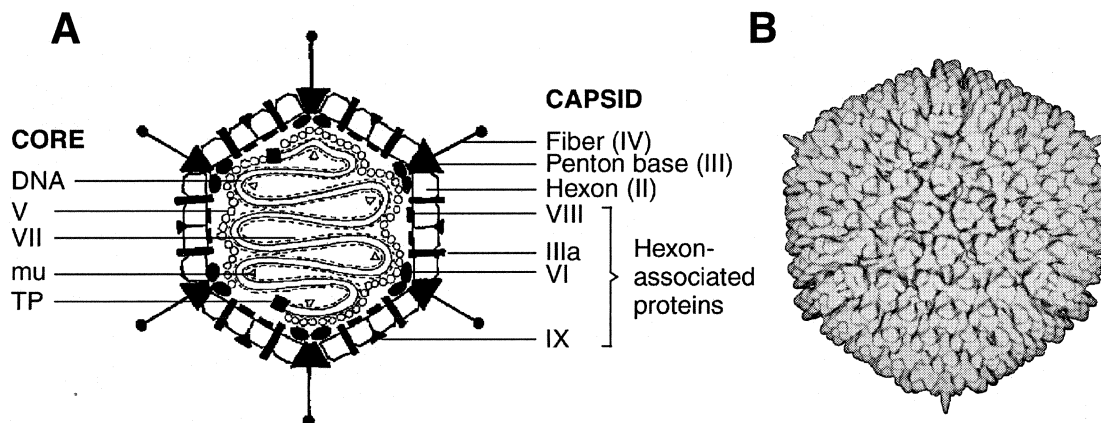


Fig 2.2 (A) The current model of the Ad5 virion, illustrating the positions and spatial arrangements of most of the protein components [164]. (B) Three-dimensional cryo-EM reconstruction of the Ad5 capsid at ~21 Å resolution. Fibers are not perfectly straight, so their density is lost during the reconstruction.

Major Capsid Proteins

The major structural protein of the Ad5 capsid is the 105 kDa hexon polypeptide. The twenty interlocking facets of the icosahedron are built from twelve hexon trimers, resulting in a stoichiometry of 240 trimers per virion. Solution of the hexon crystal structure [129] revealed a complex design whereby extended loop structures wrap tightly around one another to form a highly stable trimer. Hexon trimerization occurs in the cytoplasm of infected cells and requires the assistance of the adenovirus 100 kDa polypeptide [24]. The monomers trimerize in a manner as to form a pseudohexagonal base with three tower structures at the top of the molecule. These towers are clearly visible in the cryo-EM reconstructions of the capsid (Fig 2.2). Analysis of the structure and sequence alignments to other Ad serotypes has revealed several hypervariable regions (HVR's) present on surface loops of the towers (Fig 2.3). Interestingly, the major coat protein of a bacteriophage PRD1, also present at 240 trimers per virion, was shown to have the same fold as the adenovirus hexon, suggesting an ancient common origin for these diverse viruses [13].

Present at each of the twelve vertices are the penton complexes, each consisting of a pentameric penton base (63 kDa monomer) and a trimeric fiber (62 kDa monomer) extending approximately 300 Å outwards. The X-ray crystal structures of the full length Ad2 penton base [184] and a truncated fragment of the Ad2 fiber [156] have been solved. Adenovirus fibers consist of three domains, a short N-terminal tail that attaches the fiber to the penton base, a shaft domain comprised of a repeating sequence motif, and a globular knob domain required for primary receptor binding and trimerization of the monomers [137, 179]. The shaft length is highly variable among Ad serotypes, and is

determined by the number of pseudorepeats present, ranging from 6 repeats in subgroup B Ad3 to 22 repeats in subgroup C Ad5 [128]. Recently the shaft domain has been shown to have heparan sulfate binding activity, important for *in vivo* biodistribution and bioactivity. Interestingly, Ad5 fibers appear to have a flexible kink corresponding to a non-consensus sequence present within the third pseudorepeat [97, 178]. A lysine-lysine-threonine-lysine (KKTK) sequence residing at this position is thought to mediate the interaction with the negatively charged heparan sulfate [140, 141].

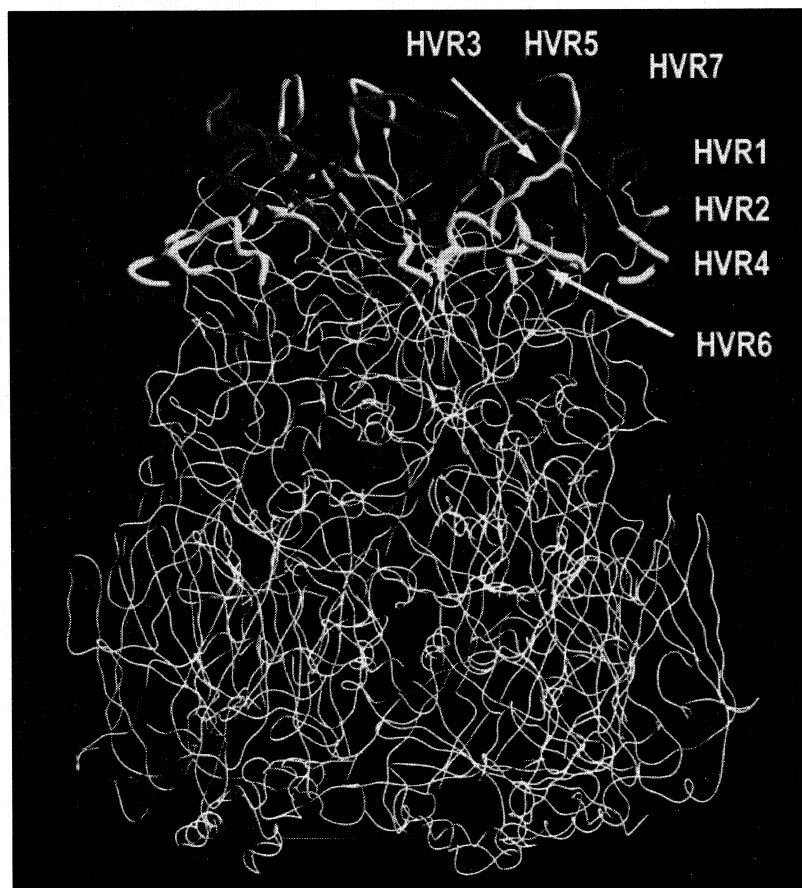


Fig 2.3 Backbone trace of the Ad5 hexon trimer showing the positions of each of the HVR's present on surface loops, from [129].

Structure of the penton base revealed the answer to the 3-fold/5-fold symmetry mismatch that occurs when the trimeric fiber docks onto the pentameric base. Solution of the penton base structure with a short N-terminal peptide from the fiber tail shows that five binding sites exist between each subunit of the pentamer but steric hindrance imposed by the trimeric structure of the fiber allows only 3/5 of the sites to be filled, resulting in one fiber per base [184]. The structure has also confirmed the presence of a flexible surface exposed loop containing an arginine-glycine-aspartic acid (RGD) motif, which has been shown to bind cell surface integrins to facilitate endocytic uptake [28, 144, 168].

Minor Capsid Proteins

Detailed analysis of the Ad2 capsid structure by cryoelectron microscopy and particle reconstruction [143] combined with the crystal structure of the Ad2 hexon [5] was used to construct a quasi-atomic model of the three-dimensional Ad2 capsid. Difference imaging and subtraction of the hexon density map away from the cryo-EM map of the capsid resulted in a density map attributable to minor capsid components [145]. Proteins IIIa, VI and IX were then assigned to specific densities within the three-dimensional map based on known masses and copy numbers, predicted protein volumes, and biochemical data [29, 137, 145, 155]. None of the minor capsid protein structures have been determined. All of the minor capsid proteins with the exception of IX are processed by the viral protease to yield the mature chains present within and necessary for infectious virions [137].

Each facet of the virion is formed from twelve hexon trimers. Central to each facet are groups-of-nine (GON) hexons that remain associated after heat or pyridine disruption [29, 120]. Protein IX, a small 14 kDa polypeptide present at 240 copies per virion [155], is believed to function as a cement protein, stabilizing the GON structure. Indeed, although IX is not necessary for encapsidation, virions devoid of IX are less thermostable than wild type virions and no GON's are seen after controlled disruption [29]. Cryo-EM studies and difference imaging of purified GON's have identified density assigned as IX [53], present as four small trimers positioned between the bases of the hexon trimers central to the GON. The C-terminus of IX is exposed on the surface of the virion [1], despite being assigned to an inaccessible position well below the surface of the hexon trimers. Protein IX and its position within the Ad capsid is the focus of chapter 6 and will be discussed in greater detail.

Protein IIIa, a 63 kDa monomeric protein present at 60 copies per virion, is located on opposite and adjacent sides of the 2-fold axis of symmetry just outside the peripentonal hexons, apparently rivets the interlocking facets together. Density assigned as IIIa can be seen on both the inner and outer surfaces of the capsid, intimately associated the hexon trimers at these positions [145].

Protein VI, a 23 kDa polypeptide present at 360 copies per virion, has been localized to regions underneath and between the five peripentonal hexon trimers and the penton base at each vertex. Six molecules of VI, present as trimers of dimers are thought to be associated with each of the peripentonal hexon trimers, stabilizing the vertex regions. Recently protein VI has been identified as the lytic factor necessary for endosomal membrane disruption during the early stages of infection [173]. Apparently

VI resides under the vertex region until low pH from endosomal acidification triggers the release of vertex components, exposing VI and allowing it to lyse the endosomal membrane.

Protein VIII, a small 15 kD polypeptide present at 120 copies per virion, is associated with hexons [49], but its precise location within the capsid remains a mystery. VIII is predicted to have a disordered structure due to its high content of proline (8%) and basic lysine/arginine (11%) and is thought to reside underneath the hexon shell [145].

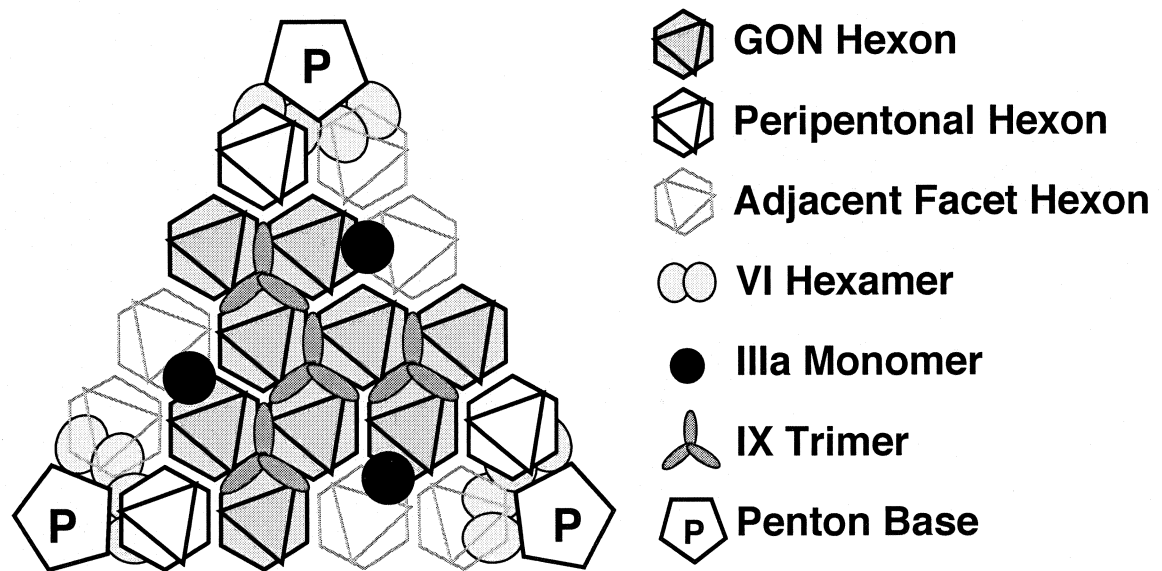


Fig 2.4 Organization of the minor capsid proteins within one facet of the adenoviral icosahedron. The GON hexons central to each facet are stabilized by four trimers of IX. Monomers of IIIa rivet neighboring facets together while hexamers of VI are associated with each of the peripentonal hexons, providing vertex stability. Adapted from [132].

Core Structure

The 36 kilobase Ad genome is associated with proteins V, VII, X and the terminal protein forming a condensed core structure. Cryo-EM reconstructions of Ad virions show a featureless density present underneath the highly ordered capsid [143]. Early studies on the structure of the nucleoprotein core have resulted in different models for core organization. Nuclease digestion experiments suggest that core proteins may form nucleosome-like structures, protecting 150-200 bp fragments of DNA from enzymatic digestion [30]. Other studies suggest a model whereby the core is organized into 12 lobes present under each of the vertices of the capsid, as visualized by ion-etching and electron microscopy of sarkosyl treated cores [19, 106].

Biochemical analysis of core protein interactions supports a model where 840 molecules of the 19 kDa protein VII and ~100 molecules of the 4 kDa protein X are tightly associated with the genomic DNA [27, 155]. Two copies of the 55 kDa TP are covalently linked to the ends of each genome, functioning as protein primers during replication. Protein V, a 42 kDa protein present at 160 copies per virion, has a weaker interaction with the genome and is thought to form a coating around the tight DNA-VII-X nucleoprotein core. Protein V interacts with both core proteins VII and X as well as dimers of capsid protein VI [27, 91], thereby linking the core to the vertices of the outer capsid (Fig 2.2). Although the 23 kDa viral protease is not considered a core protein, it is thought to be present at ~10 copies within the capsid. In addition to several of the capsomers, core proteins VII, X, and TP are cleaved into mature forms by the protease [137].

Genome Organization

The 36 kilobase linear double stranded DNA genome contains several highly organized complex transcription units flanked by 100-140 bp inverted terminal repeats (ITR's) on each end (Fig 2.5). The ITR's are critical elements, acting as the origins of replication. Just inside the left ITR is a short sequence that functions as the packaging signal (Ψ). This cis-acting element is necessary for packaging of the viral genomes during the process of encapsidation in the host cell nuclei [137].

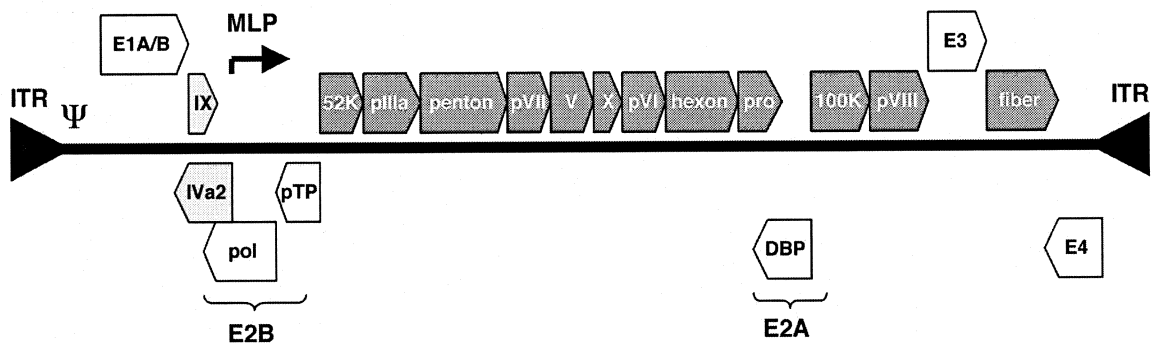


Fig 2.5 Organization of the Ad5 genome. Early regions are shown in white, intermediate genes in gray and late genes in dark. Adapted from [42].

Immediately downstream of Ψ is the E1 region containing two major transcription units, E1A and E1B. This region is the first to be expressed during viral infection and encodes functions important for all downstream events of infection. The E2 cassette is encoded in the antisense strand and is spread across the length of the linear genome. E2 encodes the DNA replication machinery. E3 encodes proteins that counteract the host immune and anti-viral defense systems. The E3 unit lies on the sense strand, nestled between the pVIII and fiber ORF's to the right of the genome. E4, the final early transcription unit is encoded on the antisense strand just downstream of the fiber gene on

the far right end of the genome. E4 proteins include other important regulatory factors necessary for various events.

Protein IX is encoded on a small unspliced mRNA just downstream of the E1B unit. IX is the only capsid protein whose expression is uncoupled from the major late promoter (MLP) and it is expressed at intermediate times during infection. All other capsid proteins and other late proteins are under control of the MLP and expressed from a long ~29 kilobase transcription unit spread across the sense strand. Extensive splicing occurs for all the Ad transcripts with the exception of the IX and IVa2 mRNA's [137].

2.4 Adenoviral Biology and Life Cycle

The process of Ad5 infection begins with the initial binding of virions to the host cell surface followed by endocytic uptake, endosomal escape, cytoplasmic trafficking, and accumulation at the nucleus. Once the Ad genome reaches the nucleus, an elaborate and highly coordinated program of viral gene expression begins. Early genes are the first to be expressed, setting the stage for genome replication and finally transcription of the late capsid genes, culminating with the production of new virions and the death of the host cell.

Binding, Entry, and Trafficking

In vitro work has demonstrated the initial attachment of Ad5 is mediated by the high affinity binding ($K_d = 15$ nM) of the distal knob domain of the adenoviral fiber to cell surface coxsackievirus B and adenovirus receptor (CAR), a type 1 transmembrane protein in the immunoglobulin superfamily [14, 70, 76]. In addition to CAR, heparan sulfate glycosaminoglycans (HS-GAGs) have been shown to promote virion attachment to certain cell types [43]. Although the mechanisms of *in vivo* attachment and uptake are poorly understood they are thought to involve interactions between lysine-lysine-threonine-lysine (KKTK) motifs present within the Ad5 fiber shaft and cell surface HS-GAGs in addition to CAR-mediated infection [140, 141]. Secondary interactions between exposed arginine-glycine-aspartic acid (RGD) motifs present within surface loops of the penton base and cell surface $\alpha_v\beta_1$, $\alpha_v\beta_3$, $\alpha_v\beta_5$, or $\alpha_3\beta_1$ integrins promotes uptake through clathrin-mediated endocytosis [83, 130, 168]. This classical model of

Ad5 uptake has recently been elaborated and new data suggests that in addition to endocytosis, Ad triggers other uptake mechanisms like micropinocytosis [93]. The presence of cholesterol has also been shown to be important both for Ad uptake and the latter process of endosomal escape [71].

Receptor binding and uptake of Ad5 occurs relatively quickly, with the majority (80-85%) of the bound virions being taken up within 5-10 minutes [59]. During uptake, the Ad5 virion undergoes a process of disassembly, beginning with the release of upwards of 90% of the fibers during the early stages of entry [59, 103]. Once the virion has been taken up, the natural process of endosomal acidification [95] triggers a conformational change in the Ad5 capsid, ultimately resulting in endosomolysis and release of the virion into the cytoplasm. Recently, it has been shown that protein VI contains an N-terminal amphipathic α -helical domain that possesses the membrane lytic activity responsible for endosomal escape. The current working model suggests that the Ad capsid somehow senses the decrease in pH and responds by releasing various vertex components including the peripentonal hexons, protein IIIa, and protein VI. Upon release the N-terminal amphipathic α -helical domain of VI becomes free to disrupt the endosomal membrane [173]. Again the process of endosomal escape is believed to occur relatively rapidly, with the majority of virions reaching the cytoplasm by 15-20 minutes post infection [59, 94].

Once free in the cytoplasm, the partially dismantled capsid interacts with dynein, a cytoplasmic motor protein [75]. The association of Ad5 with dynein enables the virions to translocate along microtubules towards the microtubule organizing center (MTOC) eventually accumulating around the host cell nucleus [6]. Previous work has

demonstrated specific interactions between the Ad5 capsid and cell nuclei using both *in vitro* binding assays as well as direct visualization with electron microscopy [175]. More detailed analysis has revealed that Ad specifically binds to the CAN/Nup214 protein of the nuclear pore complex (NPC) and this association leads to further disassembly and eventual import of the adenoviral genome into the nucleus [58, 152]. Overall, the entire process from initial cell surface binding to docking at the NPC is rapid (Fig 2.6) and usually occurs within 30-60 minutes depending on the cell type and morphology [59].

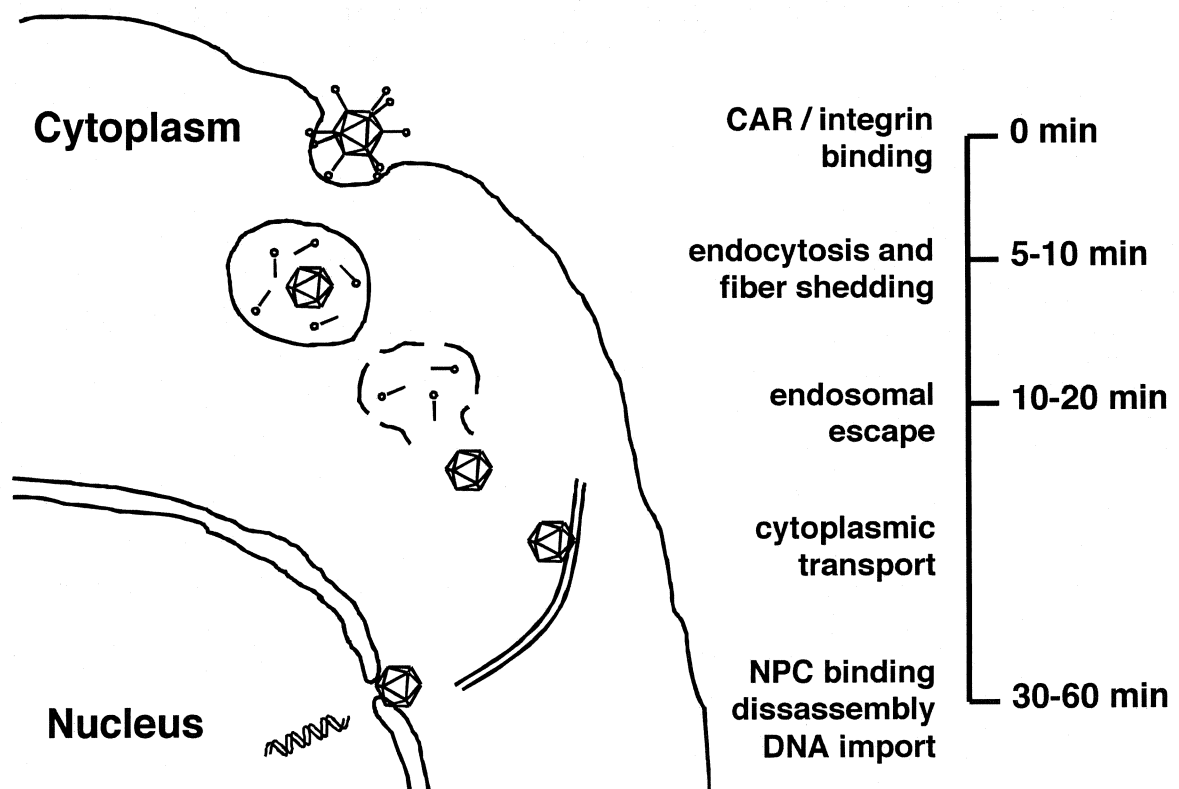


Fig 2.6 Timecourse of adenovirus binding, entry, and cytoplasmic translocation.

Early Gene Expression and DNA Replication

Once the Ad genome reaches the nucleus, viral transcription and remodeling of the host cell begins. Early Ad gene expression ultimately results in the transactivation of other early viral and cellular genes, thereby pushing the host cell forward into the S phase and creating an environment conducive for Ad genome replication. The first gene to be transcribed is the E1A transactivator, expressed from a constitutive promoter.

Differential splicing of the E1A transcript produces two different species of mRNA, encoding two different polypeptides. In addition to the direct binding and activation of TATA-binding proteins and other basal transcription factors [137], one of the main functions of the E1A proteins is to bind with the cellular tumor suppressor retinoblastoma (pRb). pRb normally functions as a tumor suppressor by binding and sequestering the cellular transcription factor E2F. Direct binding of E1A to pRb leads to the release E2F which can then activate transcription from a variety of viral and cellular promoters, leading to expression of the Ad E1 and E2 genes as well as the up-regulation of cellular genes necessary for transition into the S phase [15]. This deregulation of the cell cycle can result in the accumulation of the cellular tumor suppressor p53, which can in turn lead to activation of the apoptotic pathway. Ad counteracts this cellular defense mechanism through the actions of the E1B-55 kDa protein, which directly binds and inhibits the proapoptotic functions of p53 [134]. Another anti-apoptotic protein expressed from the E1B region is a small 19 kDa polypeptide. The E1B-19 kDa protein is a member of the Bcl-2 protein family, and blocks apoptosis by localizing to the mitochondrial membrane and inhibiting the release of cytochrome c to the cytoplasm [146]. The functions of the E1A and E1B proteins are extensive and their interactions

with the pRb and p53 tumor suppressors and cellular apoptotic signaling molecules represent only a small portion of their biological activities. Ultimately, expression of the E1 proteins results in the activation of various viral and cellular promoters, eventually shifting the host cell into the S phase while upregulating expression of the Ad E2, E3 and E4 genes. The Ad E1A and E1B proteins are capable of immortalizing primary cells in culture and have been shown to cause tumors in rodents. However, despite their oncogenic activities, the E1 genes are not associated with any human cancers, perhaps due to the lytic mode of Ad infection [137].

The immediate targets for transactivation by the effects of the E1 proteins are the E2 genes, which encode proteins involved in Ad DNA replication. Although Ad replicates in the nucleus of infected cells, special machinery is needed to replicate its linear double stranded genome. The E2 genes encode a single stranded DNA binding protein (DBP), the preterminal protein (pTP), and a viral DNA polymerase (pol). These proteins work in concert with several cellular factors to replicate the Ad genome, reviewed in [44]. Briefly, The ITR's of the Ad genome serve as the replication origins. These regions are bound by a pTP-pol complex, in conjunction with cellular factors. The pTP functions as a protein primer for extension by the polymerase and thereby becomes covalently attached to each end of the Ad genome, protecting the integrity of each end. The polymerization reaction starts with the formation of a covalent bond between the hydroxyl side chain of a serine residue and dCMP. After synthesis of the first three or four nucleotides, pol separates from pTP and continues the extension along the entire length of the linear dsDNA template, aided by the strand displacement

activities of the DBP. Ad DNA replication typically begins 4-8 hours post infection and can continue until the death of the host cell [137].

Ad E1 expression also results in transactivation of the E3 and E4 regions in addition to the E2 genes involved in DNA replication. E3 generally encodes products that counteract the host immune response. Briefly, some of the main functions of the Ad E3 proteins include the inhibition of antigen presentation by MHC class I molecules, the inhibition of antigen transport and processing by the ER protein TAP, and the down-regulation of apoptotic signaling through TNF- α , Fas ligand, and TRAIL [92]. These functions, although necessary for the persistence of infected cells *in vivo*, are dispensable for Ad replication in tissue culture and are typically deleted in first-generation Ad vectors [164]. E4 encodes more cell-cycle regulators and transactivators that work in concert with the other early proteins to remodel the cellular environment for Ad infection. The precise roles of these proteins have not been as well characterized as the E1 proteins [92] and specific functions will be discussed in relevant sections.

Late Gene Expression and Inhibition of Cellular Gene Expression

Once the process of Ad genome replication is underway, expression of the late genes begin. These genes encode for DNA binding core proteins, components of the icosahedral capsid, and the scaffolding/machinery needed to build infectious virions. The late genes are all transcribed from the major late promoter (MLP), encoded on one large ~29,000 nucleotide transcript [105]. Differential splicing and poly(A) site utilization produces five distinct groups of mRNA transcripts. These L1-L5 mRNA's are grouped together on the basis of shared poly(A) signal sequences [183]. Although the Ad E1

proteins and various cellular TATA-binding transcription factors can activate the MLP [137], the underlying element responsible for the temporal control of activation is thought to be the adenoviral IVa2 protein [137]. IVa2 is a multifunctional protein transcribed from the E2 region and it is classified as a delayed early protein. The accumulation of early Ad proteins is believed to release repression of the IVa2 promoter, leading to its expression at intermediate times [137]. IVa2 can then bind downstream of the MLP and activate transcription of late genes.

During these late stages of expression, nuclear export of host cell mRNA is blocked [12]. Nascent cellular transcripts continue to be synthesized but they simply fail to exit the nucleus while transcripts of viral origin are efficiently exported and translated. This blockade of cellular gene expression is rather indirect, and results from the actions of a complex of the E1B-55 kDa protein and the E4-34 kDa proteins [63, 118]. This E1B-E4 complex efficiently binds mRNA transcripts and shuttles them to the cytoplasm through a nuclear export signal within the E4 protein. There is no direct discrimination of cellular versus viral transcripts, but rather the early genes have collectively caused a remodeling of nuclear structure by this time and E1B-E4 complex together with cellular transport factors are localized to intranuclear inclusions containing viral transcription/replication centers [110].

Direct mechanisms do exist for the preferential translation of viral mRNAs in the host cell cytoplasm. Build up of double stranded RNA species at the late stages of infection can trigger the protein kinase R (PKR) dependent phosphorylation and inactivation of eukaryotic initiation factor-2 α (eIF-2 α). Ad encodes two RNA species termed VA RNAs that inhibit the activation of PKR and thereby prevent translation

inhibition. The VA RNAs are believed to be associated with pools of viral mRNA transcripts, thereby providing localized protection against host cell shutdown of protein synthesis [90, 109]. The decrease in host cell mRNA transport and expression also causes the inactivation of another host translation factor eIF-4F. This factor binds the caps of cellular transcripts and facilitates ribosomal scanning and initiation at an AUG start codon. The Ad L1-L5 transcripts all contain a leader sequence at their 5' ends termed the tripartite leader (TPL). The TPL enables viral mRNAs to be efficiently translated in the absence of functional eIF-4F [84, 181].

Encapsidation and Virion Assembly

The processes of Ad genome replication and late gene expression lead to the assembly of new progeny virions within the host cell nucleus (Fig 2.7). Most of the Ad structural proteins like penton base and fiber contain a nuclear localization signal (NLS) for transport into the nucleus. In the case of hexon, which lacks its own NLS, immature pVI acts as a shuttle for the accumulation of hexon trimers in the nucleus [176]. The actual process of DNA packaging and capsid assembly is still unclear, but pulse-chase experiments and the analysis of various temperature sensitive mutants support a model whereby the Ad DNA is inserted into preformed capsid shells [37, 47]. Several viral proteins have roles in the packaging of the Ad genome during encapsidation. The L1-52/55 kDa protein and the IVa2 protein are both necessary for DNA packaging and IVa2 has been shown to directly bind the packaging signal [61, 182]. Mutants in the L4-33 kDa protein are defective in capsid assembly, indicating a role for this protein in encapsidation [51].

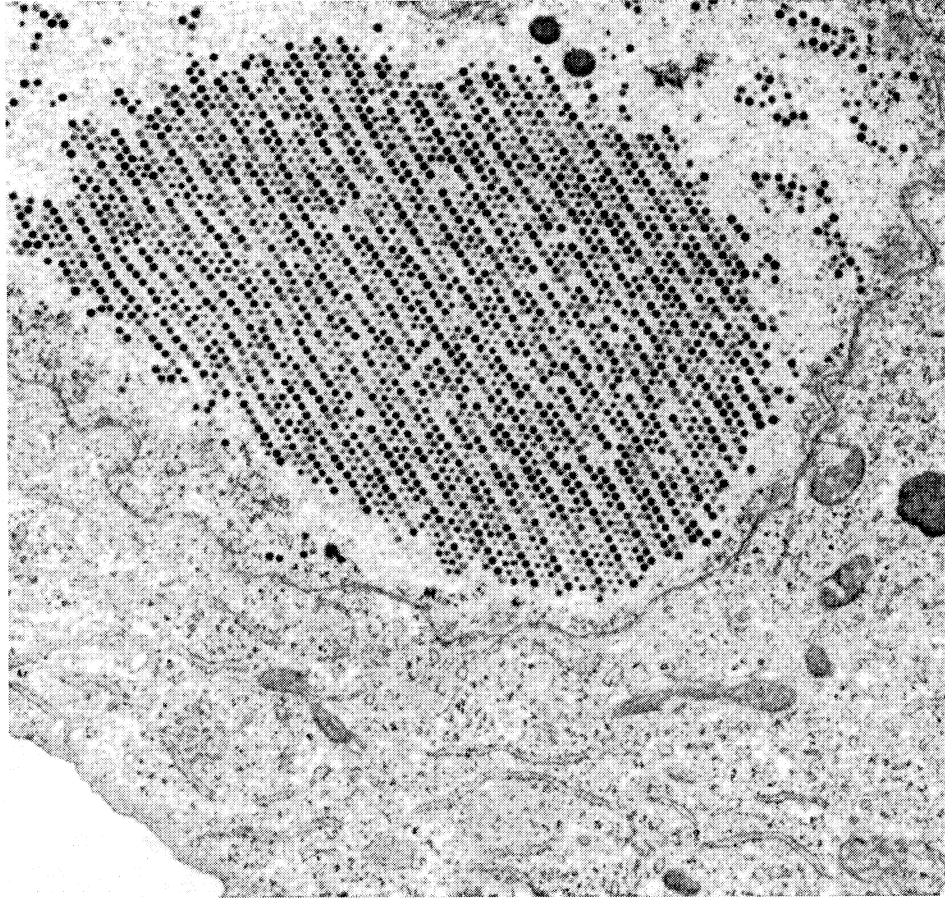


Fig 2.7 Electron micrograph showing the accumulation of progeny virions within the nucleus of a host cell during the latter stages of viral infection (http://dbb.urmc.rochester.edu/labs/smith/photo_gallery.htm).

Once the Ad genome has been properly encapsidated, the viral protease cleaves immature core and capsid proteins pIIIa, pVI, pVII, pVIII, and pX into their mature forms rendering the virions fully infectious [87]. This proteolytic processing is very important as a virus encoding a temperature sensitive mutant protease produces noninfectious virions capable of binding and entering cells, but lacking the ability to escape the endosomes and is therefore destroyed in the lysosomal compartment [57, 167]. The protease has two main cofactors necessary for full enzymatic activity: viral DNA and the 11 amino acid C-terminal peptide of VI, which is thought to be located just

underneath the peripentonal hexons. It therefore appears that the protease is only switched on when the DNA and capsid proteins are all in the proper spatial orientation, as defined by the icosahedral capsid [87]. Remarkably, as many as 10,000 progeny virions can be produced per infected cell [69], as shown in Fig 2.7. The entire process, from initial infection to cell death and release of progeny virions, reaches completion 30-40 hours post infection [164].

2.5 Adenoviral Vector Targeting

Systemic administration of Ad vectors results in rapid and efficient clearance of the vector by hepatic Kupffer cells, macrophage, and monocytes [2, 147]. Large amounts of vector can be administered to overcome this clearance mechanism, thereby allowing high levels of transduction of liver hepatocytes [147]. Adenoviral vectors are immunogenic and the large amounts of vector needed to overcome liver clearance can lead to rapid and dangerous responses by the innate immune system, causing acute toxicity [85] and even death [88]. Many efforts are underway to improve the efficacy of Ad vectors by altering their interactions with the body. The ablation of native tropism combined with the introduction of new targeting moieties should lead to safer vectors with improved dose-response profiles [98]. This section will highlight the major advances towards achieving targeted adenoviral gene delivery.

Genetic Modification of the Capsid

Many of the therapeutically relevant target cells for gene therapy are refractory to Ad transduction due to low expression of primary receptors. Multiple strategies have been pursued to improve the efficacy of Ad vectors by targeting their transduction to specific cell and tissue types. Genetic manipulation of the adenoviral capsid (Fig 2.8) is the most direct approach to modify vector tropism. The detailed structural data on the major capsid proteins have facilitated the genetic incorporation of foreign peptides and proteins into exposed regions of the Ad capsid. Short peptides and epitopes have successfully been grafted into the surface exposed HI loop [11, 79] and C-terminus [169] of the fiber

knob domain, the RGD-containing loop of penton base [170], the HVR5 loop of the hexon [32], and the C-terminus of protein IX [46].

C-terminal fusions of poly-lysine residues [169] and HI loop insertions of RGD peptides [45] have created vectors with expanded tropisms towards cells expressing HS-GAG's and integrins including cells normally refractive to Ad5 transduction like endothelial cells, skeletal and smooth muscle cells, and CAR-deficient cancer cells. Similarly, the insertion of RGD peptides into HVR5 of hexon [163] or the C-terminus of IX [159] have resulted in vectors with broader tropism. Incorporation of mammalian cell-binding peptide ligands isolated by phage display [9, 117] into the HI loop of the knob has generated vectors with more specific activity towards the target cells [107, 177]. Despite the numerous reports of successful modification of the fiber C-terminus and HI loop, there is no guarantee that any given peptide will be tolerated. Often insertion of foreign peptides into these locations interferes with fiber folding and trimerization, preventing rescue of the modified vectors. Conversely, peptide ligands that are tolerated may lose their original function once displayed within the structural context of the knob domain [114, 171].

Molecular Conjugates and Adaptor Molecules

Genetic modification of the Ad capsid and the fiber protein in particular is generally limited to small peptide insertions. Not only does their size preclude the incorporation of larger, higher affinity ligands, but the nuclear life cycle of Ad also limits the repertoire of ligands to those that can fold properly in the reducing environment of the cytoplasm and cell nuclei. Naturally secreted ligands like cytokines, immunoglobulins,

and growth factors require the oxidative environment of the Golgi and ER compartments to fold correctly and form proper disulfide bonds [86]. One targeting method to circumvent the problems of capsid-ligand incompatibility is the use of bifunctional fusion proteins. These molecular adaptor proteins consist of a capsid-binding domain genetically or chemically fused to a cell-binding ligand. These molecules can physically bridge the vector to the cell surface, thereby redirecting vector transduction to the target cell (Fig 2.8). Successful strategies have described anti-capsid antibody fragments or soluble CAR fragments fused to a diverse set of ligands including antibody fragments against a variety of cellular receptors, growth factors like the basic fibroblast growth factor (FGF-2) and epidermal growth factor (EGF), and even small molecules ligands like folate [7].

Although this technology is versatile, the preparation of these adaptors, which are typically recombinant fusion proteins or chemically conjugated proteins, can vary from batch to batch. Also, the adaptor molecules rely on non-covalent protein-protein interactions for their conjugation to the Ad capsid, which are generally considered too weak to work *in vivo*. Naturally occurring antibodies or CAR receptors could compete for and displace the molecular adaptors from the capsid, abolishing the vector targeting activity.

Chemical Modification of the Ad Capsid

Another general strategy to redirect Ad vector transduction is the direct chemical modification of the Ad capsid (Fig 2.8). Primary-amine reactive chemical groups can be used to covalently attach molecules to the surface of the Ad capsid. Direct attachment of

ligands like FGF-2 and EGF as well as phage-selected peptides through bifunctional polyethylene glycol (PEG) or poly-N-(2-hydroxypropyl) methacrylamide (pHPMA) molecules has been shown to augment CAR-independent gene transfer [52, 80, 123]. Not only is this technology suitable for the display of ligands from the capsid, but native vector tropism can either be maintained or masked, depending on the specific reaction conditions. Reaction to an excess of PEG has been shown to improve the *in vivo* pharmacokinetics of the vector by increasing vector persistence in the blood [2], preventing antibody neutralization [35], and decreasing the innate immune response against the vector [99].

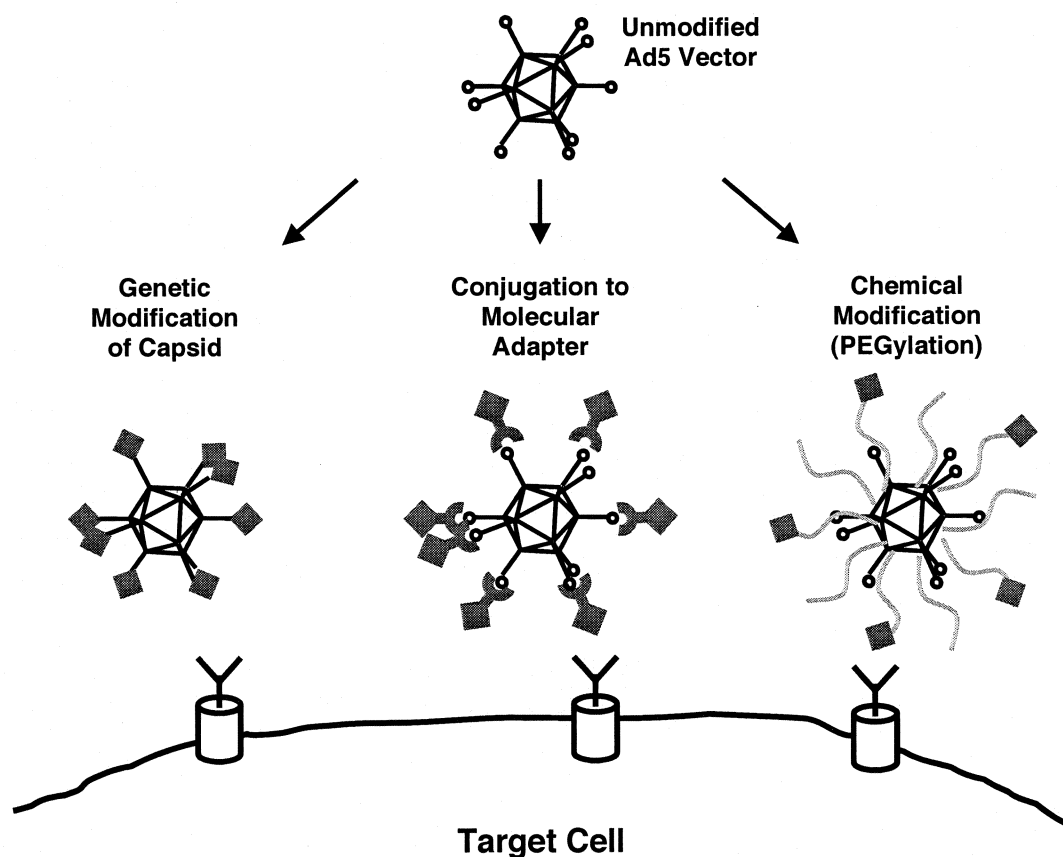


Fig 2.8 Schematic of three major strategies for the alteration of Ad vector tropism.

Fiber-Swapping and Alternate Serotypes

Another strategy for redirecting Ad5 vectors to alternate cell types exploits both the natural diversity and evolutionary conservation of the adenoviridae family. Previous work has shown that the Ad5 fiber can be swapped with fibers of other Ad serotypes thereby creating “pseudotyped” hybrid vectors [65]. The fiber-swapping of Ad5 fibers with those from subgroup B adenoviruses like Ad3, Ad35, or Ad11 results in vectors with CAR-independent transduction, mediated through the group B Ad receptors CD80/CD86, and CD46 [54, 138, 139]. Although this strategy does introduce alternate tropism into the Ad5 capsid, it does not result in truly targeted vectors, as the natural cellular receptors for the group B adenoviruses are present on many cell types. An interesting case of fiber-swapping was recently described whereby the Ad5 fiber was replaced with the structurally similar $\sigma 1$ protein from reovirus [96]. The resulting chimera vector could transduce cells through the reovirus receptors JAM1 and sialic acid. This vector is currently being tested as a vaccine vector as reovirus naturally infects cells involved in mucosal immunity. Even more extreme cases of fiber replacement have been described in the literature such as the replacement of the shaft and knob domains of fiber with the T4 phage fibrin protein fused to cell binding domains like CD40-ligand, which is structurally similar to the fiber knob domain [10, 78]. Other reports of “knobless” vectors whereby the knobs are proteolytically removed after vector production, thereby exposing cell targeting domains have also been described [67].

2.6 Metabolic Biotinylation and the Biotin Acceptor Peptide

The small molecule biotin (also known as vitamin H) is an essential cofactor for a group of metabolic enzymes known as the biotin-dependent carboxylases. These essential enzymes catalyze the addition, removal, or transfer of carboxyl groups to and from various metabolites and are vital for amino acid metabolism, gluconeogenesis, lipogenesis, and various other metabolic processes [25]. The vitamin cofactor is covalently attached to a specific lysine residue of a highly conserved sequence of the apocarboxylase domain of such enzymes and acts as the actual carrier of the carboxyl group during catalysis. The addition of biotin to these apoenzyme protein substrates is catalyzed by a group of enzymes known as biotin-protein ligases (BPL's). These BPL's are ubiquitous in nature and a great deal of functional conservation exists between evolutionary divergent species [131]. Holocarboxylase synthetase (HCS), the mammalian BPL is capable of recognizing and biotinylating prokaryotic apocarboxylase domains and the human HCS gene was actually identified by its ability to complement *birA*, the *E. coli* BPL [82].

Despite the ubiquitous nature of biotin containing enzymes, the covalent attachment of biotin is a relatively uncommon posttranslational modification. Only four apoenzymes are biotinylated by HCS in mammalian cells: acetyl-CoA, methylcrotonyl-CoA, propionyl-CoA, and pyruvate carboxylases [77]. Although these four apoenzyme substrates are targeted to either the cytoplasmic or mitochondrial compartments, HCS has been shown to primarily localize to the nucleus [104], where it is believed to play a role in the biotin-dependent regulation of gene expression [142].

Avidin is a 16 kDa chicken egg white glycoprotein with a very high affinity for biotin [60]. The avidin-biotin affinity system has been extensively commercialized, and represents an extremely versatile technology, with applications in molecular labeling, targeting, detection, purification, and imaging [8]. With an extremely high affinity ($K_d \approx 10^{-15}$ M), the interaction between tetrameric avidin and biotin is the strongest known non-covalent interaction in nature. To put the strength of this interaction into perspective, a K_d of 10^{-15} M corresponds to a free energy of dissociation of 87.9 kJ/mol [122], roughly one-quarter the strength of a typical C-C bond with a free energy of 348 kJ/mol [20]. The exceptional specificity and strength of this interaction makes the avidin-biotin system a powerful tool for a variety of biochemical and biomedical applications [60, 174].

A wide variety of methods have been developed for the covalent attachment of biotin molecules to proteins. Chemical biotinylation is easily accomplished but lacks reaction homogeneity. The extent and position of biotinylation vary in these chemical reactions and the ablation of protein function due to the reaction of a critical amine group is always a possibility. Additionally, proteins must first be isolated and purified prior to chemical biotinylation. Recent studies have shown that the chemical spacers present between the biotin group and the amine reactive succinimidyl ester are quite sensitive to hydrolysis in the presence of blood plasma [17].

An alternative to chemical biotinylation is site-specific *in vivo* metabolic biotinylation of proteins through genetic fusion of biotin-accepting apocarboxylase domains like the 123 amino acid *Propionibacterium shermanii* transcarboxylase domain (PSTCD) [33, 115, 116]. Endogenous BPL's like *birA* or human HCS will recognize the

PSTCD biotin acceptor peptide (BAP) and catalyze the addition of biotin to a specific lysine residue.

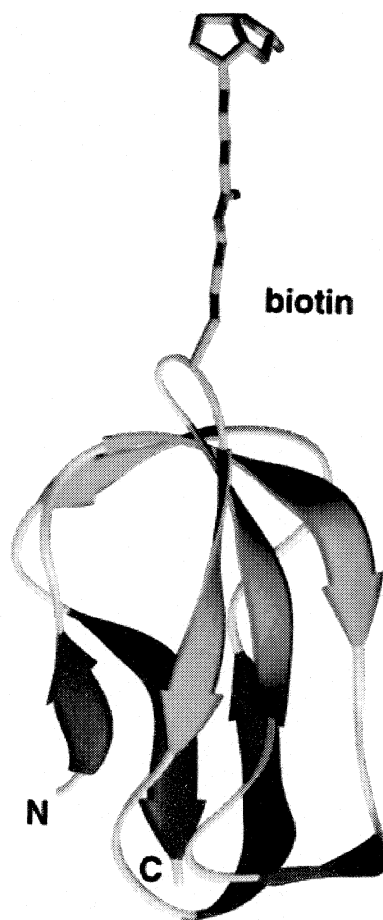


Fig 2.9 Ribbon diagram of the C-terminal 70 amino acids of the BAP from *P. shermanii* trans-carboxylase, from [121].

Previous work [115] has demonstrated that the 70 C-terminal residues of the PSTCD BAP are sufficient to enable *in vivo* metabolic biotinylation in mammalian cells. The NMR solution structure of the PSTCD [121] reveals that these 70 residues fold into a compact β -sandwich structure, with the N and C termini in close proximity on the end opposite the biotinyl-lysine residue (Fig 2.9). The small size and efficient substrate

activity of the BAP warranted its use as a convenient fusion partner for the metabolic biotinylation of the adenoviral capsid.

Chapter III

Construction of BAP-Modified Adenoviral Vectors Through Bacteriophage λ Red Recombination

Abstract

Manipulation of the adenoviral genome by standard *in vitro* restriction endonuclease digestion and ligation dependent cloning procedures can be difficult and cumbersome due to the relatively large size of the Ad genome. Methods for the rapid construction of capsid modified adenoviral vectors through the high efficiency phage λ Red system are presented herein. Efficient recombination of either PCR products or linearized shuttle plasmids resulted in the insertion of the BAP domain onto the C-termini of fiber and protein IX, as well as into the HVR5 loop of hexon. The BAP modifications resulted in viable E1/E3-deleted vectors that were propagated in 293A cells and purified by CsCl density gradient centrifugation. The λ Red system represents a simple and efficient platform for *in vivo* recombination-based genetic engineering of the adenoviral genome.

3.1 Introduction

First generation adenoviral vectors ($\Delta E1/\Delta E3$) represent an important technology for gene transfer into mammalian cells. The relatively large transgene capacity and the ease to which they can be replicated to high titer preparations makes these vectors invaluable tools for applications ranging from gene therapy and genetic immunization to a basic tool for the *in vitro* transduction of mammalian cells. Many different methods have been developed for the construction of such vectors [38]. Early methods were based on observations that transfection of plasmid-encoded adenoviral genomic DNA into mammalian cells could support the production of viable adenoviruses [16].

These early methods for recombinant Ad vector construction rely on the recombination between two DNA molecules, one encoding the left end of the Ad genome with the transgene expression cassette in place of the E1 region and the other molecule containing the remaining right end of the adenoviral genome with a small overlap in viral sequence between the two. The two molecules would be cotransfected into the 293 cell line that stably express the E1 proteins in *trans* [56] and recombination between the two molecules would result in a $\Delta E1$ adenoviral genome that replicates and produces progeny virions in E1-expressing producer cells. Initially, the right end of the Ad genome was obtained from digestion of genomic DNA isolated from purified Ad virions. Separation of the digested right end from the full length Ad genome was difficult and problems arose due to the production of high amounts of background parental virus. Several laborious rounds of plaque assays and screening were required to effectively separate and identify recombinant virus from the background parental virus.

Several methods were developed to facilitate identification and isolation of recombinant virus from parental background. These methods included the use of parental viruses encoding visual reporters like GFP [40] or β -gal [135] within the E1 region such that any recombinants could be visually screened by the lack of reporter expression. Another method utilizes a vector containing the HSV thymidine kinase [107] gene within the E1 region [72]. Non-recombinant parental vector can then be selected against by the addition of the nucleoside analogue ganciclovir, as only recombinants lacking the *tk* gene would be able to grow. All these early methods depend on an inefficient recombination event within the mammalian host cells and typically require a few weeks for the desired recombinant to emerge. Schemes based on the expression of the efficient bacteriophage P1 Cre-*lox* recombination system within the mammalian producer cells have been developed [64], but the persistence of non-recombinant parental viruses requires laborious plaque assays and screening.

Methods involving the use of bacterial homologous recombination have been developed to circumvent the problems associated with the emergence of parental virus within the mammalian host cells. Additionally, bacteria offer a faster and simpler system for the identification and isolation of recombinant Ad vector genomes prior to transfection into mammalian cells. Since the desired recombinants are first cloned in bacteria, the possibility of background parental virus is severely reduced if not eliminated altogether. One disadvantage is that these systems lack selective pressure for the Ad sequences and mutations resulting in decreased viability can arise. Several methods have been developed for the plasmid-based production of recombinant Ad vector genomes in

E. coli [26, 34, 66] but the AdEasy system described by [66] has been commercialized and is now widely used for the construction of Ad vectors:

cDNA cloning in transfer plasmid

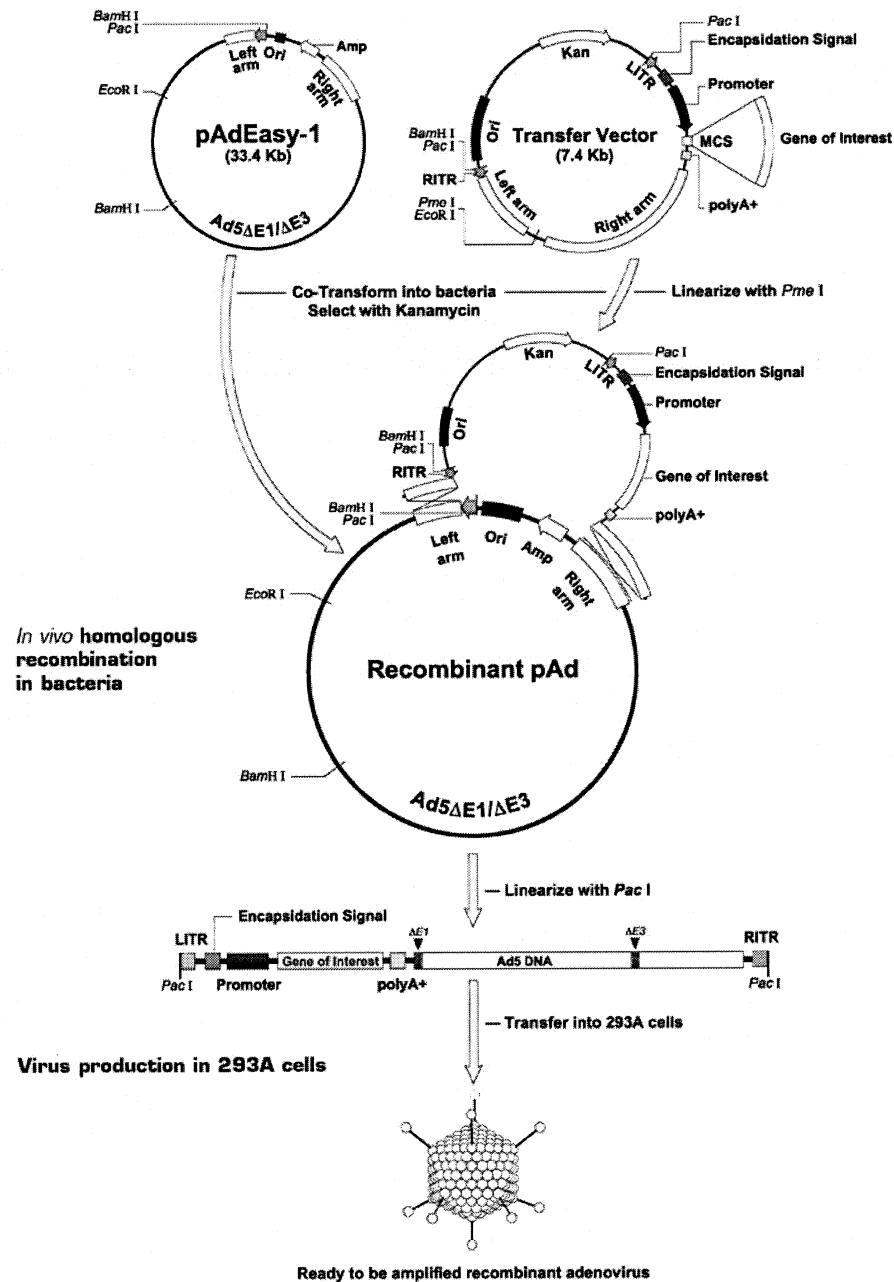


Fig 3.1 Diagram depicting the AdEasy system, taken from <http://www.adenovirus.com/products/kits/adeasy/>

The AdEasy system is a two-plasmid system consisting of a shuttle construct (pShuttle) containing the left end of the Ad genome and containing a MCS in place of the E1 region and a larger pAdEasy-1 plasmid encoding the remaining right end of the Ad genome. The transgene of interest is cloned into pShuttle and the resulting construct is linearized and cotransformed with pAdEasy-1 into the recombinogenic strain BJ5183. Recombination between the two DNA molecules results in the joining of the left and right ends along with the swapping of ampicillin resistance for kanamycin resistance. Selection on kanamycin yields colonies containing the desired recombinant Ad genomes. These resulting pAd plasmids are low copy number pBR322-based plasmids containing the entire Δ E1/ Δ E3 adenovirus type 5 genome with a transgene expression cassette in the E1 region. Digestion of pAd plasmids with *PacI* results in the excision of the full recombinant Ad genome, which is then transfected into 293 cells for the production of recombinant adenoviral vectors. All vectors described herein were derived from the AdEasy system and they contain expression cassettes encoding the dsRed2 red fluorescent protein, a GFP-luciferase fusion protein, or a Luc-IRES-hrGFP cassette allowing for simultaneous translation of Luc and hrGFP from the same transcript.

Bacteriophage λ Red Recombination

The production of metabolically biotinylated adenoviral vectors involves the fusion of sequences encoding the PSTCD biotin acceptor peptide (BAP) to the open reading frames of the Ad capsid proteins, resulting in the display of the BAP from the surface of the Ad capsid. The pAd plasmids used for vector construction are too large (~34-35 kb) for easy manipulation by standard *in vitro* digestion and ligation cloning

techniques. To facilitate the construction of capsid-modified pAd genomes, an efficient recombination system from bacteriophage λ was utilized: the Red recombination system.

The bacteriophage λ Red genes were originally discovered in a mutant recombination defective strain that was severely defective for recombination in a *recA* deficient host strain [31]. The mutation mapped to three gene products clustered within the λ P_L operon that all work in concert to efficiently mediate recombination across short homologous sequences. The *exo* gene encodes an exonuclease that digests the 5' end of a linear double stranded DNA (dsDNA) molecule, generating a 3' single stranded overhang to which the β single-stranded DNA (ssDNA) binding protein binds to promote complimentary annealing and recombination. The γ protein mediates recombination indirectly by binding and inhibiting the RecBCD complex, which can rapidly degrade linear dsDNA molecules [100]. Recombination between the linear dsDNA (with β -coated ssDNA ends) and a circular dsDNA molecule is thought to occur via a *recA*-dependent strand invasion mechanism. The system works so efficiently that recombination across as few as 36 nucleotides of homologous sequence is possible. Homologous recombination between two linear dsDNA molecules also occurs with high efficiency through *recA*-independent, β -mediated strand annealing mechanisms [31] [119].

3.2 Materials and Methods

Materials. Plasmid DNA purification kits were purchased from Qiagen. The Ad-Easy vector system was purchased from Quantum Biotechnologies. pEM7-Zeo was purchased from Invitrogen. Restriction endonucleases and T4 DNA ligase were purchased from New England Biolabs. Herculase thermophilic polymerase was purchased from Stratagene. High-glucose DMEM with L-arginine, antibiotic-antimycotic (Ab/Am), fetal bovine serum (FBS), and lipofectamine were purchased from Gibco BRL. All other reagents and supplies were purchased from Sigma, Fisher, or VWR.

Bacterial Strains. XL-1 blue cells (Stratagene) were used for all restriction based clonings and DNA preps unless indicated otherwise. BJ5183 (Quantum Biotechnologies) was used for traditional *recA* based homologous recombination. DH5 α /pCP20 and BW25113/pKD46 were obtained from the *E. coli* Genetic Stock Center (<http://cgsc.biology.yale.edu>) and were originally described in [39].

Red Recombination Using PCR Products. The BAP was previously subcloned adjacent to a cassette encoding zeocin resistance in pIX-BAP-Shuttle-Zeo^R [22]. This construct was then PCR amplified with oligos BAP-Zeo5' fiber (*GCCACATCCTCTTACACTTTTTCATACATTGCCCAAGAAGGGGGCAGTGGCGGATCCGGCGGGTCCG* GAGAGGGCGAGATTCCC) and BAP-Zeo3' fiber (*TGAAAAATAAACACGTTGAAACA* *TAACACAAACGATTCTGCAGGTCGACTCTAGAGG*). Italicized sequences

correspond to the 39 nt homology regions for insertion of the BAP-Zeo fragment at the 3' end of the fiber gene on pAd-dsRed. The underlined sequence codes for the (Gly-Gly-Ser)₃ linker peptide. The resulting product was *DpnI* digested to remove any template plasmid, gel purified, and 0.5 µg was co-transformed along with 1 µg pAd-dsRed into electrocompetent BW25113 cells. Transformed cells were rescued with 1 ml SOC (lacking glucose and supplemented with 0.1% L-arabinose) and incubated for 10 hours at 30 °C. Transformants were then plated at 37 °C on LB agar containing kanamycin and zeocin to select for proper recombinants. Several clones were picked, grown in 3 ml liquid cultures and minipreped. Recombinant pAd-dsRed-Fiber-BAP was screened by restriction digestion and PCR and transformed back into XL-1 blue cells to isolate the recombinant plasmid from any parental pAd-dsRed that failed to undergo recombination. Proper recombination was verified by sequencing and the pAd-dsRed-Fiber-BAP construct was midipreped and linearized with *PacI*.

Red Recombination Using Shuttle Plasmids. The BAP sequence was cloned into the two shuttles and used for the construction of protein IX and hexon modified vectors. Construction of pFZF was done by cloning annealed oligo-nucleotides containing the FRT sequence (GAAGTTCCTATTCTCTAGAAAGTATAGGAACTTC) into the *NheI/XhoI* and *EcoRI/BamHI* sites of pEM7-Zeo, thereby flanking the zeocin resistance cassette with FRT sites. The resulting pFZF (FRT-Zeo-FRT) was then used for the construction of pIX-display. Briefly, the IX coding sequence was PCR amplified from the pAd-Easy genome and subcloned into the *HindIII* and *SalI* sites of pFZF. A short fragment of the human apoE4 cDNA was then PCR amplified and cloned in frame

into the *SalI* and *BamHI* sites of the construct. This apoE4 sequence, primary sequence RARLSKELQAAQARLGADMEDVCGRLVQYRGEVQA, encodes an α -helical peptide linker approximately 45 Å in length [159]. *AgeI* and *ClaI* sites were included in the apoE4 oligo design to allow fusion of ligand sequences downstream of the IX-45 fusion. A short 175 bp sequence from the protein IX 3'UTR was then PCR amplified and cloned into the *NheI* and *BglII* sites of the construct thereby placing the FZF cassette between the IX-45 fusion sequence and the IX 3'UTR sequence for homologous recombination.

pHVR5-display was derived from pUT18, a pUC derivative, described in [74]. Briefly, a ~1950 bp fragment encoding a C-terminal fragment of pVI and residues 1-268 of hexon was PCR amplified and cloned into the *HindIII* and *KpnI* sites of pUT18. An additional *SalI* site was engineered into the oligonucleotide to create *SalI/KpnI* cloning sites flanking the HVR5 sequence of the hexon. Next, a ~2050 bp sequence encoding the remainder of hexon was amplified and subcloned into the *KpnI* and *EcoRI* sites of the construct. Finally, the FZF cassette was PCR amplified and inserted between the pVI and hexon ORF's by Red recombination as described above.

pIX-45-BAP was made by PCR cloning the BAP into the *AgeI/ClaI* sites of pIX-display with BAP5'A (ATGCTCCTGACCGGTGGCGGAGAGGGCGAGATTCC) and BAP3'C (CCATCGATGGTTACCCGATCTTGATGAGACCCTG). The construct was linearized with *Acc65I*, *BglII*, and *PvuI* and the 1508 bp fragment was gel purified.

pHVR5-BAP was made by PCR cloning the BAP into the *SalI/KpnI* sites of pHVR5-display with BAP5'S (ACGCACGCGGGTCGACCGGCGGAGAGGGCGAGATTCCCGCTCCG) and BAP3'K (TCGGGGTACCGCCGCGGAGCCCCCGATCTTGAT

GAGACC). The resulting construct was linearized with *PvuI* and the 3552 bp fragment was gel purified. Red recombination of each of the fragments was then performed with 0.5 μ g fragment and 1 μ g pAd-dsRed as described above. Positive clones were identified by PCR and/or restriction digestion, and the recombinant pAd genomes were transformed into electrocompetant DH5 α cells harboring pCP20, a temperature sensitive replicon expressing FLP recombinase for the excision of the Zeo^R cassette. Transformants were incubated for 4 hours at 30 °C and plated at 30 °C on LB agar containing kanamycin and chloramphenicol. Four colonies were picked for each construct and screened by zeocin sensitivity. Typically at least two of the four clones lost resistance to zeocin upon transfer into DH5 α /pCP20 indicating proper excision of the FRT-flanked Zeo^R cassette. Positive clones were then grown up in 30 ml liquid cultures at 37 °C to lose pCP20 and the plasmid DNA was midipreped and linearized with *PacI*. pAd-IX-BAP, without the 45 Å spacer, was produced by similar methods involving Red recombination. Specific details are provided in [22].

Vector Amplification. 293A cells were maintained at 37 °C in DMEM containing 10% FBS and Ab/Am (cDMEM). Recombinant vectors were produced by transfection of 293A monolayers with lipofectamine reagent (Invitrogen). Plaques typically appeared within 9-14 days at which the monolayers were overlaid with 1.25% agarose-cDMEM and picked. Viruses were amplified in five successive rounds of growth on 293A cells, going from 24-well plates to cell factories, typically using ~20-30% of each round's lysate supernatant as inoculum in the next round. Cell lysates containing the virions underwent three rounds of freeze/thaw cycles in DMEM plus 5%

FBS between each round. 293A cells were cultured in cDMEM supplemented with 30 μ M D-biotin for the final two rounds of amplification to allow for maximum levels of metabolic biotinylation.

CsCl-Density Gradient Purification. Cells were collected 3-4 days post infection, once they completely detached from the plate. Infected cells were concentrated in ~10 ml of 50 mM Tris-Hcl, pH 8.0 and subjected to three cycles of freeze-thaw. Lysate was spun down at 1200 rpm for 15 minutes and the supernatant was loaded onto a discontinuous CsCl gradient consisting of 10 ml of light CsCl (~1.23 g/ml) carefully underlayed with 8 ml of heavy CsCl (~1.43 g/ml). CsCl solutions were prepared in Tris buffer. The tubes were centrifuged at 20,000 rpm for 4 hours at 4 °C. The bottom band, containing the infectious virions, was collected by side puncture with an 18-gauge needle syringe and was diluted to 4 ml with Tris buffer. The virions were then loaded onto a second smaller gradient (4 ml and 4 ml) and centrifuged as before for 16 hours. The banded infectious virions were collected with a needle and desalted on a DG-10 buffer exchange column (BioRad). Final preps of virus were collected in either 20 mM HEPES, 150 mM NaCl, 30% glycerol pH 7.8 or buffer A195 [48].

3.3 Results and Discussion

Red Recombination Using PCR Products

Genetic engineering based on Red recombination relies on the transfer and subsequent selection of an antibiotic resistance gene. To utilize the method for construction of a BAP-modified fiber gene, the BAP was previously subcloned adjacent to a cassette encoding zeocin resistance in pIX-BAP-Shuttle-Zeo^R [22]. The resulting construct was used as template for PCR with primers containing 39 nt overhangs complementary to sequences within the Ad genome for proper fusion of the BAP to the C-terminus of the fiber gene. A short (Gly-Gly-Ser)₃ linker was included between fiber and the BAP in the oligo design. The resulting PCR product was *DpnI* digested to remove any template plasmid and gel-purified. Electrocompetent BW25113 cells were co-transformed with pAd-dsRed expressing the red fluorescent protein and the purified PCR product. Transformants were incubated for 10 hours at 30 °C to induce expression of the Red genes and allow recombination (Fig 3.2).

The cells were then plated at 37 °C on selective media for the isolation of proper recombinants. Individual colonies were picked and screened by PCR and restriction digestion. 100% of the screened clones contained the proper recombination construct. Single clones that are both zeocin and kanamycin-resistant can contain both the recombinant and parental pAd-dsRed plasmid, so it is important to colony purify each positive clone by transforming a non-recombinogenic strain such as XL-1 blue or DH5 α . The resulting pAd-Fiber-BAP constructs from these strains were confirmed by restriction digestion and sequencing. The construct was then linearized with *PacI* and transfected

into 293A cells, with plaques forming after about 14 days. Plaques were overlayed with agarose and picked for amplification and purification of the fiber-modified vector.

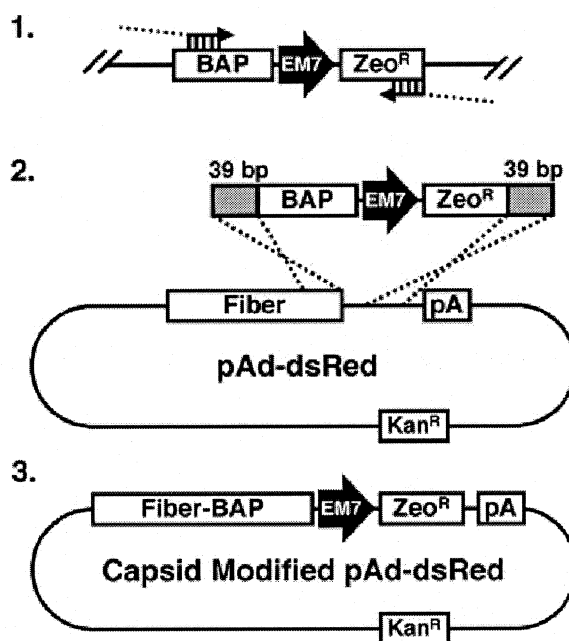


Fig 3.2 Modification of the fiber gene with the λ Red system. (1) The BAP-Zeo^R cassette was amplified with oligos containing 39 nt homology extensions for targeted insertion. (2) Expression of the λ Red genes within BW25113 promotes recombination across the short homologies, thereby creating (3) the capsid-modified pAd-dsRed genome construct.

Red Recombination Using Shuttle Plasmids

The use of linear PCR products for the construction of plasmids with Red recombination is quick and convenient but PCR amplification always runs the risk of the introduction of unwanted mutations. Additionally, new recombinogenic oligos must be designed and purchased for the fusion of different ligands to the C-terminus of fiber.

Shuttle plasmids were constructed to create a stable platform for the modification of pIX

and hexon proteins. Insertion of the selectable Zeo^R cassette is well tolerated immediately downstream of the fiber gene [114] however it is not known whether the insertion of this small bacterial expression cassette will be tolerated in other locations of the Ad genome. To avoid any problems in this regard, pFZF, a modified form of pEM7-Zeo (Invitrogen), was constructed. pFZF contains the Zeo^R expression cassette flanked by 34 nt FRT sites for subsequent excision of the cassette by FLP recombinase.

pIX-display, a shuttle plasmid for the construction of pIX-modified Ad vectors was constructed from the pFZF backbone. Briefly, sequences encoding the full length IX gene with a 3' multi-cloning site and the downstream IX 3' untranslated region (3'UTR) were PCR cloned into pFZF. Previous work has shown that the presence of an alpha helical spacer peptide between IX and a c-myc epitope increased the accessibility of the peptide tag [159]. Based on these findings the sequence encoding the 45 Å alpha helical peptide from human apolipoprotein E (herein referred to as "45") was incorporated into the shuttle. The resulting shuttle (Fig 3.3) contains *AgeI* and *ClaI* sites for the fusion of ligands to the C-terminus of the pIX-45 fusion. Alternatively, *SalI* and *ClaI* could be utilized for the insertion of ligands without the 45 spacer or *SalI* and *AgeI* could be used to swap out 45 for other spacer sequences. The BAP was PCR cloned into the *AgeI/ClaI* sites of pIX-display to create pIX-45-BAP. The plasmid was then linearized with *Acc65I*, *BglII*, and *PvuI* and the linear recombination fragment containing the IX-45-BAP fragment was gel purified.

Previous work has described the modification of hypervariable region 5 (HVR5) of the hexon protein [32, 163]. Based on these results the shuttle plasmid pHVR5-display was created for the addition of various peptide or protein ligands into this surface loop of

hexon (Fig 3.3). The shuttle contains a small portion of the upstream pVI gene followed by the complete hexon gene, containing *SalI* and *KpnI* cloning sites in place of HVR5. The FRT-Zeo^R-FRT cassette from pFZF was PCR amplified and inserted immediately after the pVI gene using Red recombination. The BAP was then PCR cloned into HVR5 of the hexon shuttle to create pHVR5-BAP. *PvuI* was used to linearize the plasmid and the Hexon-BAP recombination fragment was gel purified.

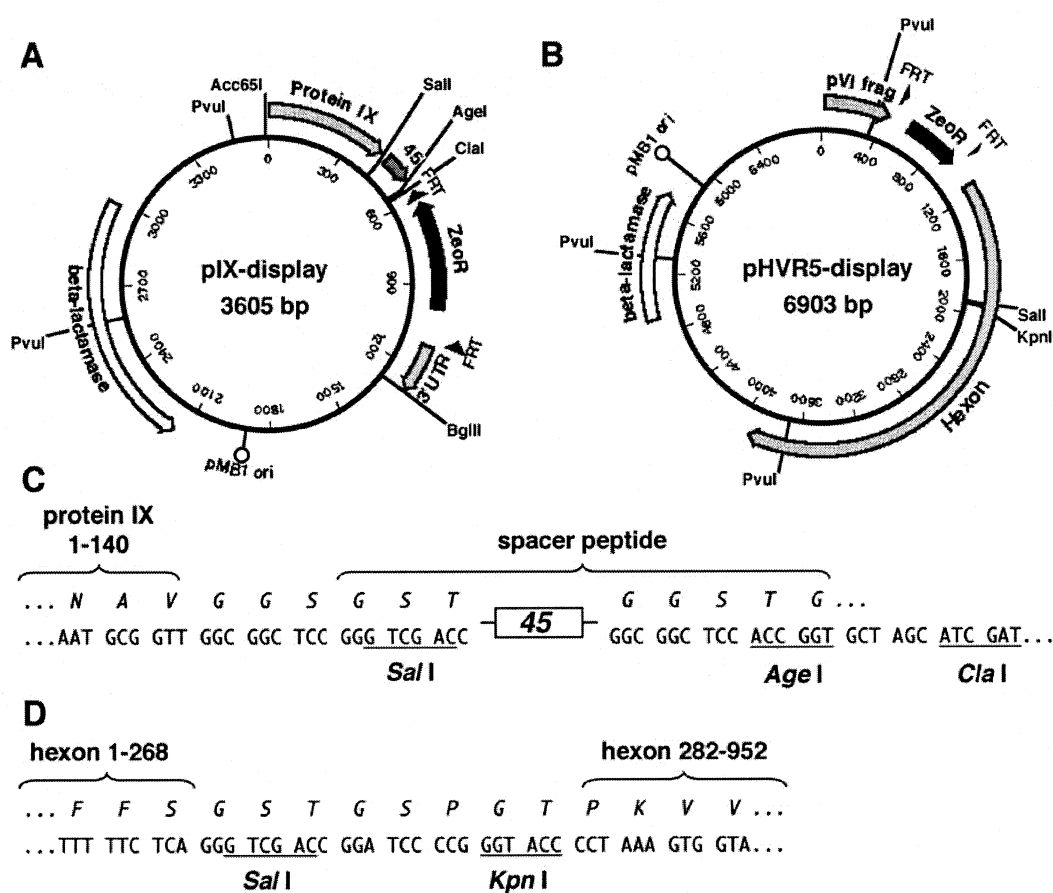


Fig 3.3 Plasmid maps and selected restriction sites of pIX-display (**A** and **C**) and pHVR-display (**B** and **D**). The 45 Å spacer in pIX-display corresponds to nucleotides 322-426 of the human apoE4 open reading frame, encoding a 35 residue α -helical peptide.

To create IX and hexon modified genomes, BW25113 cells were co-transformed with pAd-dsRed and the respective linear fragments as described above. All of the screened clones constructed from pIX-display contained the correct construct. It is particularly important to screen hexon recombinants for the presence of the HVR5 insert, as recombination may occur between the pVI fragment and the first 804 bp of hexon rather than the last 2015 bp, thereby creating a zeocin resistant clone that lacks the insert. On average, 3/8 zeocin resistant clones actually contained the HVR5 modification. Direct comparison to BJ5183 (*endA sbcBC recBC galK met thi-1 bioT hsdR;Str^r*), a standard strain used for homologous recombination [66] demonstrates that shuttle-based recombination via the Red system in BW25113 is 500-1000 times more efficient than the BJ5183 platform. In addition, recombination of PCR products, across short 39 nt homology regions was only possible in BW25113. Positive clones were isolated and transformed into a DH5 α strain harboring pCP20, a chloramphenicol-resistant temperature sensitive plasmid for the expression of FLP recombinase [39]. Transformants were plated on media containing kanamycin and chloramphenicol and incubated at 30 °C to enable FLP-mediated removal of the FRT-flanked Zeo^R cassettes. Colonies were picked and screened by sensitivity to zeocin as well as restriction digestion.

Properly modified pAd-Fiber-BAP, pAd-IX-BAP, pAd-IX-45-BAP and pAd-Hexon-BAP genomes were then *PacI* linearized and transfected into 293A cells to create capsid-modified Ad vectors. Plaques formed within 9-14 days and the vectors were propagated and amplified by standard methods as previously described. All vectors were amplified and purified by CsCl density-gradient centrifugation, yielding normal titers.

3.4 Conclusions

In summary, the use of the λ Red system for genetic manipulation of the adenoviral genome is presented. Molecular cloning based on the Red genes is extremely efficient and allows for recombination between as little as 36 bp of homology, thereby enabling the targeted homology sequences to be incorporated directly into oligonucleotide design. Rapid construction of a fiber-BAP fusion within the context of the Ad genome is demonstrated through the use of Red recombination between a simple PCR product and the Ad genome in BW25113 cells.

Additionally, the construction of two useful shuttle plasmids for the insertion of peptides or domains onto the C-terminus of protein IX or into the HVR5 surface loop of hexon is presented. These shuttles were used with the Red system to quickly engineer BAP-modified vectors that could be rescued and amplified to normal titers in 293A cells.

Red recombination represents an extremely simple and useful methodology for the genetic engineering of Ad vectors. The highly efficient Red system will be of great use not only for the modification of capsomer genes, but also for the alteration or knockout of other adenoviral sequences as well.

Chapter IV

Characterization and Avidin-Based Applications of Metabolically Biotinylated Adenoviral Vectors

Abstract

The genetic incorporation of the BAP domain into the fiber, IX, and hexon capsomeres of the adenoviral virion results in viable Ad vectors. These vectors are all comparable to unmodified wild type Ad vectors with regards to CAR-dependent infectivity and transduction, with the exception of Ad-fiber-BAP, which suffers a slight decrease in infectivity. All BAP-modified vectors are metabolically biotinylated during propagation in 293A cells and the biotins are accessible to avidin binding on the surface of the capsid. The number of biotin molecules per capsid correlates well with the stoichiometry of each of the modified capsomeres within the virion. The metabolically biotinylated vectors readily bind avidin and streptavidin functionalized resins, enabling avidin-based physical targeting of vector transduction to refractory cells. In addition the use of monomeric avidin resin for the effective purification of metabolically biotinylated Ad vectors is presented, demonstrating the valuable potential of this application. Direct comparison of each vector reveals that the IX-modified vectors are superior for avidin-based purification of Ad vectors.

4.1 Introduction

Infectivity, transduction, and morphology of all four BAP-modified vectors is presented herein. Incorporation of the BAP results in metabolic biotinylation and surface display of biotins from the modified vectors. A wide variety of avidin/biotin-based reagents are commercially available for applications in molecular labeling, detection, capture, conjugation and affinity purification. The use of avidin-based resins for affinity purification and physical targeting of metabolically biotinylated adenoviral vectors is presented herein. The transduction of Ad-BAP vectors, when conjugated to streptavidin coated paramagnetic μ particles, was greatly enhanced in the presence of a magnetic field. CAR-deficient CHO cells were efficiently transduced by the μ particle-bound Ad-BAP vector, while unmodified Ad vector resulted in negligible transduction under the same conditions. This simple method is useful for the *in vitro* transduction of refractory cells or the transduction of specific populations of cells within a monolayer.

Immobilized monomeric avidin, with a substantially reduced affinity for biotin ($K_d \approx 10^{-7}$ M) than native tetrameric avidin ($K_d \approx 10^{-15}$ M), was evaluated as an affinity purification matrix for the capture and gentle release of Ad-BAP vectors from crude 293A cell lysates. While all BAP-modified vectors were equally capable of binding the monomeric avidin resin, they exhibited unique differences upon elution, attributable to the biology of the modified capsomeres. Purification of Ad-fiber-BAP resulted in co-purification of excess free fiber-BAP protein, which could then inhibit the bioactivity of the vector by directly competing for cell binding. Similarly, the co-purification of massive amounts of excess free hexon-BAP, together with its interaction partners,

resulted in relatively dirty preparations of Ad-hexon-BAP. Overall, the IX-modified vectors proved the most effective for purification on monomeric avidin. Taken together, this data demonstrates that avidin-based purification represents a potentially viable method for the enrichment of adenoviral vectors from crude lysates.

4.2 Materials and Methods

Plaque Assay. 293A cells were plated in 24 well plates and grown to ~75% confluence. Purified preps of each vector were serially diluted in serum-free DMEM and used to infect subconfluent 293A monolayers for 3 hours at 37 °C in a minimal volume, after which time 1 ml of cDMEM was added to each well. Media was regularly changed for seven days and the monolayer was overlaid with cDMEM plus 1.25% agarose. Fresh agarose containing media was added daily and plaques were counted 14 days post-infection. The highest dilution that produced visible plaques on the monolayers was used to calculate the particle:plaque forming unit ratio (VP/PFU) for each vector. Assay was done in triplicate and values are reported as mean VP/PFU \pm standard deviation.

Cell Transduction. HeLa cells were plated to ~80% confluence in a 24 well plate and transduced in triplicate with each vector at MOI's (multiplicities of infection) of 5000, 500, and 50 VP/cell for 2 hours in a minimal volume of DMEM plus 2% FBS. Vector was removed and 2 ml of fresh cDMEM was added to each well. Transduction was measured 48 hours post transduction by flow cytometry. For the vector thermostability assay, virus diluted in serum-free DMEM was incubated at 47.5 °C for various times before transduction of HeLa cells in triplicate at an MOI of 1000 VP/cell. Expression of dsRed was quantified by flow cytometry 48 hours post transduction. Results were plotted as percent positive cells versus time at 47 °C for each vector.

Fluorescent Microscopy. Micrographs were taken on an Olympus CK40 fluorescent microscope using the appropriate UV absorbtion and emission filters. Digital pictures were taken with a Spot RT color camera system and images were processed with Adobe Photoshop. All fluorescent micrographs depicting cellular dsRed expression are representative of the entire sample and were collected with identical exposure times and gain levels for each separate experiment.

Flow Cytometry. Reporter gene expression (transduction) was quantitated by flow cytometry and analyzed using the CellQuest software (Beckton Dickinson). Briefly, cell monolayers were detached with 0.25% trypsin solution, diluted to ~1.5 ml with PBS and transferred to 5 ml round bottom polystyrene tubes. Samples were run through the flow cytometer and 10,000 events (cells) per sample were collected for data analysis. Gates between transduced and non-transduced (i.e. “positive” and “negative”) cells were determined on a one-dimensional histogram by excluding 99% of the mock-infected cells from the threshold value for determining positively transduced cells. Data was expressed as either % positive cells or mean fluorescence intensity (MFI).

Transmission Electron Microscopy. CsCl-purified virions were adsorbed onto carbon/formvar 300-mesh copper TEM grids (Ted Pella). Samples were negatively stained with 1% phosphotungstic acid for 1 minute and washed once in distilled H₂O. Specimens were visualized with a Hitachi 7500 transmission electron microscope at 100 kV and 40,000x magnification.

Western Blot. Purified virions were diluted into Laemmli's loading buffer, heated to 95 °C for 3 minutes, and electrophoresed on a 7.5% polyacrylamide gel. Proteins were then blotted onto a polyvinylidene difluoride (PVDF) membrane and blocked in Tris-buffered saline with 0.1% Tween-20 (TBST) plus 5% (w/vol) powdered milk overnight at 4 °C. The blot was probed with NeutrAvidin-HRP [0.5-2 µg/ml] at room temperature for 1 hour, washed 5x in TBST, and detected by chemiluminescence with supersignal west dura substrate [80].

ELISA. All washes and incubations performed at 4 °C unless otherwise stated. Serial dilutions of each vector in PBS were adsorbed onto the wells of a high-binding microtiter plate for 3 hours. The plate was then blocked with TBST plus 5% milk for 3 hours. 100 µl of NeutrAvidin-HRP [2 µg/ml in PBS] was added to each well and the plate was incubated for an additional 2 hours. The plate was washed extensively and bound HRP was detected by colorimetric reaction with 100 µl tetramethylbenzidine substrate for 30 minutes at room temperature. The reaction was stopped by the addition of 50 µl 1.8 M H₂SO₄ and absorbance at 450 nm was measured with an automated microplate reader. Values are reported as mean absorbances of triplicate samples ± standard deviation.

Biotin Quantification. Metabolically biotinylated recombinant maltose binding protein (MBP-biotin), with a known MBP:biotin stoichiometry of 1:1, was diluted to 1 µg/ml in PBS and various amounts ranging from 1-12 ng were immobilized on the wells of a microtiter plate. The different amounts of biotin were then quantified for

NeutrAvidin-HRP binding as described above. The known amounts and molecular weight of the MBP-biotin allowed a standard curve of biotin content versus A_{450} to be plotted. Serial two-fold dilutions ranging from 5×10^8 VP to 1.56×10^7 VP were quantified for avidin binding by ELISA as described above. Comparison of average A_{450} values from the known amounts of vector to those of the MBP-biotin standard curve resulted in the approximation of the number of biotin molecules per capsid of each BAP-modified vector.

Avidin Neutralization. 200,000 HeLa cells were plated in 24-well plates in cDMEM. 2×10^8 VP of each vector was diluted into 500 μ l serum free media containing none, [0.33 nM], or [0.33 μ M] neutravidin. Samples were incubated for 20 minutes on ice and 400 μ l was overlayed on the HeLa cell monolayer, corresponding to a final MOI of 800 VP/cell. Cells were transduced for 3 hours prior to the addition of 1 ml cDMEM. Transduction was measured 48 hours later by flow cytometry and MFI relative to the control condition was calculated for each vector. Results are presented as the mean % transduction of three replicates \pm standard deviation.

Magnetofection. CHO cells were grown to confluence in 12-well plates (approximately 570,000 cells per well). Rare-earth 5 mm diameter magnet disks (Indigo Instruments) were affixed underneath half of the wells prior to seeding. Each vector (6×10^8 VP) was diluted into 500 μ l serum-free DMEM, to which 2 μ l of streptavidin-coated superparamagnetic μ beads (New England Biolabs) or 2 μ l control buffer was added. Samples were mixed by pipetting and complexed for 15 min at 4 °C. CHO cell

monolayers were washed twice in serum-free DMEM and overlaid with 500 μ l of each vector complex (MOI = 1000 VP/cell). Plates were placed on an orbital shaker for 10 min at room temperature and then shifted to 37 °C with the addition of 1.5 ml of cDMEM to each well. Cells were photographed 24 hours post-transduction under a fluorescent microscope to show transduction. Groups with magnets were photographed in the location where the magnet was affixed. To better illustrate the phenomenon, samples containing the Ad-Fiber-BAP vector expressing the GFP-luciferase fusion were also analyzed for luciferase expression with the Night Owl CCD camera. Samples were washed once with PBS and 1 ml of D-luciferin (1 mg/ml) was added to each well. Samples were immediately photographed with the Night Owl camera to visualize luciferase expression.

Purification on Monomeric Avidin Resin. Softlink monomeric avidin resin (Promega) was pre-adsorbed with biotin and regenerated according to the manufacturer's protocol. Resin was pre-blocked with 2.5% BSA and equilibrated in buffer A195 [48]. 293A cells were plated in T225 flasks, grown to ~80% confluence, and infected with each vector at an MOI of 50 VP/cell. Cells were harvested 3-4 days post infection, once they displayed complete cytopathic effect. Cells were washed twice in buffer A195 and lysed in 10 ml A195 by three freeze/thaw cycles. Lysate was centrifuged and 500 μ l of monomeric avidin resin was added to 9 ml of the supernatant and incubated for six hours at on a nutator. Resin was pelleted and washed 5x with 10 ml of A195. All unbound and wash fractions were stored. Vector was eluted overnight by the addition of 4 ml A195 containing 5 mM d-biotin. The elution fraction was collected and a second elution was

performed. All washes and incubations were performed at 4 °C. To determine the vector bioactivity present in each fraction, 50 µl aliquots were diluted into 250 µl serum free DMEM and added to HeLa cell monolayers (~70% confluence) plated in 24-well plates. Transduction (dsRed expression) was visually assessed 36 hours later by fluorescence microscopy and quantitated 48 hours post-transduction by flow cytometry. Transduction values (MFI) of the fractions of each vector were normalized to their corresponding input values. Aliquots of each fraction were assayed for protein content by SDS-PAGE and western blotting.

4.3 Results and Discussion

Characterization of BAP-Modified Vectors

The direct insertion of the 70 amino acid BAP domain into Ad capsid proteins might interfere with capsid structure and virion function. Purified BAP-modified vectors were tested for infectivity by standard plaque assays on 293A cell monolayers. Results (table 4.1) indicate that all vectors with the exception of Ad-fiber-BAP have particle to plaque forming unit (VP/PFU) ratios comparable to unmodified Ad-wt vectors. Ad-fiber-BAP appears to suffer a 3.5-fold decrease in infectivity, perhaps due to steric inhibition of CAR binding due to the presence of the 7.4 kDa BAP on the C-terminus of the fiber.

Table 4.1 Plaque Assays of BAP-Modified Vectors.

Vector	VP/PFU ratio
Ad-wt	75 ± 23
Ad-fiber-BAP	261 ± 67
Ad-IX-BAP	84 ± 19
Ad-IX-45-BAP	74 ± 22
Ad-hexon-BAP	79 ± 10

Plaque assays on 293A cells provides a measure of the process of infectivity. BAP modification of capsomeres may lead to defects in numerous processes like protein stability, folding, nuclear localization, encapsidation, as well as host cell interactions during the stages of vector binding, uptake and trafficking. To determine whether the drop in Ad-fiber-BAP infectivity is due to defects in actual vector binding and or uptake in host cells, vector transduction was measured. CAR-positive HeLa cells were transduced with each vector at various multiplicities of infection (MOI). Results show a

small but significant decrease in vector activity for Ad-fiber-BAP, while the IX and hexon-modified vectors transduce HeLa cells to levels similar to Ad-wt (Fig 4.1). This decrease in transduction for Ad-fiber-BAP again suggests that the addition of the BAP to the C-terminus of fiber results in steric hindrance of CAR binding, leading to a less efficient transduction and infectivity.

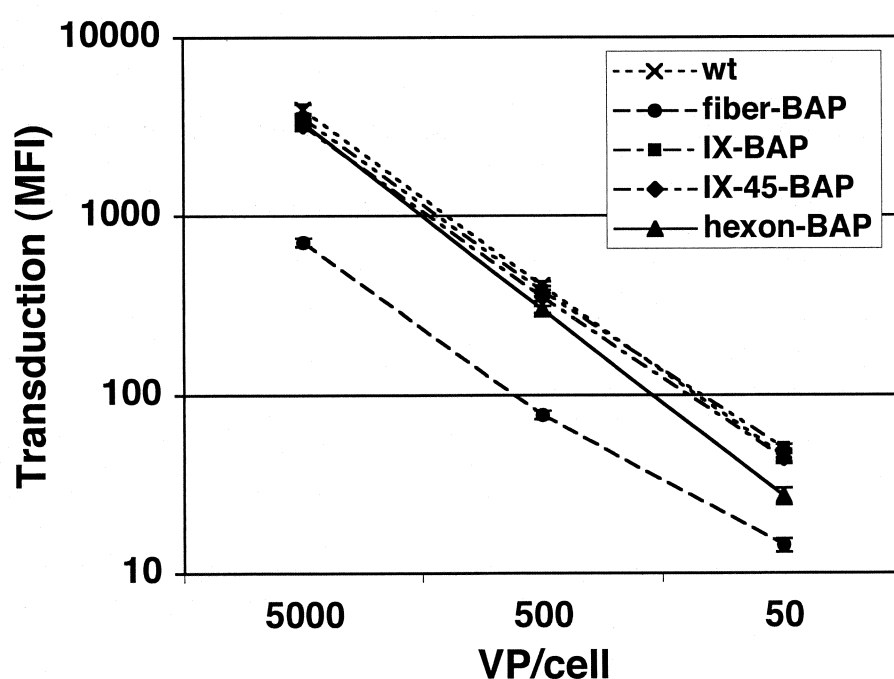


Fig 4.1 CAR-mediated transduction of BAP-modified vectors. HeLa cells were transduced with each vector at the indicated MOI and mean fluorescence intensity (MFI) was measured 48 hours later by flow cytometry.

Protein IX functions as a capsid cement, and is involved in capsid thermostability.

Virions devoid of IX, while still infectious, are rendered thermolabile and are more sensitive to heat denaturation than wild type vectors [29]. A thermostability assay was performed to indirectly test the functionality of the IX-BAP fusion in comparison to wild

type IX. Vectors were heated to 47.5 °C for various times and then tested for transduction activity on HeLa cells. Ad Δ IX, a vector deleted for protein IX, was constructed and included as a control for thermosensitivity. There is no significant difference in the transduction profiles as a function heating time between wild-type and Ad-IX-BAP, as measured by flow cytometry (Fig 4.2). In contrast, Ad Δ IX displays a marked drop in transduction, a reflection of its thermolabile phenotype. The thermostability of Ad-IX-45-BAP was also comparable to wild type, indicating that the addition of the BAP to the C-terminus of IX has no significant detrimental effects towards IX function.

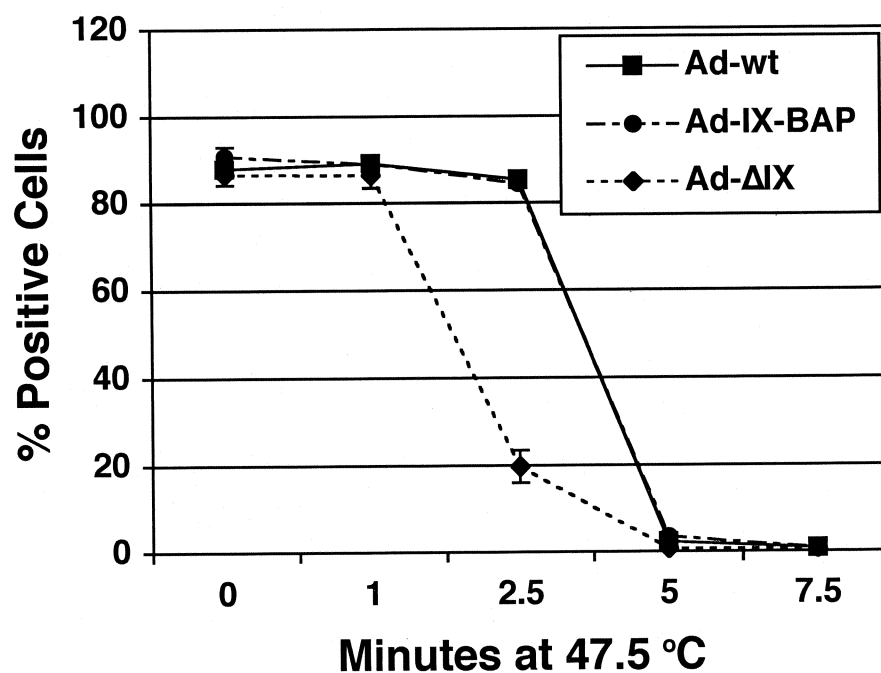


Fig 4.2 Virion thermostability assay. Vectors were heated for various times and assayed on HeLa cells. Transduction efficiency was measured 48 hours later by flow cytometry.

Virion morphology of BAP-modified vectors was examined with negative stain transmission electron microscopy. All vectors with the exception of Ad-45-BAP were examined and none show any discernible differences in overall morphology as compared to wild type Ad (Fig 4.3). It should be noted that subtle differences in the composition of the capsid cannot be determined by this technique.

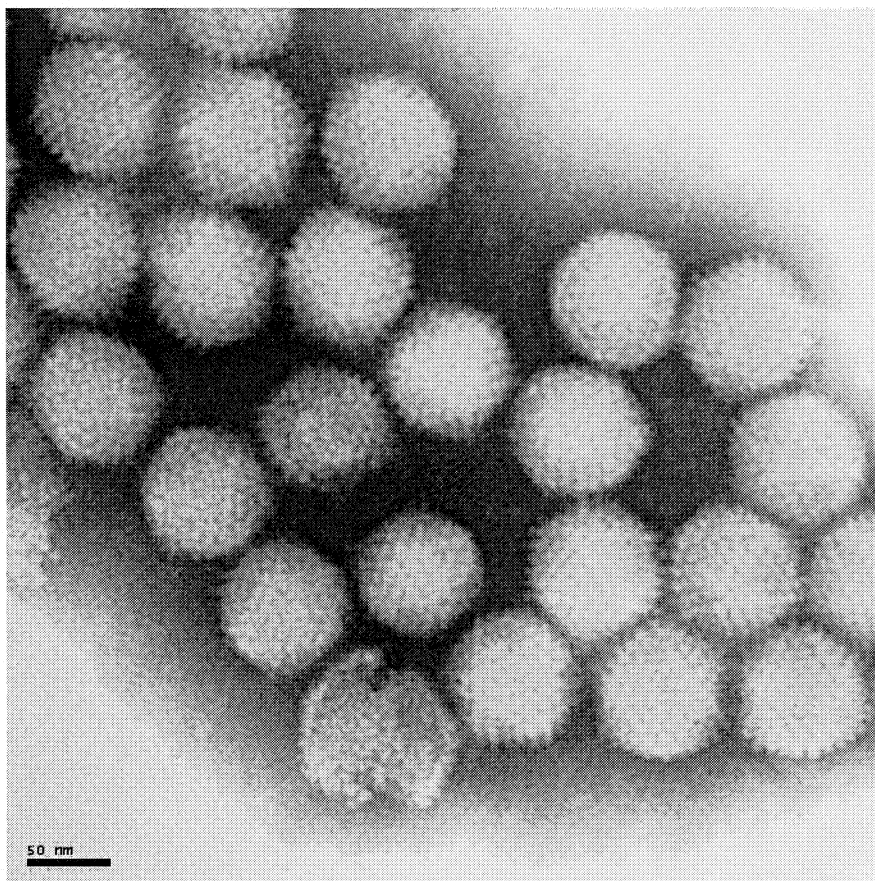


Fig 4.3 Negative stain TEM micrograph of Ad-wt. Image is representative of those obtained with all BAP-modified vectors. The occasional presence broken capsids are typical for TEM of Ad specimens. Scale bar represents 500 Å.

Metabolic Biotinylation of BAP-Modified Vectors

Infectivity data shows that the incorporation of the BAP domain into various proteins of the Ad capsid is generally well tolerated, without substantial defects in vector function. Function of the incorporated BAP domain as a substrate for metabolic biotinylation by cellular HCS was first tested by western blot of the BAP-modified vectors. CsCl-purified virions were denatured, separated by SDS-PAGE, blotted and probed with an avidin-HRP conjugate to directly assess biotinylation of the capsid proteins (Fig 4.4). The blot reveals that the encapsidated BAP fusions are indeed metabolically biotinylated during production in 293A cells.

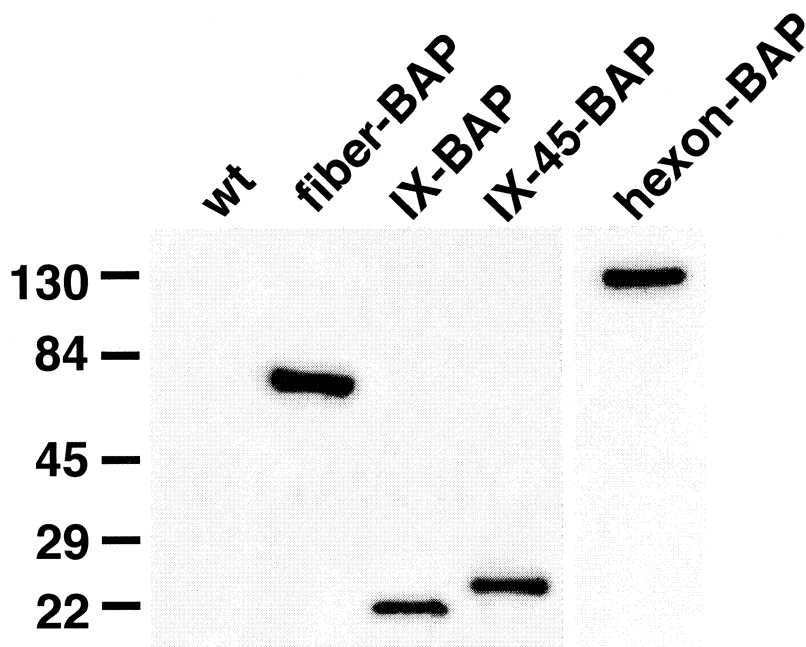


Fig 4.4 Western blot shows encapsidation of biotinylated BAP fusions. 10^9 (wt, fiber-BAP, IX-BAP, and IX-45-BAP) or 10^8 (hexon-BAP) particles were blotted and probed with avidin-HRP to detect biotinylated capsomeres.

Biotinylation of the BAP-modified capsomeres could conceivably occur before encapsidation, whereby the biotin molecules could become inaccessible once the fusion

protein is incorporated into the Ad capsid. Surface accessibility of the biotin molecules is critical for their function as molecular adaptors in vector targeting applications. ELISA was used to ascertain the presence of biotin molecules on the surface of the virions. Immobilized vectors were probed with avidin-HRP to determine the relative extent of exposed biotin molecules (Fig 4.5A). Results agree well with the known stoichiometry of the capsid proteins. Vector with modified fiber (36 monomers per virion) yielded the lowest signal whereas those with modified hexon (720 monomers per virion) had the highest signal. Ad vectors with modified protein IX (240 monomers per virion) had intermediate levels of signal, with the presence of the 45 Å spacer peptide boosting levels about two-fold, in good agreement with previous data [159].

Comparison of the ELISA data to a standard curve of biotin concentration versus absorbance at 450 nm enables an approximation of the average number of biotins per virion for each of the BAP-modified vectors (Fig 4.5B). This ELISA assay is based on avidin binding, so the values obtained reflect the number of avidin-accessible biotins per capsid. Two or more biotin molecules in close proximity due to the architecture of the adenoviral capsid could only be detected as one biotin because of the steric issues associated with the binding of avidin-HRP conjugates. In accordance with these concerns, the measured number of biotins for Ad-IX-BAP, Ad-IX-45-BAP, and Ad-hexon-BAP are substantially less (30%, 54%, and 34%, respectively) than the theoretical maximums. In contrast, Ad-fiber-BAP apparently displays the maximum of 36 biotins per capsid, perhaps because the C-terminal BAP is relatively distant from the bulk of the capsid, allowing efficient avidin binding. Interestingly, the apparent number of biotins displayed by Ad-hexon-BAP is very close to 1/3 the theoretical value. The close

proximity of the HVR5 loops of the monomeric hexons within a given trimer may be imposing this binding limitation of one avidin-HRP per hexon trimer.

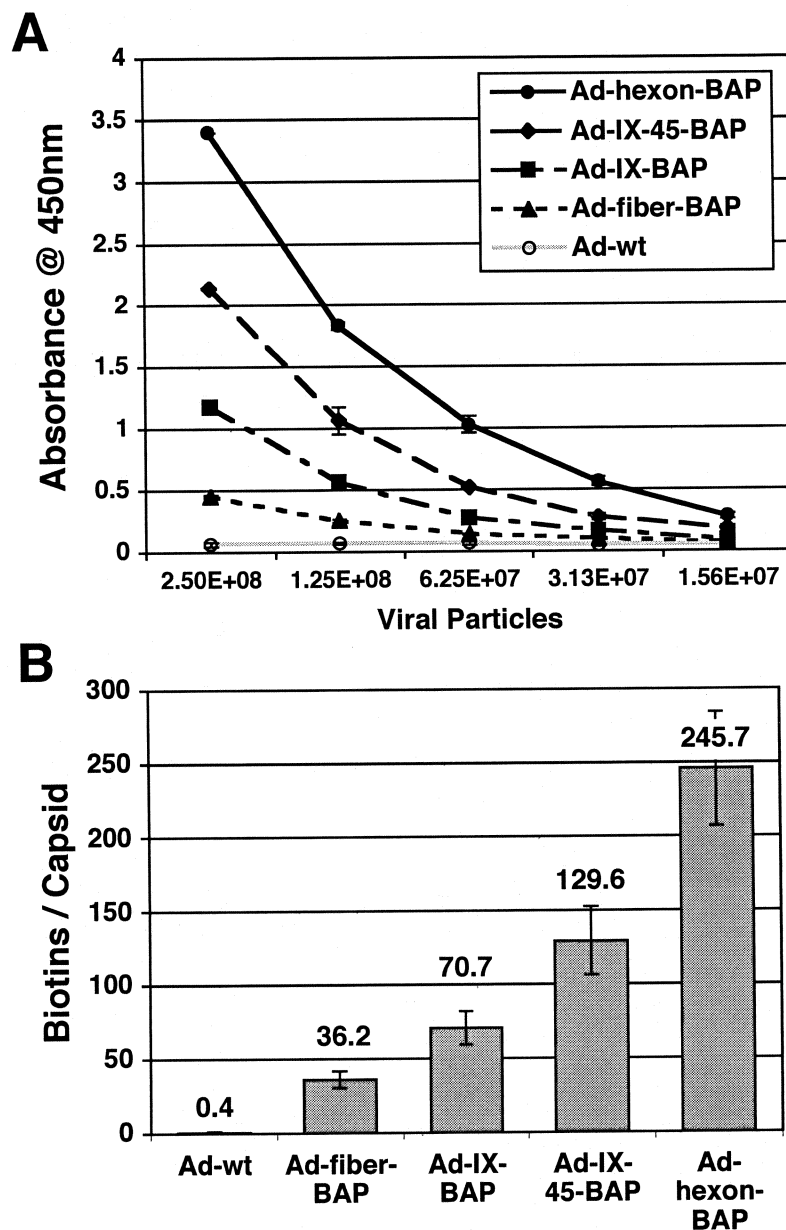


Fig 4.5 (A) Capsid Biotinylation ELISA. Avidin-HRP binding to immobilized virions reveals the relative extent of surface biotinylation. (B) Comparison of the data to a standard curve with known quantities of biotin results in an approximation of the number of biotins displayed per capsid.

To rule out the possibility of denatured or broken virions accounting for the positive ELISA signals, the neutralization activity of tetrameric avidin was assessed. Vectors were incubated with [0.33 nM] or [0.33 μ M] free avidin prior to HeLa cell transduction. These concentrations correspond to molar ratios of 500:1 and 500,000:1 of free avidin molecules to viral particles, enough to fully saturate any surface biotins. Results reveal a concentration-dependent neutralization activity for avidin (Fig 4.6). The presence of a low concentration of free avidin causes a small decrease in vector transduction for all metabolically biotinylated vectors, with no effect on wild type virions. Higher concentrations of avidin result in dramatic decreases in transduction for Ad-fiber-BAP and Ad-hexon-BAP, with a lesser effect on both of the IX-modified vectors.

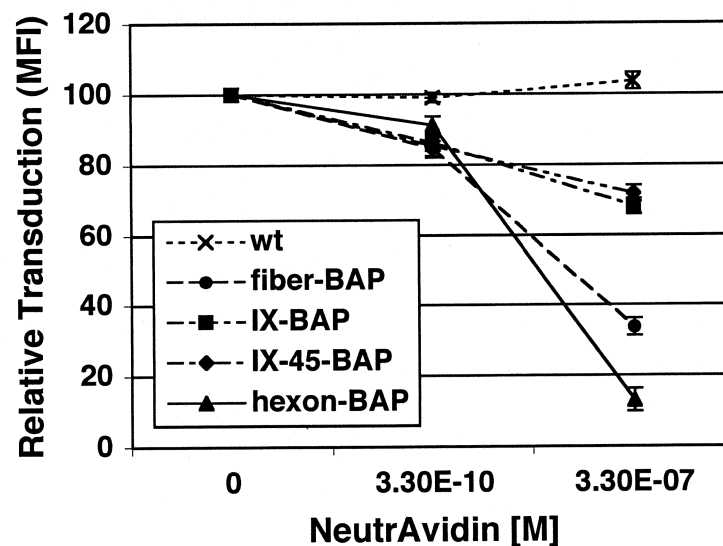


Fig 4.6 Partial neutralization of virion transduction by tetrameric avidin. Vectors were incubated with various concentrations of free avidin prior to HeLa cell transduction. MFI was measured by flow cytometry 48 hours later and data was plotted as the percentage of transduction activity without any avidin.

Saturation of Ad-fiber-BAP with 60 kDa avidin most likely leads to further steric inhibition of CAR binding and vector uptake. Neutralization of Ad-hexon-BAP is probably due to the shielding of the virion and prevention of capsid-cell interactions critical for one or more steps of vector uptake, endosomal escape, and/or trafficking. Recent studies [157] show that an anti-[hexon] neutralizing antibody functions by crosslinking hexon trimers on the surface of the capsid, preventing uncoating and nuclear import of the genome. Tetrameric avidin may act in a similar manner, by crosslinking the surface biotins of Ad-hexon-BAP to prevent proper disassembly. Interestingly, the IX-modified vectors were the most resistant to avidin neutralization, suggesting that additions of large proteins to the C-terminus of IX can be tolerated without major consequences for vector transduction. Complete neutralization of vector activity was not observed under any of the conditions tested.

Physical Targeting of Metabolically Biotinylated Vectors

Previous studies have demonstrated that chemically biotinylated vectors can be complexed with biotin-binding paramagnetic μ beads and that transduction of refractory cells can be enhanced by physically localizing the vector onto cells using magnetic force [112]. To test this application for the BAP-modified vectors, refractory CAR-deficient CHO cells were transduced with biotinylated vectors in the absence or presence of 1 μ m streptavidin-coated paramagnetic beads and in the absence or presence of a small 5 mm magnet.

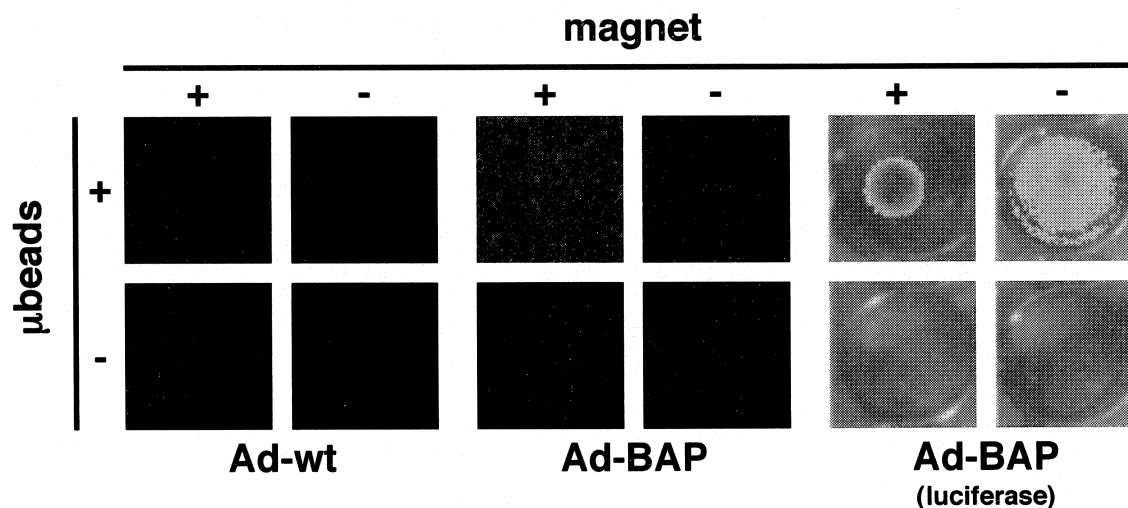


Fig 4.7 Physical targeting of metabolically biotinylated Ad vectors to refractory cells through magnetic force. No enhancement of wild type Ad transduction was observed (left). All BAP-modified vectors had greatly enhanced transduction when bound to streptavidin-coated paramagnetic μ beads as shown by expression of dsRed (middle). Luciferase imaging (right) reveals that the enhanced transduction is confined to the area directly above the magnet.

As expected, the wild type vector and metabolically biotinylated vectors alone failed to significantly transduce the CHO cells under all conditions. In contrast, incubation of the biotinylated vectors with magnetic beads alone caused an increase in

transduction of the metabolically biotinylated vectors, but not by wild-type Ad5 vector. In the absence of the magnet, transduction was increased by the biotinylated vectors because the heavy paramagnetic beads eventually settle to the bottom of the dishes, bringing the vectors in close contact with the CHO cell monolayer. In the presence of a magnetic field, transduction was markedly increased. Luciferase imaging using the Night Owl camera system demonstrated that this transduction was focused to the precise area of where the magnet was placed (Fig 4.7).

Avidin-Based Purification of Metabolically Biotinylated Vectors

The accessibility of the biotin molecules on all BAP modified vectors warranted an investigation into the feasibility of avidin-based affinity purification. The use of an affinity-based method for vector purification is an attractive alternative to traditional CsCl density gradient centrifugation, especially for very small or large scale preparations that cannot be effectively banded by CsCl-based techniques. 293A cells were infected at low MOI, harvested 3-4 days later, and crude lysates were incubated with monomeric avidin resin. Unbound lysate was removed, resin was washed five times, and the bound vector was eluted twice in buffer containing 5 mM biotin. All fractions were collected and analyzed for vector activity by transduction of HeLa cells (Fig 4.8A). Unmodified Ad-wt vector exhibited weak non-specific binding to the resin, with the majority of the bioactivity disappearing by the second wash. All varieties of BAP-modified vectors bound tightly to the resin with very little bioactivity present in the unbound and wash fractions. Elution with the addition of 5 mM biotin resulted in the release of the BAP-modified vectors as seen by the dramatic increase in HeLa cell transduction.

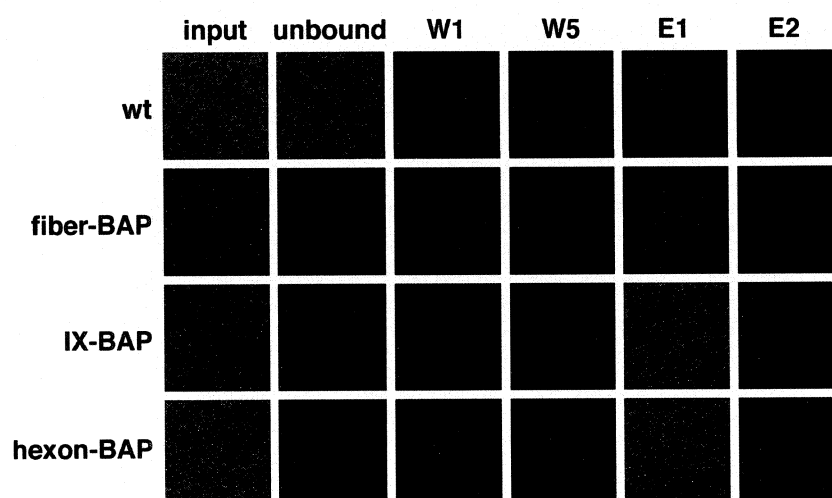
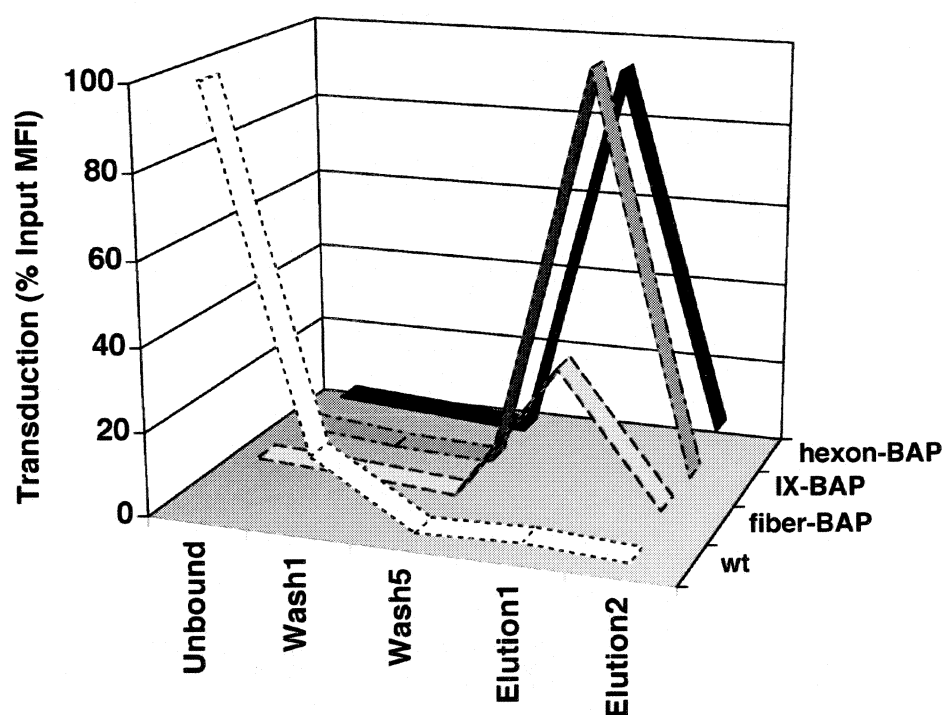
A**B**

Fig 4.8 Purification of metabolically biotinylated vectors on monomeric avidin resin. **(A)** Vector bioactivity of each fraction as revealed by fluorescence microscopy of HeLa cell transduction, as described in materials and methods. **(B)** Quantification of vector transduction by flow cytometry, normalized as a percentage of the input fractions, as described in materials and methods. For simplicity only the first and last wash fractions are shown. Both IX-modified vectors behaved similarly, so only data for Ad-IX-45-BAP is presented.

Quantification of vector transduction by flow cytometry (Fig 4.8B) reveals that while elution of the IX and hexon-modified vectors results in the recovery of nearly 100% of the input, the elution of Ad-fiber-BAP only yields 30-35% of the input bioactivity. The second elution fractions of all BAP-modified vectors show that the vast majority of the bound vector is efficiently released in the initial elution fraction, with little remaining activity present.

Equivalent volumes of various fractions were analyzed for protein content by SDS-PAGE and western blot (Fig 4.9) to determine the cause of the apparent low elution recovery with Ad-fiber-BAP. Comparison of the input and elution fractions for each sample reveals that the majority of cellular proteins were removed during the purification. Elution of Ad-hexon-BAP results in the co-purification of massive amounts of free hexon-BAP protein, as seen by the Coomassie stained gel (Fig 4.9A).

Further analysis by western blot, probed with an anti-[Ad5] polyclonal antibody (Fig 4.9B) shows that purification of each of the biotinylated vectors results in co-purification of free BAP-fusion proteins. This is not unexpected since Ad capsid proteins are produced in excess and the majority of them are not encapsidated into virions during infection [68, 137]. Therefore, even though Ad-fiber-BAP can bind and elute just as effectively as the IX and hexon-modified vectors, the presence of the excess fiber-BAP fusion protein in the elution fraction will interfere with bioactivity by directly competing for cell binding [45, 163].

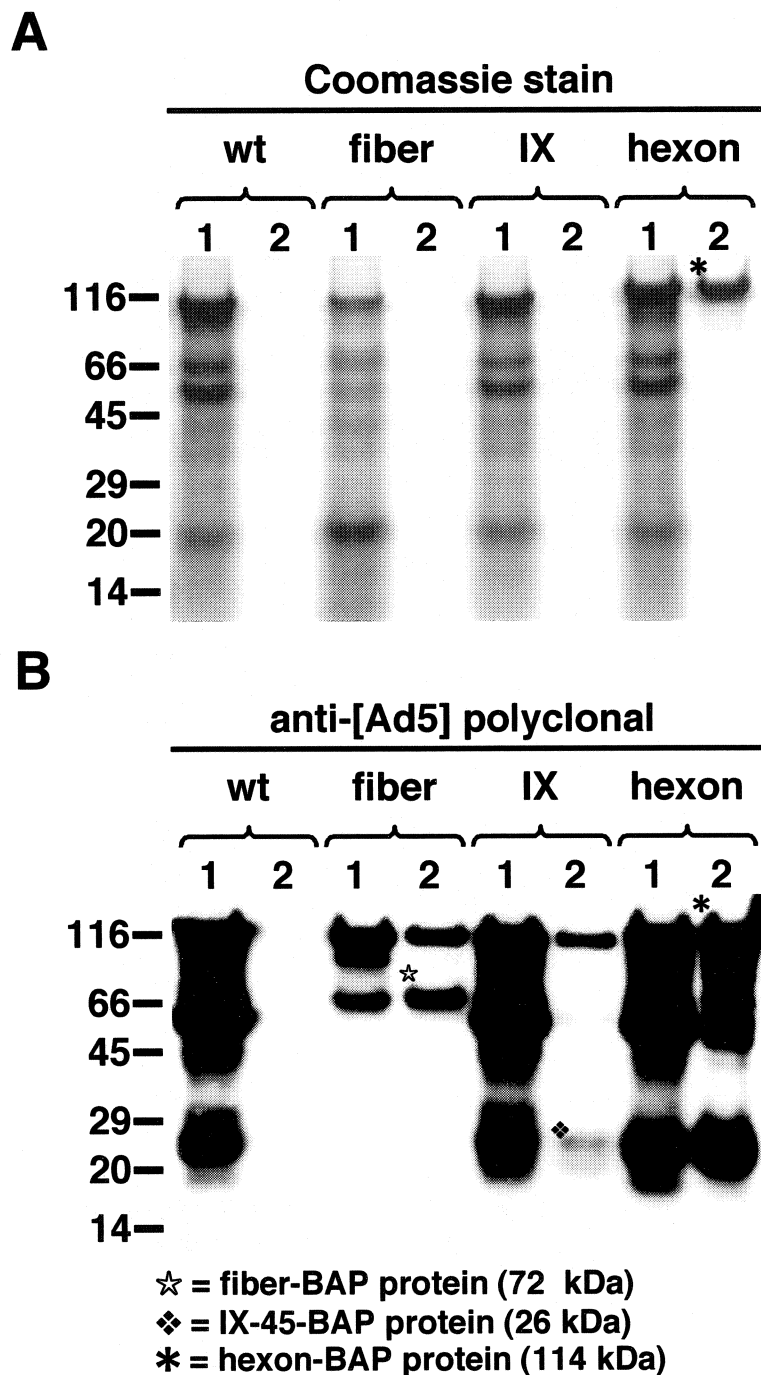


Fig 4.9 SDS-PAGE analysis of input (lane 1) and elution (lane 2) fractions. (A) Coomassie protein staining, note the abundance of hexon-BAP protein in the elution fraction (asterisk). (B) Western blot of the identical gel, note the absence of signal from the Ad-wt elution and the presence of BAP-fusion proteins, marked with symbols, in the elution fractions of metabolically biotinylated vectors.

With the exception of Ad-hexon-BAP, all the elution fractions were too dilute for Coomassie staining. This problem was overcome by 30-fold concentration of the samples with centrifugal ultrafiltration devices, resulting in good Coomassie staining (Fig 4.10). Comparison of the elution fractions to 3×10^9 VP of a CsCl-purified prep of Ad-wt demonstrates that the purity of some of the fractions is close to that of the CsCl method.

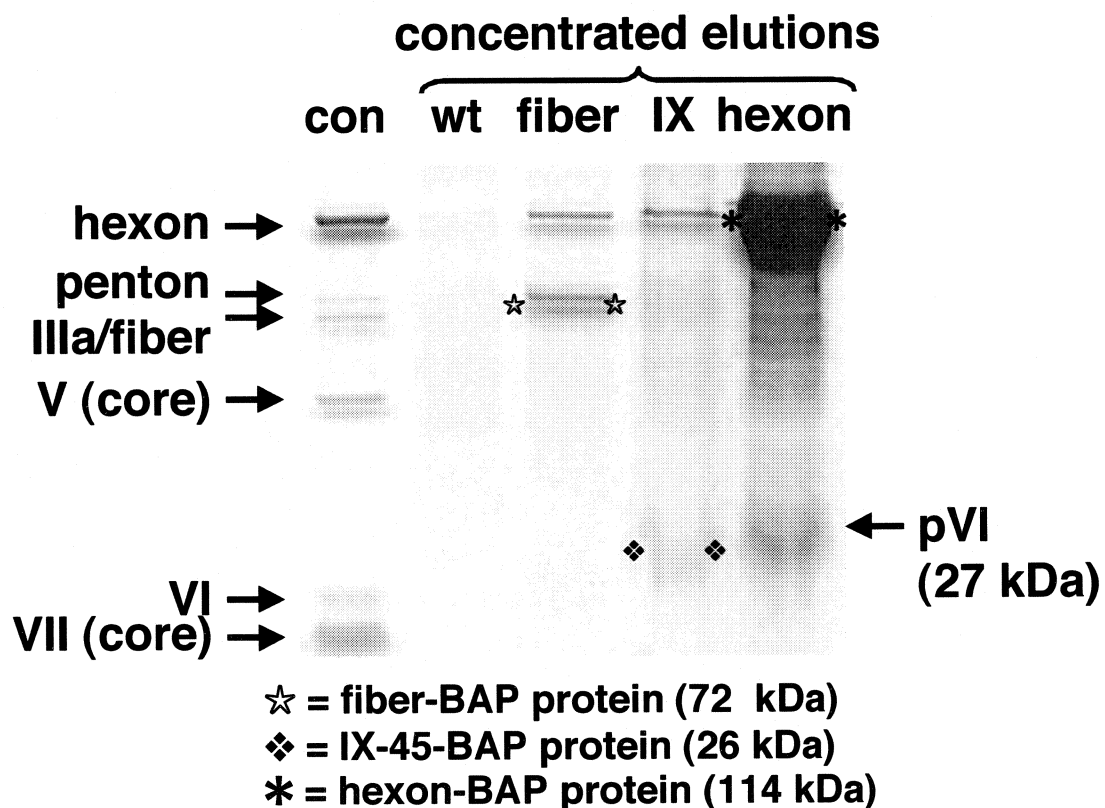


Fig 4.10 Coomassie stained gel of concentrated elution fractions. 3×10^9 VP of a CsCl-purified prep was loaded in the control lane. Note the absence of core protein bands, resulting from contamination by empty capsids. Positions of the free BAP-fusions are marked with symbols.

Despite the absence of the majority of the cellular proteins, one major difference between the CsCl purified sample and the elution fractions is the ratio of the capsid proteins and the notable absence of detectable core proteins, indicative of the presence of

empty capsids. One major disadvantage of affinity methods for adenoviral purification is the inability to separate empty and immature particles from fully assembled infectious virions. Differences in the densities of these populations allows for their separation through a CsCl gradient. Overall, the IX-modified vectors performed best for avidin-based purification. Ad-IX-45-BAP has the highest recovery of bioactivity and elution of Ad-IX-45-BAP results in mainly hexon antigen, along with some excess IX-45-BAP fusion as well as the empty capsid components, skewing the observed ratios. Ad-fiber-BAP also performs well, resulting in a relatively clean elution, except for the large amounts of free fiber-BAP that co-purify and lower the perceived bioactivity. Further separation of the Ad-fiber-BAP elution by dialysis or gel filtration should lead to a fairly pure preparation with good bioactivity. Purification of Ad-hexon-BAP results in the least pure of the elution fractions, containing massive amounts of free hexon-BAP and many smaller species as well. Interestingly, it appears that a large amount of immature pVI (27 kDa) co-purified with the hexon-BAP. pVI functions as a shuttle for the nuclear import of hexon trimers in addition as its role as a capsid protein [176].

4.4 Conclusions

In summary, the addition of the BAP domain into the adenoviral capsid is well tolerated as fusions to the C-termini of both fiber and protein IX, as well as an insertion into the HVR5 surface loop of hexon. The BAP-modified vectors retain infectivity near wild type levels with the exception of Ad-fiber-BAP, which suffers a small but significant decrease in infectivity and CAR-mediated transduction. All BAP modified vectors are metabolically biotinylated during production in 293A cells and they each have different magnitudes of biotin display, correlating well with the known stoichiometry of each modified capsomere within the virion.

The extremely tight interaction between the small molecule biotin and tetrameric avidin ($K_d \approx 10^{-15}$ M) is the basis behind a multitude of commercially available avidin/biotin products. The introduction of covalently attached biotin molecules to the surface of the virions facilitates their use in conjunction with a wide variety of commercially available avidin-based reagents. Physical targeting of refractory cells through magnetic force is demonstrated by complexing the BAP-modified vectors with streptavidin coated paramagnetic particles. Other potential applications could include the use of avidin-based resins to remove helper adenoviruses from preparations of adeno-associated virus (AAV) vectors or the immobilization of intact virions on resins for affinity chromatography applications to identify cellular/serum factors that interact with capsids.

Immobilized monomeric avidin has a reduced affinity for biotin ($K_d \approx 10^{-7}$ M) than tetrameric avidin, enabling its use for the reversible capture and recovery of

biotinylated proteins. Avidin-based purification of metabolically biotinylated vectors therefore represents a potentially valuable alternative to the traditional CsCl-based techniques. All of the BAP-modified vectors specifically bind and elute from the resin with the addition of free biotin. Analysis of the purification reveals that unencapsidated excess biotinylated capsomeres are also purified, which in the case of Ad-fiber-BAP, results in an apparently lower bioactivity upon elution. All elutions contain substantial amounts of empty capsids, as evidenced by the relatively lower amounts of the core proteins in the elution fractions, as compared to CsCl-purified virions. The elution fraction of Ad-hexon-BAP has strong bioactivity, comparable to the input fraction, despite the fact that the large abundance of unencapsidated free hexon protein produced during adenoviral infection of 293 cells results in the contamination of the Ad-hexon-BAP elution with large amounts of free hexon and hexon-associated proteins. The IX-modified vectors perform best overall, with the cleanest elution profiles containing the highest bioactivity. Avidin-based methods could become very useful for the enrichment and purification of large-scale batches of Ad vectors, prior to HPLC and other chromatographic methods. The method also represents a quick and easy alternative to CsCl banding, especially for laboratories without ultracentrifugation capabilities.

Chapter V

Ligand-Targeted Transduction of Metabolically Biotinylated Adenoviral Vectors

Abstract

The utility of the metabolically biotinylated vectors for avidin-based ligand-targeted transduction is explored herein. The panel of BAP-modified vectors has, for the first time, enabled a direct comparison of ligand-targeted transduction through the fiber, protein IX, and hexon capsomeres. Redirection of transduction through the fiber protein is generally efficient and can be mediated through a wide range of cell surface receptors including transmembrane receptors like the transferrin receptor (CD71) and the epidermal growth factor receptor (EGFR), GPI-linked surface proteins like CD59, and glycolipid ganglioside molecules like G_{M1} . Rerouting of vector transduction through the more abundant capsomeres like IX and hexon was generally inefficient and resulted in negligible enhancements of transduction. Although the precise mechanisms behind these differences in vector function are not yet known, they likely involve the dissociation of fibers from the capsid at early times of uptake and trafficking, a major functional difference between the fiber and protein IX/hexon. These results suggest that effective vector targeting by genetic means is only possible through modifications to the fiber protein, the natural cell binding protein of the adenovirus capsid.

5.1 Introduction

Genetic insertion of protein and peptide ligands for the retargeting of adenoviral vectors to new receptors is hampered by the unpredictable nature of the effects of such manipulations. Incorporation of peptides and proteins within the fiber protein often either disrupts the proper folding/trimerization of the fiber or the ligands that are tolerated lose their inherent binding properties [86, 171]. The successful incorporation of the metabolically biotinylated BAP domain into several locales of the Ad capsid provides a unique platform for the avidin-based attachment of a diverse array of cell targeting ligands to the virion surface. The construction of metabolically biotinylated vectors bearing different magnitudes of biotin molecules at different positions on the surface of the adenoviral capsid warranted investigation into their potential for avidin-based, ligand-targeted gene delivery.

Experimentation with several cell lines refractory to Ad5 transduction revealed that biotin display from the surface of the virions does not correlate with their capacity for targeted transduction. Ad-fiber-BAP, with the lowest degree of biotin display, overwhelmingly outperformed the protein IX and hexon modified vectors for targeted gene delivery through multiple ligand-receptor pairs. The observed phenomenon is most likely due to functional differences between the biology of the fiber protein and the other capsomeres during the process of vector transduction. Normally the fiber protein functions as the primary point of cell attachment, and rapidly dissociates from the virion during cellular uptake [59, 103]. This event may be of great importance for the successful trafficking of the virion, as it frees the capsid from its bound receptor and

enabling it to traverse towards the nucleus. Hexon comprises the bulk of the icosahedral particle, so cell binding through this protein could conceivably result in improper trafficking of the virions, preventing transduction. Analysis of the fate of protein IX through fluorescence microscopy and immunoprecipitation experiments with IX-modified vectors suggests that unlike the fiber protein, IX does not rapidly dissociate from the incoming virions during endocytosis, in good agreement with recent biophysical data from another group [89].

Regardless of the reasons behind the inefficient transduction through IX and hexon-modified vectors, Ad-fiber-BAP is an extremely useful platform for ligand screening and the identification of functional targeting ligands compatible with adenoviral transduction, as well as for the direct attachment of ligands to the virion surface through the extremely tight avidin-biotin interaction. This methodology is very useful for targeted transduction through complex ligands like cholera toxin, growth factors, antibodies, and carbohydrate moieties, which cannot be genetically engineered into the Ad capsid.

5.2 Materials and Methods

Ligand-Targeted Transduction of Suspension Cells. K562 erythroid leukemia cells were maintained in cDMEM. 5×10^5 cells were aliquoted into 5 ml round bottom polystyrene tubes and pelleted by gentle centrifugation. Cells were washed twice in 2 ml Hank's balanced salt solution with 1% BSA (HBSS-BSA) and pelleted. Cells were incubated in 250 μ l of a 1:50 dilution of biotinylated cell targeting ligand in HBSS-BSA for 20 min with occasional mixing. Cells were then washed three times in 2 ml HBSS-BSA and incubated in 500 μ l of NeutrAvidin [100 μ g/ml] in HBSS-BSA for 20 minutes. Cells were washed twice in HBSS-BSA and incubated with vectors at an MOI of 5000 VP/cell for 20 minutes. Cells were then washed 3 times in HBSS-BSA and plated in 1 ml cDMEM at 37 °C. All washes and incubations were performed at 4 °C. All concentrations of ligands and avidin were at saturating levels. Transduction was assessed 24-48 hours later by fluorescence microscopy and/or flow cytometry. All fluorescent micrographs depicting cellular dsRed expression are representative of the entire sample and were collected with identical exposure times and gain levels.

Ligand-Targeted Transduction of Adherent Cells. Adherent cells (A431, C2C12, and SkBr3) were plated in 24 well plates and grown overnight in the appropriate growth medium. Cells were washed twice in HBSS-BSA and incubated in 250 μ l of various ligands diluted 1:50 in HBSS-BSA as described above. Cell monolayers were thoroughly washed and incubated with excess avidin in 250 μ l as described above. Cell monolayers were washed again and incubated with Ad vectors at various MOI's in 250

μl, as described above. After thorough washing, cell monolayers were rescued with complete media and incubated at 37 °C. All washes and incubations were done at 4 °C. Transduction was assessed 24–48 hours later by fluorescence microscopy and/or flow cytometry. All fluorescent micrographs depicting cellular dsRed expression are representative of the entire sample and were collected with identical exposure times and gain levels. A431 transduction (Fig 5.2) was quantitated by measuring the overall transduction (MFI) or transduction efficiency (% positive cells) of each vector/ligand combination relative to their corresponding values with non-targeted transduction. Data expressed as mean values of three independent experiments ± standard deviation.

Tracking of Targeted Transduction. Ad-fiber-BAP and Ad-IX-BAP (5×10^{11} VP) were labeled with Alexafluor-555 succinimidyl ester at 40 μg dye per 10^{12} virions, as recommended by the manufacturer (Molecular Probes). Excess dye was removed by banding on a CsCl gradient. Banded vector was desalted and stored at –80 °C in A195 buffer. Addition of the 555 fluorescent label caused no significant decreases in transduction on HeLa cells. C2C12 cells were sparsely plated in permanox 4-chamber slides and attached overnight. Cells were targeted with indicated ligands as described above, and shifted to 37 °C for 0 or 45 min to allow uptake of 555-labelled vector. Cells were then washed extensively to remove unbound vector and samples were processed for fluorescent microscopy as described below.

Construction of Ad-IX-45-EGFP. The enhanced green fluorescent protein (EGFP) gene from pEGFP-N1 (Clontech) was PCR amplified with EGFP5'A (TTGCTC

CTGACCGGTGGCATGGTGAGCAAGGGCGAGG) and EGFP3'C (CCATCGATGGT TACTTGTACAGCTCGTC) and the product was gel-purified and digested with *AgeI* and *ClaI* (sites underlined) overnight at 37 °C. Digested product was purified and cloned into the *AgeI/ClaI* sites of pIX-display, resulting in the fusion of the IX-45 coding sequence with the EGFP gene. The resulting pIX-45-EGFP construct was digested with *Acc65I*, *BglII*, and *PvuI*, and the large fragment was recombined into pAd-dsRed using Red recombination, as described in chapter 3. Removal of the Zeo^R marker by FLP-mediated excision resulted in pAd-dsRed-IX-45-EGFP, which was linearized with *PacI* and transfected into 293A cells to produce Ad-IX-45-EGFP. Vector fluorescence is readily visible upon CsCl banding and illumination with an ultraviolet lamp (Fig 5.5A).

Tracking Ad-IX-45-EGFP. HeLa cells were sparsely plated in permanox 4-chamber slides and grown overnight in cDMEM. Cells were washed once in HBSS-BSA and incubated with 10¹⁰ VP of Ad-IX-45-GFP diluted in 250 µl HBSS-BSA for 30 min at 4 °C. Cells were washed three times in HBSS-BSA and incubated in cDMEM for 30 min at either 37 °C to allow endocytic uptake and trafficking, or 4 °C to prevent uptake. Cells were then fixed, stained, and imaged as described below. High MOI was necessary to visualize the EGFP signal of the internalized vector.

Fluorescence Deconvolution Microscopy. Samples, plated in permanox 4-chamber slides, were thoroughly washed in PBS and fixed in 10% formalin for 20-30 minutes at 4 °C. Samples were washed once in PBS plus 30 mM glycine and twice in PBS at room temperature prior to mounting. For actin staining, samples were

permeabilized in PBS plus 0.1% Triton X-100 for 5 min at room temperature, followed by a PBS wash and a 30 min block in PBS plus 2% BSA at room temperature. Samples were then stained with Texas-Red conjugated phalloidin (Molecular Probes) diluted in PBS-BSA for 20 min at room temperature. Samples were washed twice in PBS and mounted in VectaShield containing DAPI (Vector Laboratories). Specimens were visualized at 100x magnification under oil immersion with a Zeiss Axioplan II fluorescence microscope using the appropriate filter sets. Images were processed using the MetaMorph software package and deconvolution was performed using the “no neighbors” algorithm.

Immunoprecipitation of Trafficking Ad-IX-BAP. HeLa cells were gently detached with cell dissociation buffer (Gibco) and 5×10^5 cells were aliquoted into 5 ml round bottom polystyrene tubes. Cells were washed once in cold cDMEM and all subsequent steps were performed at 4 °C. Ad-IX-BAP vector (5000 VP/cell) was bound to the cells for 2 hours, followed by two washes in cDMEM to remove unbound vector. Cells were resuspended in 500 μ l cDMEM and shifted to a 37 °C water bath for various times (0, 5, 10, 15, 30, 45, 60, 90 minutes) to allow internalization and trafficking. Samples were shifted back to 4 °C and washed twice in cold serum-free DMEM. Cells were incubated in 250 μ l cold trypsin (0.25%) for 1.5 hours to digest any surface virus that failed to endocytose. Cells were washed twice with cold cDMEM and once with cold PBS. Cells were lysed in 750 μ l cold immunoprecipitation lysis buffer (IPLB; 30 mM Tris-HCL, 20 mM MES, 100 mM NaCl, 0.5% Empigen BB zwitterionic detergent, 1 x Roche complete protease inhibitor, pH = 7.5) for 20 min with occasional mixing.

Lysates were collected and combined with 20 μ l protein A/G sepharose (Sigma) in microfuge tubes to preclear the lysate (remove any non-specific binding proteins). Lysates were precleared for 1 hour with gentle mixing on a nutator. Resin was pelleted and supernatant was transferred to new tubes, combined with 20 μ l fresh protein A/G sepharose and 5 μ g mouse anti-[hexon] clone 8C4 (Abcam). Samples were mixed well and incubated for 2 hours on a nutator. Resin was pelleted, washed twice with IPLB, once with PBS and eluted with SDS-PAGE loading buffer. Samples were denatured at 95 °C and stored at -20 °C prior to SDS-PAGE and western blotting, as described earlier. Band intensities of the fiber and IX-BAP signals at each timepoint were quantified by densitometry on a Storm phosphoimager/densitometer. Ratios of the intensities of fiber bands relative to IX were calculated for each timepoint and plotted, with the earliest timepoint representing 100%.

Ad-fiber-BAP/CTx-B complexing. Ad-fiber-BAP, expressing firefly luciferase (Luc) and humanized *Renilla* GFP (hrGFP) from a bicistronic CMV-driven transcript containing an internal ribosome entry site (IRES) element, was propagated on 293A cells and crude lysate was loaded onto a large CsCl gradient as previously described. After the first CsCl gradient, vector was split into equal fractions and each was diluted to 4 ml in 50 mM Tris, pH = 8. Saturating amounts of tetrameric NeutrAvidin (1.8 mg per 10^{12} VP, corresponding to a 500:1 molar ratio of avidin to capsid biotin, assuming 36 biotins/virion) was included in one of the fractions and the samples were incubated for 30 min at 4 °C with occasional mixing. The two 4 ml fractions were loaded onto a second CsCl gradient and spun at 20,000 rpm for three hours. Bands were collected with an 18

gauge needle and the samples were diluted to 4 ml with buffer as before. Excess biotin-CTx-B (Sigma) was included in the sample containing avidin, again at saturating levels (0.36 mg Ctx-B per 10^{12} VP, corresponding to a 100:1 molar ratio of Ctx-B to capsid biotin, assuming 36 biotins per virion). Samples were incubated for 30 min at 4 °C with occasional mixing to allow complex formation. Samples were then banded in a third CsCl gradient and bands were collected and desalted in a DG-10 column (BioRad). Vectors were stored at 4 °C in A195 buffer. Complex formation was shown by western blot of 10^9 VP, probed with anti-[hexon] antibody, anti-[avidin] antibody, and avidin-HRP to demonstrate presence of avidin and biotin-CTx-B on the virions. Ad-IX-BAP was complexed to biotinylated transferrin (Molecular Probes) in a similar manner tested for CAR-mediated transduction on HeLa cells as previously described.

CTx-B Complex Transduction. C2C12 cells were plated and grown to confluence in cDMEM in 24 well plates. Cells were allowed to partially differentiate into myotubes by serum starvation for 10 days. Myotubes were incubated at 37 °C with Ad-fiber-BAP or Ad-fiber-BAP/CTx-B complex for 90 minutes in a minimal volume of serum-free DMEM prior to the addition of 1 ml cDMEM. Transduction was assessed 36 hours later by fluorescence microscopy for hrGFP expression or by luciferase assay. All fluorescent micrographs depicting cellular hrGFP expression are representative of the entire sample and were collected with identical exposure times and gain levels.

Luciferase Assay. Cell monolayers were washed twice in PBS and overlaid with 1 x reporter lysis buffer (Promega). The plates were then frozen at -80 °C and

thawed to disrupt the membranes. Lysates were collected in microfuge tubes and vortexed to mix. Samples were pelleted and aliquots of the supe were assayed for protein content by BCA assay, according to the manufacturer's recommendations [80] and for luciferase activity according to the manufacturer's protocol (Promega). Results of triplicate experiments are reported as mean relative light units per mg protein (RLU/mg) \pm standard deviation.

5.3 Results and Discussion

Biotin Display Does Not Correlate with Targeted Transduction

The display of biotin molecules on the surface of the Ad virion enables conjugation to various biotinylated ligands through a tetrameric avidin bridge. The construction of the panel of metabolically biotinylated BAP-modified vectors allows for the direct comparison of transduction through different Ad capsid proteins. These experiments were initiated with the notion that the redirection of transduction through protein IX and hexon might allow for more efficient avidin-dependent, ligand-targeted transduction than Ad-fiber-BAP, given that Ad-IX-BAP, Ad-IX-45-BAP, and Ad-hexon-BAP display significantly higher numbers of avidin-accessible biotin molecules than the fiber-modified vector. CAR-negative K562 cells, normally refractory to transduction by Ad5 vectors, were first used to test whether biotin display correlates with transduction capability. K562 cells express high levels of cell surface CD59, a glycosyl phosphatidyl inositol (GPI) linked complement regulatory protein, as well as CD71, the transferrin receptor. Cells were labeled by saturation with biotinylated antibodies against CD59 and CD71, as well as the cognate ligand transferrin, followed by extensive washing and saturation with avidin, thereby converting cell surface CD59 and CD71 into potential Ad vector receptors through the extremely strong avidin-biotin interaction. Cells were then incubated with metabolically biotinylated vectors and transduction was assessed 48 hours later by fluorescence microscopy. Surprisingly, the qualitative data (Fig 5.1) reveals that while K562 cells are transduced through a variety of ligand-receptor pairs with Ad-fiber-BAP, transduction is not permitted through protein IX and hexon. Inclusion of the 45 Å

spacer peptide, which boosted biotin accessibility by 2-fold, had no effect on ligand-targeted transduction. Controls without avidin or using a non-specific biotinylated IgG isotype antibody result in no enhancement of transduction.

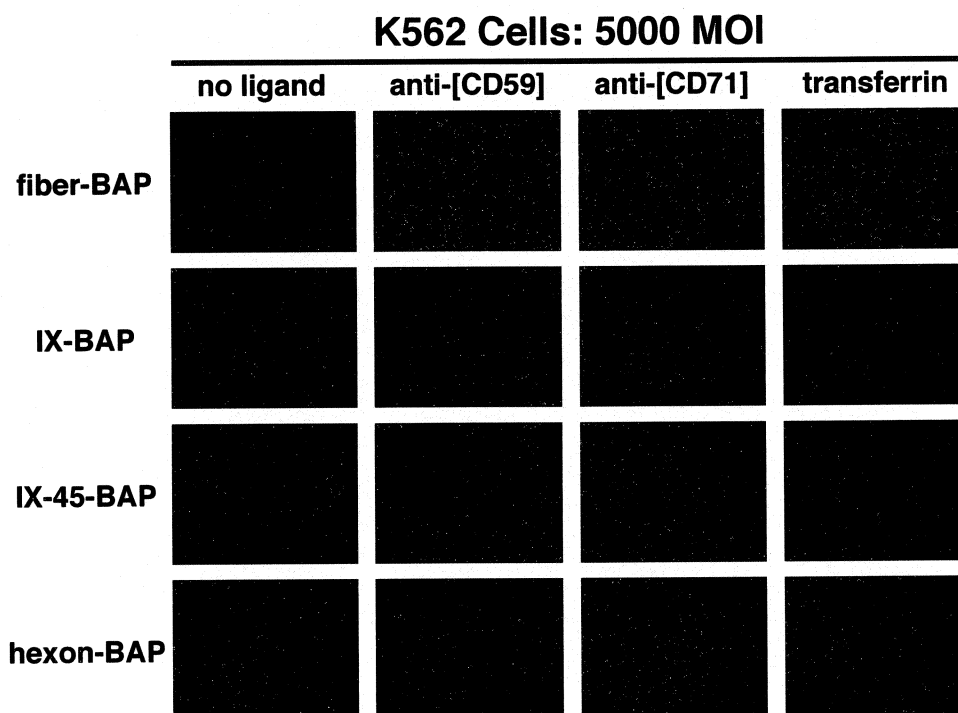


Fig 5.1 Comparison of targeted transduction of refractory K562 cells through antibody and protein ligands. Cells were transduced with the indicated ligands and cellular dsRed expression was visualized by fluorescence microscopy 48 hours post transduction.

A431 cells, another CAR-negative refractory human cell line, were similarly tested for ligand-targeted gene delivery. A431 cells express very high levels of the epidermal growth factor receptor (EGFR), in addition to moderate levels of CD59 and CD71. Transduction of metabolically biotinylated Ad vectors was evaluated using biotinylated epidermal growth factor (EGF), CD59, CD71, and transferrin as targeting ligands, as described above. Quantification of dsRed expression by flow cytometry again

reveal that avidin-based transduction through the fiber protein is efficient with a wide variety of ligand-receptor pairs. Ligand-targeted delivery in this manner typically results in 30-50 fold enhancement of transduction efficiencies, leading to 40-60 fold increases in overall transduction levels as measured by total fluorescence (Fig 5.2). As before, redirection of transduction through the more abundant protein IX or hexon results in low levels of transduction with all ligands tested.

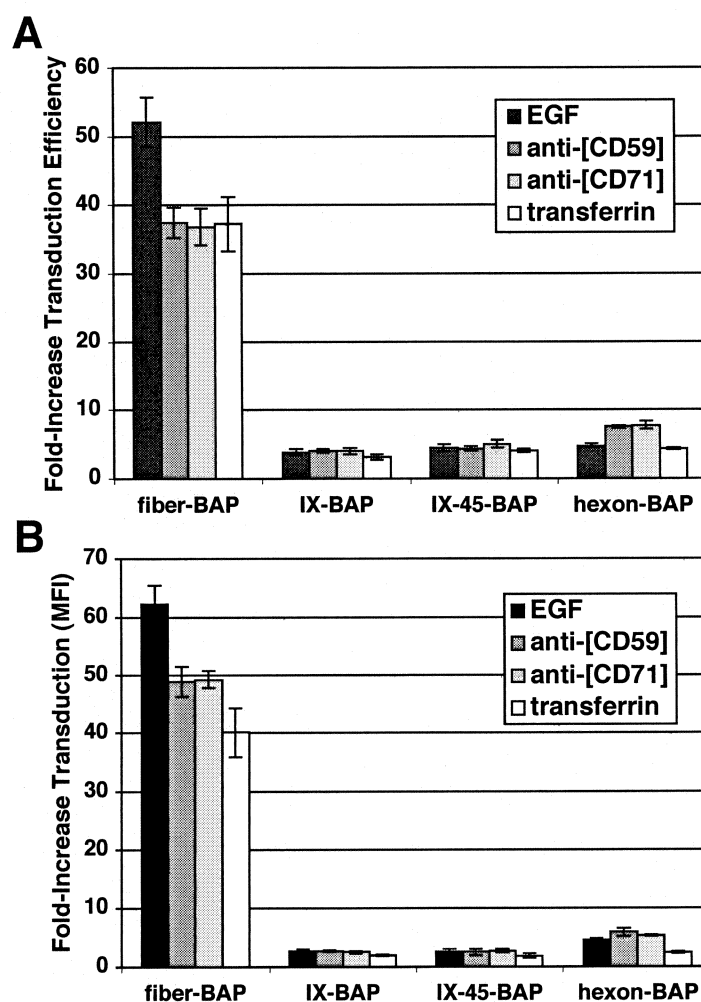


Fig 5.2 Comparison of targeted transduction of A431 cells with protein and antibody ligands. Quantification of the fold-increase in transduction efficiency (**A**) and the fold-increase in dsRed fluorescence (**B**) as compared to untargeted vectors.

Additional experiments were performed on partially differentiated murine C2C12 myoblasts. This cell line, derived from mouse skeletal muscle, is low for CAR expression and can be differentiated by serum deprivation, leading to the fusion of cells into multinucleated fibers, reminiscent of muscle tissue. Cultures of these myotubes were established and transduced with the BAP-modified vectors. Flow cytometry of labeled myoblasts had previously shown that these cells express high levels of ganglioside G_{M1} and stain brightly with the cholera toxin B subunit (CTx-B). These cells also stain positive for CD71. As before, transduction of Ad-fiber-BAP is improved when targeted through either receptor, although higher levels of vector are required for efficient transduction through CD71. Transduction of Ad-fiber-BAP through Ctx-B was very efficient, resulting in transduction of nearly 75% of the cells and high levels of fluorescent reporter. In contrast, transduction of IX and hexon-modified vectors is strikingly low when redirected through CTx-B, even at the higher MOI. Surprisingly, comparable levels of transferrin-mediated transduction are obtained through all BAP-modified vectors at the higher MOI (Fig 5.3).

Additional studies with refractory SkBr3 cells again demonstrate that while targeted transduction through the fiber protein is possible with a wide variety of cell surface receptors, transduction mediated through capsomeres other than fiber is generally inefficient. Table 5.1 emphasizes this trend and provides a summary of results obtained for multiple cell types using a variety of ligands. One exception to this trend appears to be the transduction through the transferrin receptor. For certain cell types, transferrin mediated transduction is equivalent for all BAP-modified vectors tested. In the case of mouse C2C12 cells, the vectors could be targeted through either the natural ligand

transferrin or a monoclonal antibody against murine CD71. For the human cell lines, the monoclonal antibody against human CD71 only worked with Ad-fiber-BAP, failing to enhance transduction when bound through protein IX or hexon.

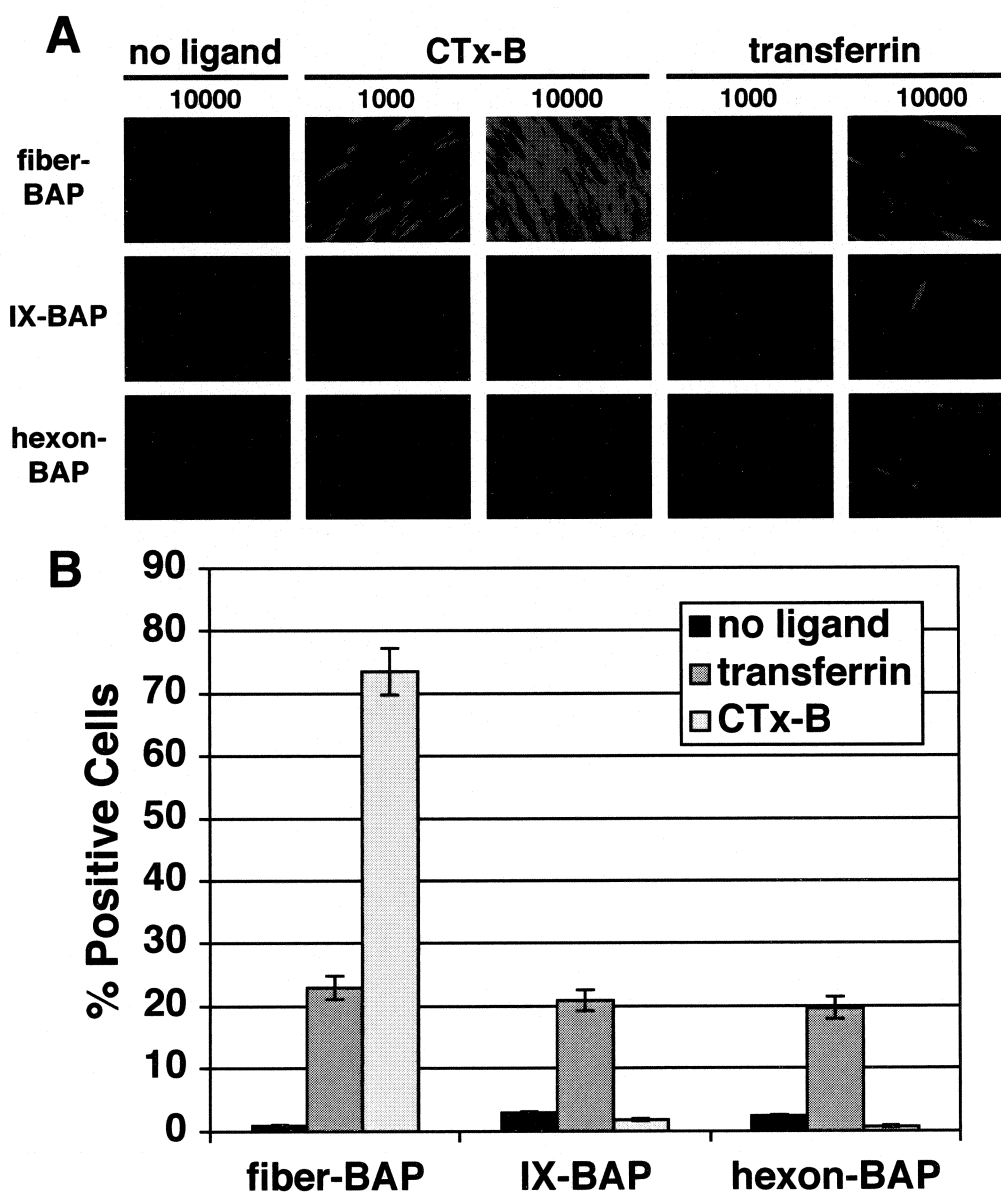


Fig 5.3 Targeted transduction of murine C2C12 myotubes with CTx-B and transferrin. (A) Fluorescence microscopy of myotubes transduced with the indicated MOI of vector. (B) Transduction efficiency of the cells transduced at 10,000 VP/cell as measured by flow cytometry.

Table 5.1 Summary of BAP Vector Targeting Results*

Target Cell	Ad-fiber-BAP	Ad-IX-BAP	Ad-hexon-BAP
A431			
anti-[CD59]	+	-	-
anti-[CD71]	+	-	-
transferrin	+	-	-
EGF	++	-	-
C2C12			
anti-[mCD71]	+	+	+
transferrin	+	+	+
cholera toxin B	+++	-	-
EGF	-	-	-
K562			
anti-[CD59]	+++	-	-
anti-[CD71]	+++	-	-
transferrin	+++	-	-
SkBr3			
anti-[CD59]	++	-	n.d.
herceptin	++	-	n.d.
anti-[CD71]	++	-	n.d.
transferrin	++	++	n.d.
EGF	-	-	n.d.

* untargeted transduction typically resulted in $\leq 5\%$ positive cells, with “+”, “++”, and “+++” representing efficiencies of 10-33%, 33-66%, and 66-90% positive cells as measured by flow cytometry, n.d. not determined.

In an attempt to further investigate the differences in transduction through fiber or protein IX, CTx-B targeted binding and trafficking was analyzed by fluorescence microscopy. C2C12 blasts are extremely adherent and provide a suitable model system that can withstand the multiple washes/incubations required for this type of experiment. Purified Ad-fiber-BAP and Ad-IX-BAP virions were covalently labeled with amine-reactive Alexafluor 555 succinimidyl ester, a bright orange/red fluorophore. 555-labeled vectors were separated from the excess free dye by CsCl banding and desalting through a 10 kDa size exclusion column. There were no significant differences in infectivity

between the fluorophore conjugated and unlabeled vectors. C2C12 blasts, plated on microscope chamber slides were targeted for CTx-B-mediated transduction with the 555-labeled vectors. Half of the samples were maintained at 4 °C to visualize binding and the other half of the samples were shifted to 37 °C for 45 minutes to observe intracellular trafficking of the vectors. Samples were then fixed, stained with DAPI, and visualized by fluorescence microscopy.

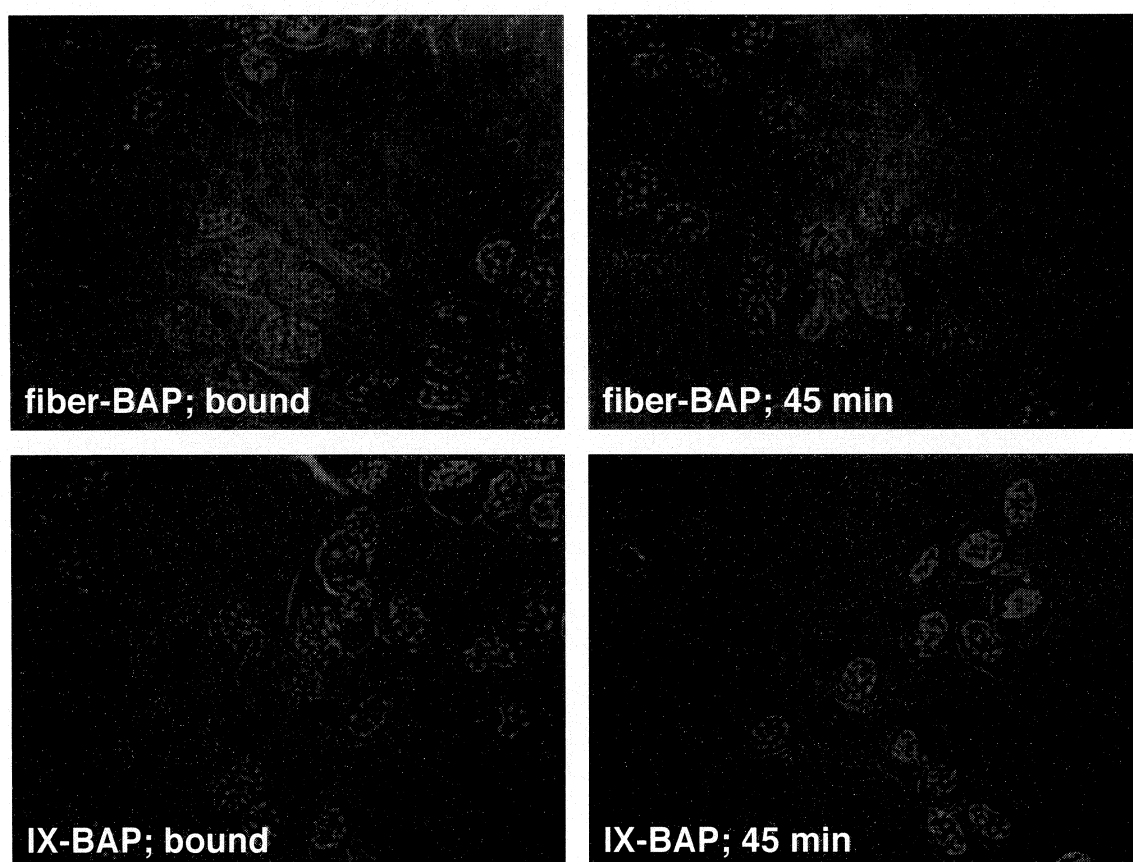


Fig 5.4 Fluorescence deconvolution microscopy of the binding and internalization of AlexaFluor 555-labeled vectors (red) through CTx-B on C2C12 myoblasts. Nuclei were stained with DAPI. Original magnification was 100x.

At the initial timepoints, 555-labeled vector particles are present across the cell surface, indicative of vector binding through CTx-B. Shifting the temperature to 37 °C

for 45 minutes results in the accumulation of Ad-fiber-BAP at the nuclear periphery, while targeting Ad-IX-BAP through CTx-B leads to altered trafficking, with accumulation of 555-labeled vector as bright aggregates within and sometimes seemingly on the surface of the C2C12 cells (Fig 5.4). Clearly this altered trafficking pattern leads to non-productive infection, as Ad-IX-BAP fails to transduce the C2C12 cells through CTx-B (Fig 5.3).

These experiments clearly show that avidin-based redirection of adenoviral transduction through biotinylated ligand-receptor interactions is greatly dependent on the nature of the BAP-modified capsomer. While transduction of Ad-fiber-BAP can be targeted to refractory cells through a wide variety of ligand-receptor pairs, Ad-IX-BAP and Ad-hexon-BAP are surprisingly inefficient as targeting platforms, despite having a higher display of biotins than Ad-fiber-BAP. Some of these observed differences in transduction might be explained by fundamental aspects of adenoviral capsid biology as well as the properties of specific receptor-ligand interactions. The versatility of Ad-fiber-BAP may be due in part to the inherent biology of the fiber protein and the early events of Ad trafficking during vector uptake and endocytosis. Adenovirus binds its natural receptor, CAR, with high affinity through interaction with its knob domain, located at the very end of the molecule, extended away from the icosahedral capsid. Once bound, vectors are taken up into early endosomes. The natural process of endosomal acidification acts as a trigger, causing a conformational change in the capsid, ultimately resulting in endosomal lysis and escape. Previous work [59] has shown that ~90% of the fiber molecules are released within the first 10 minutes of uptake during these early stages of trafficking. This process of fiber dissociation may function to release the virion

from CAR, thereby allowing the capsid to continue with normal cytoplasmic trafficking, dynein-mediated microtubule association [75], and docking at the nuclear pores [152].

Ad-fiber-BAP binding and transduction with exogenous ligands might be tolerated so well because the fiber-BAP proteins naturally dissociate from the capsid upon uptake, allowing the vector to escape from its bound receptor, whether its CD59, CD71, ganglioside G_{M1} or EGFR. Protein IX normally functions as a capsid cement [124] and may remain tightly associated with the capsid during uptake and trafficking, unlike the fiber protein. Receptor binding and uptake through protein IX or hexon might therefore result in entrapment of the vector on its bound receptor, leading to altered trafficking possibly resulting in the recycling of virions back to the cell surface or retention of the vector in endosomes and eventual destruction of virions in lysosomes. Indeed, Ad-*ts1*, a temperature sensitive mutant adenovirus fails to release its fibers and is eventually degraded in lysosomes [167, 173].

The success of transferrin, a ligand that seems to work with IX or hexon-modified virions in certain cell types, may be due to the specific biology of the transferrin-CD71 interaction. Transferrin naturally binds CD71 and is taken up through classical clathrin-dependent endocytosis. Bound transferrin naturally releases iron in response to endosomal acidification, near pH 5.5. Ad virions also sense this drop in pH and respond by lysis of the endosome and eventual neutralization of the pH as the endosomal contents are diluted into the cytoplasm. If Ad-IX-BAP is attached to membrane bound CD71 through apotransferrin (iron has released), the neutralization of pH caused by endosomal disruption could conceivably cause apotransferrin to release from CD71, an event that normally occurs at the cell surface and functions as part of the transferrin recycling and

iron uptake mechanisms of the cell [172]. Interestingly, the monoclonal antibody against mouse CD71 was just as effective as transferrin for targeting of Ad-IX-BAP and Ad-hexon-BAP in C2C12 cells while the monoclonal against human CD71 failed and only transferrin was effective for the targeting of SkBr3 cells. These differences could be attributable to different binding affinities towards the transferrin receptor. If the anti-[human CD71] monoclonal binds very tightly it may not release like transferrin during uptake. On the other hand, if the anti-[mouse CD71] monoclonal binds with less affinity or is sensitive to acidification, the antibody may dissociate from CD71 during uptake, enabling targeted transduction. These speculations require further experimentation to fully explain the puzzling observations.

Tracking Protein IX During Vector Uptake

The proposed vector entrapment hypothesis assumes that protein IX stays associated with the icosahedral hexon capsid throughout the course of uptake and trafficking. Review of the literature provides conflicting data on this matter, with some reports describing the release of IX within the first 30 minutes [59] while others describe its release at later times of 45-60 minutes, when the majority of the virions have already reached the nucleus [89]. Ad-IX-45-EGFP, a new fluorescent vector, was constructed to directly monitor the fate of IX during vector uptake and trafficking. Green fluorescent protein was fused to the C-terminus of protein IX through the 45 Å spacer using the pIX-display shuttle plasmid and Red recombination, as described in chapter 3. Fluorescence of the vector is readily apparent upon CsCl density gradient banding (Fig 5.5A), demonstrating encapsidation of the IX-45-EGFP fusion protein. Thermostability studies

reveal no significant differences between wild type vectors and Ad-IX-45-EGFP, indicating complete incorporation and proper functionality of the IX-45-EGFP fusion within the capsid. Addition of the large ~27 kDa EGFP to the capsid has no major effects on vector infectivity as demonstrated by plaque assay (data not shown). HeLa cell infections were set up on microscope slides to visually monitor where the green fluorescence of protein IX accumulates during the natural route of infection. Initially, green fluorescence is observed along the cell surface, but by 30 minutes post infection the fluorescence is localized around the cell nucleus (Fig 5.5B). These results suggest that by 30 minutes post-infection, protein IX has reached the nucleus in a manner similar to that of fluorescently labeled capsids (Fig 5.4). It is not known whether this perinuclear fluorescence is due to free protein IX that has dissociated from the incoming virions or whether it is still in fact capsid-bound.

An immunoprecipitation experiment was designed to determine whether or not protein IX stays bound to the trafficking Ad virion. Since hexon comprises bulk of the icosahedral capsid and does not release until complete disassembly at the nuclear pores [152], capture of intracellular trafficking virions with an anti-[hexon] antibody allows for the detection of virion-bound IX and fiber by western blotting. Relative levels of virion-bound IX and fiber could then be compared over time to determine the status of protein IX during the process of virion uptake and trafficking.

HeLa cells were infected for various times with Ad-IX-BAP, after which the cells were gently lysed with detergent and capsids were immunoprecipitated with an anti-[hexon] antibody and protein A/G sepharose. Trypsin was used to destroy any cell surface virions that had failed to endocytose prior to the immunoprecipitation. The

protein A/G resin was washed multiple times and bound proteins were analyzed by SDS-PAGE and western blot. The presence of capsid associated IX-BAP fusion on the blot was probed by detection with avidin-HRP. The results (Fig 5.5C) demonstrate that protein IX clearly remains associated with the hexon capsid at and beyond the 30 minute time point, in agreement with its natural role as a capsid cementing protein. The levels of IX-BAP increase within the first 15 minutes, in good agreement with the measured time for adenoviral endocytosis [59], and appear reach a steady state after 15 minutes of trafficking. Probing of the same blot with anti-[fiber] reveals that the fiber protein is also present at low levels at all time points measured (Fig 5.5C). These levels remain constant and reflect the steady state balanced by the continual uptake of new virions and the subsequent release of the fibers during trafficking. Measurement of the ratios of the fiber signal to the IX signal at each time point (Fig 5.5D) reflect the overall decrease in the levels of fiber with respect to IX, indicative of fiber dissociation during uptake.

Taken together, the visual fluorescence microscopy with Ad-IX-45-EGFP and the immunoprecipitation data with Ad-IX-BAP strongly suggests that protein IX does not release from the capsid during trafficking. The inability of protein IX and hexon to release from the virion during vector uptake and transport may lead to altered trafficking of the vector, resulting in poor transduction when receptor binding is redirected through these capsid proteins.

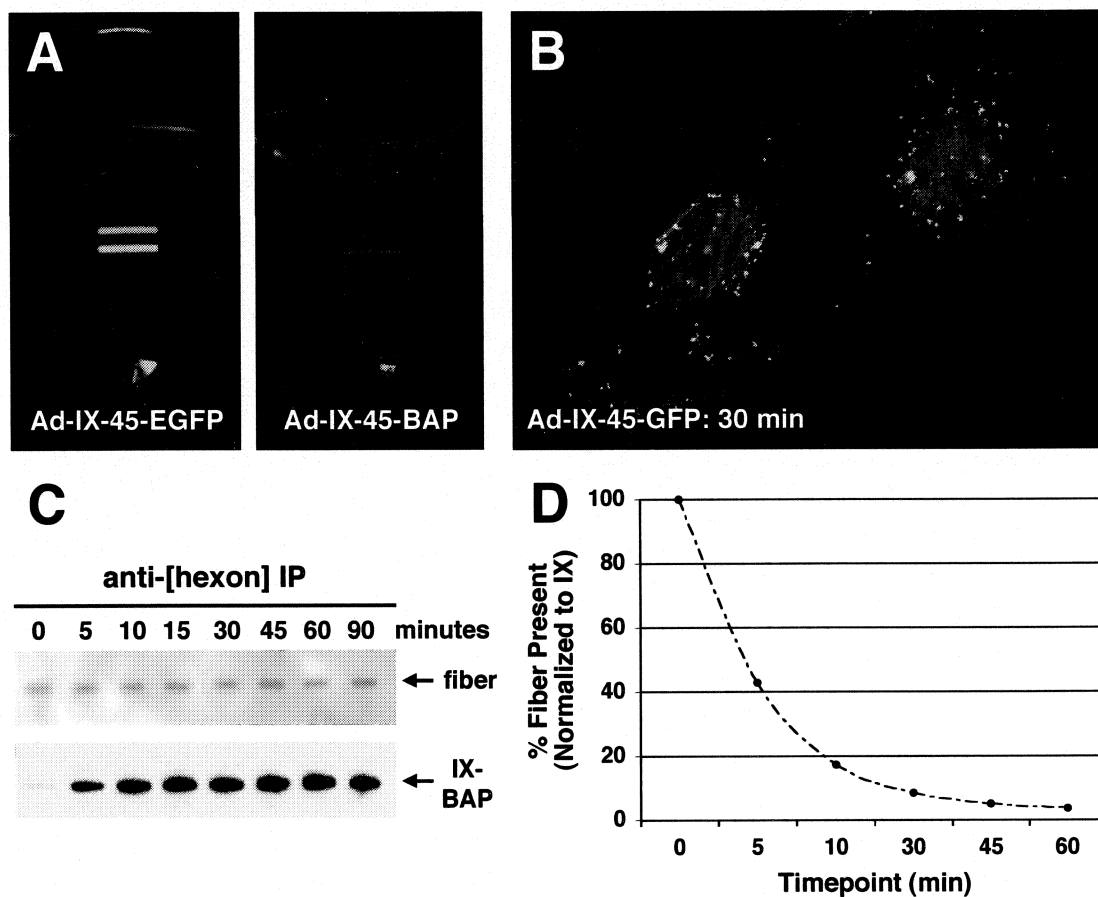


Fig 5.5 Protein IX stays associated with the virion during cellular uptake and trafficking. **(A)** CsCl banding of fluorescent Ad-IX-45-EGFP (left), bottom band is infectious virions. No fluorescence is seen with CsCl banded Ad-IX-45-BAP (right). **(B)** Intracellular trafficking and perinuclear accumulation of Ad-IX-45-EGFP (green) 30 minutes post transduction in HeLa cells. Actin was stained with Texas-Red labeled Phalloidin (red) and the nucleus was stained with DAPI (blue). Original magnification was 100x. **(C)** Analysis of Ad-IX-BAP trafficking by immunoprecipitation with an anti-[hexon] antibody. Virions captured at each timepoint were blotted and probed with anti-[fiber] or avidin-HRP to detect the IX-BAP fusion. No capture was observed with non-specific isotype antibody. **(D)** Plot of the relative band intensities between fiber and IX as a function of time, intensities quantified by densitometry.

Complex Formation and Targeting

Previous vector targeting experiments utilized a layering approach as a quick method for screening ligands for the targeted transduction of various refractory cell types. While this method is good for the identification of ligands and receptors through which

Ad vector transduction can be mediated, it is not useful for *in vivo* applications. The direct use of any BAP-modified vectors for the delivery of actual therapeutic genes *in vivo* will require the preassembly of vector-ligand complexes prior to administration. The feasibility of this approach was tested by complexing Ad-fiber-BAP to biotinylated CTx-B through tetrameric avidin. The combination of Ad-fiber-BAP and CTx-B was chosen because of the greatly enhanced levels of transduction obtained with C2C12 target cells using the layering approach (Fig 5.3). Ad-fiber-BAP, encoding a bicistronic luciferase/hrGFP expression cassette, was amplified in 293A cells and CsCl purified. Complex formation was accomplished by saturation with tetrameric avidin, followed by CsCl banding to separate virions from free proteins. This process was repeated with biotinylated CTx-B and the final bands were collected and desalted through a 10 kDa size exclusion column. SDS-PAGE and western blotting of the complex (Fig 5.6A) shows that both avidin and CTx-B are physically bound to the Ad-fiber-BAP vector particles.

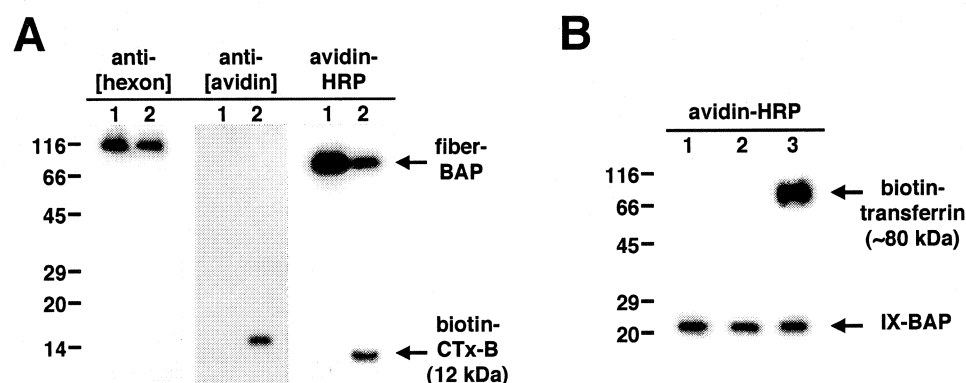


Fig 5.6 Complexing of BAP-modified vectors to targeting ligands. **(A)** Western blot of Ad-fiber-BAP (lane 1) and Ad-fiber-BAP/avidin/CTx-B complex (lane 2). **(B)** Western blot of Ad-IX-BAP (lane 1), Ad-IX-BAP/avidin complex (lane 2) and Ad-IX-BAP/avidin/transferrin complex (lane 3). 10^9 vector particles loaded per lane.

Cultures of C2C12 myotubes were established and used to test the transduction of the Ad-CTx-B complex versus unmodified Ad-fiber-BAP. Fluorescence microscopy of the transduced myotubes (Fig 5.7A) clearly shows enhanced transduction efficiency and hrGFP expression with the CTx-B complex over that of native Ad-fiber-BAP, at the two MOI's tested. Quantification of the data by luciferase assay (Fig 5.7B) reveals that complexing with CTx-B increases luciferase activity by a full log over unmodified vector.

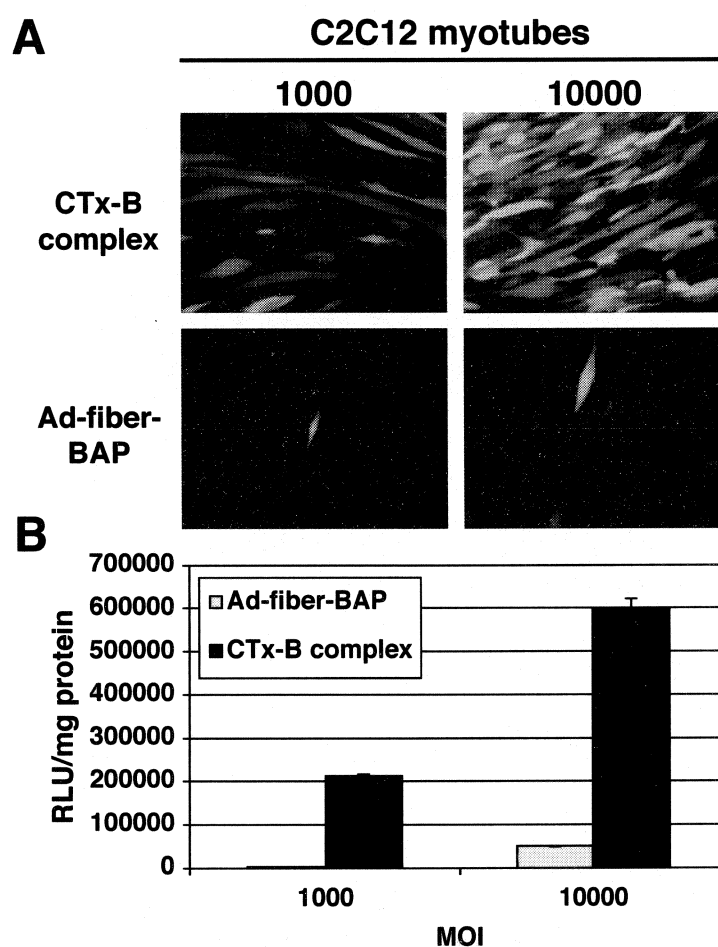


Fig 5.7 Transduction of C2C12 myotubes by Ad-fiber-BAP/CTx-B complexes. **(A)** Fluorescence microscopy of transduced cells expressing hrGFP. **(B)** Quantification of transduction by luciferase assay.

This data indicates that complexing of Ad-fiber-BAP to cell-targeting ligands through the avidin-biotin interaction is possible and can result in substantial increases in vector transduction over untargeted vectors. This methodology could be extremely useful for the targeting of Ad vectors with complex ligands like carbohydrates or disulfide-linked proteins (i.e. antibodies and growth factors) that cannot be genetically engineered into the adenoviral capsid. Recent work by others in the laboratory demonstrates that ligands including the clinically approved monoclonal antibody Herceptin® and mannosylated BSA can also be successfully complexed to Ad-fiber-BAP for the transduction of Her-2 positive breast cancer cells and antigen presenting cells respectively.

Earlier data shows that transduction through IX-linked ligands fails in most cases, although some success was observed with transferrin. Direct complexing of Ad-IX-BAP with transferrin was tested to determine whether or not the results obtained with the layering approaches will be retained when transferrin is linked to the capsid through protein IX. Complexes were made as before by CsCl banding and sequential saturation with avidin and biotinylated transferrin. Western blot (Fig 5.6B) shows that as before with the fiber-modified vector, Ad-IX-BAP can be complexed with biotinylated ligands which remain capsid associated through CsCl banding. Unlike the Ad-fiber-BAP complex, the Ad-IX-BAP transferrin complex had no targeting capabilities on C2C12 myoblasts (data not shown). In fact, transduction of HeLa cells, which express both CAR and CD71, was drastically reduced as compared to unmodified or avidin-complexed Ad-IX-BAP (Fig 5.8). Apparently the addition of large ~80 kDa transferrin molecules to the

Ad capsid through protein IX prevents both CD71-targeted transduction and normal transduction through fiber-CAR interactions.

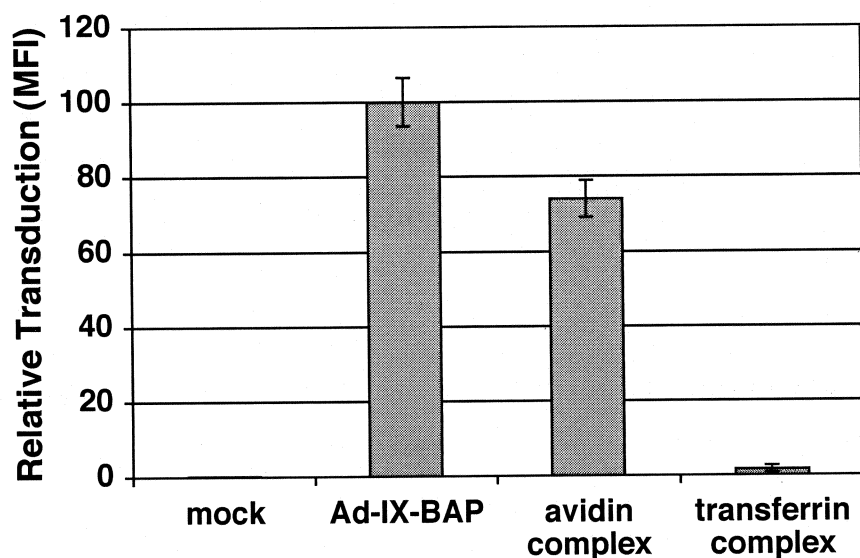


Fig 5.8 HeLa cell transduction of Ad-IX-BAP complexes. MFI was measured by flow cytometry and data was plotted as the percentage of transduction activity relative to uncomplexed Ad-IX-BAP.

Addition of the ~60 kDa avidin linkers to the capsid only result in a modest decrease of CAR-mediated transduction, in agreement with earlier avidin neutralization experiments (Fig 4.6), while the further addition of transferrin (140 kDa total) essentially inactivated the vector. The mechanisms of this inhibition were not explored further but perhaps the display of large complexes from protein IX physically blocks normal capsid-cell interactions that are essential to proper vector uptake, trafficking, and transduction. Regardless, data from the layering experiments and the direct complexing strongly suggest that avidin-based targeting through capsomeres other than the fiber is very inefficient.

5.4 Conclusions

Protein IX has received much attention lately as a useful locale for the display of large polypeptides from the adenoviral capsid [113]. Direct genetic fusion of large targeting ligands to the C-terminus of IX is an attractive alternative to fiber modification for the introduction of targeted tropism into Ad vectors. Hexon also represents an appealing candidate for the introduction of new tropism, due to the sheer abundance of the protein within the virion. Metabolic biotinylation of the adenoviral capsid has for the first time enabled a direct comparison of ligand-mediated cell targeting through the fiber, IX, and hexon capsomeres. Regardless of the multivalent biotin display achieved through fusion of the BAP to the IX and hexon capsomeres, these vectors are quite ineffective for the avidin-based redirection of transduction through a variety of ligand-receptor interactions. On the other hand, Ad-fiber-BAP is an extremely versatile platform for ligand-mediated cell targeting through the avidin-biotin system. Ad-fiber-BAP transduction can be targeted to a wide range of refractory cells through a broad array of ligands, despite the fact that it displays the fewest amount of biotins per capsid. Complexing of targeting ligands directly to the surface of Ad-fiber-BAP through the strong biotin-avidin interaction represents a convenient and flexible system for the introduction of new tropism into Ad vectors.

Although the exact mechanisms responsible for this phenomenon have not been determined, one current working hypothesis relies on functional differences between fiber and the other capsomeres during vector uptake and trafficking. The dissociation of the fibers from the trafficking capsid are well documented [59, 103] and this event

appears to enable virion escape from endosomal receptors, thereby releasing the virion into the cytoplasm for eventual accumulation at the nuclear pores and import of the Ad genome into the nucleus. Redirection of receptor binding through protein IX or hexon may perturb this natural pathway, resulting in possible entrapment of virions on receptors and altered trafficking patterns, thereby preventing normal transduction. Indeed, analysis of fluorophore conjugated Ad-IX-BAP by fluorescence microscopy shows improper accumulation of vector during nonproductive CTx-B mediated uptake. Investigation of the fate of protein IX during trafficking reveals that in contrast to the fiber protein, IX remains associated with the virion. It therefore seems possible that the differences in targeting capabilities between the vectors may be in part due to the functional differences between fiber and IX/hexon during the processes of virion uptake and trafficking. Regardless of the mechanisms involved, Ad-fiber-BAP clearly outperforms the other vectors for targeting applications.

Chapter VI

Cryo-Electron Microscopy of IX-Modified Vectors Reveals the True Position of IX Within the Adenoviral Icosahedron

Abstract

Adenovirus protein IX functions as a capsid cement and is thought to enhance stability through interactions within the group-of-nine (GON) hexons, central to each facet. Direct studies on the position of IX within the adenoviral capsid have never been reported despite decades of structural and biochemical research. Cryo-electron microscopy and particle reconstruction of the IX-modified vectors described in this chapter provides the first direct visualization of IX within the structural context of the adenoviral capsid. The data indicates that rather than being embedded within the GON hexons, IX is present as density currently assigned to protein IIIa, located along the outer edges of the GON in a surface-accessible position. This new and exciting data contradicts all previous conclusions regarding the structural biology of IX within the capsid and emphasizes the need for more rigorous studies of adenoviral virion structure.

6.1 Introduction

Adenovirus gene IX is located to the left end of the genome directly behind the E1B coding sequence and codes for a small 14.3 kDa capsid protein. Gene IX is genus-specific, unique to all known members of *Mastadenoviridae* (generally corresponding to a mammalian host range), and is absent from *Aviadenoviridae*, *Atadenoviridae*, and *Siadenoviridae* the other three genera of the *Adenoviridae* family [42]. Transcription of IX is driven from its own promoter which overlaps the E1B coding sequence, leading to repression of pIX expression until E1B transcription has subsided, shortly after the onset of adenoviral DNA replication at intermediate times post infection [154]. Protein IX is one of the few capsomers whose expression is uncoupled from the major late promoter that drives expression of most capsid and core proteins. The presence of protein IX is not required for the encapsidation of virions of sub-genomic (<36 kb) size, but virions with capsids devoid of IX are more thermolabile than wild type virions [23, 29]. Previous work [55] has shown that deletion of IX prevents the encapsidation of genomes of wild type or larger sizes (36-38 kb), though more recent work indicates that the absence of IX does not prevent encapsidation but rather the resulting Δ IX virions are somehow defective in infectivity assays [133].

In addition to its mysterious role as a capsid protein, IX has been shown to function as a transcriptional activator, enhancing transcription of TATA-containing viral and cellular promoters including the major late promoter [125], even though it has no direct DNA binding properties. The physiological role of this transcriptional activity during the viral life cycle does not appear to be very significant though, as virions devoid of IX seem to replicate with normal kinetics and only suffer a three-fold reduction in

transcription off the major late promoter [133]. Despite its lack of significant transactivation activity, protein IX has been shown to function in nuclear reorganization and sequestration of cellular promyelocytic leukaemia (PML) protein into clear amorphous inclusions, an activity shown to contribute to efficient viral replication [125]. All studies on the biology of IX have been conducted in tissue culture cells and it should be noted that the transactivation, nuclear reorganization, and structural roles of protein IX during *in vivo* infection and pathogenesis have not been elucidated.

The icosahedral adenoviral capsid is formed from twenty interlocking facets, each comprised of twelve hexon trimers organized into triangular units (Fig 6.1). The groups-of-nine (GON's) hexons that are observed after various methods of capsid disruption are central to each facet. The crystal structure of the hexon trimer [129] reveals a pseudo-hexagonal base with three towers extending upwards creating a triangular top approximately 113 Å from the bottom. The maximum radius of the hexon trimer is 50 Å. The triangular top is rotated roughly 10 degrees counter-clockwise with respect to the hexagonal base. The hexon trimers present within each facet are closely packed along their hexagonal bases, creating a continuous protein shell that is approximately 33-44 Å thick. The three towers of each hexon trimer extend roughly 69 Å above the "base shell" thereby creating cavities between the towers of different hexon trimers. Due to the 10 degree difference in rotational pitch between the bases and towers of individual hexon trimers, each GON contains four large and three small cavities between the nine different hexon trimers (Fig 6.1).

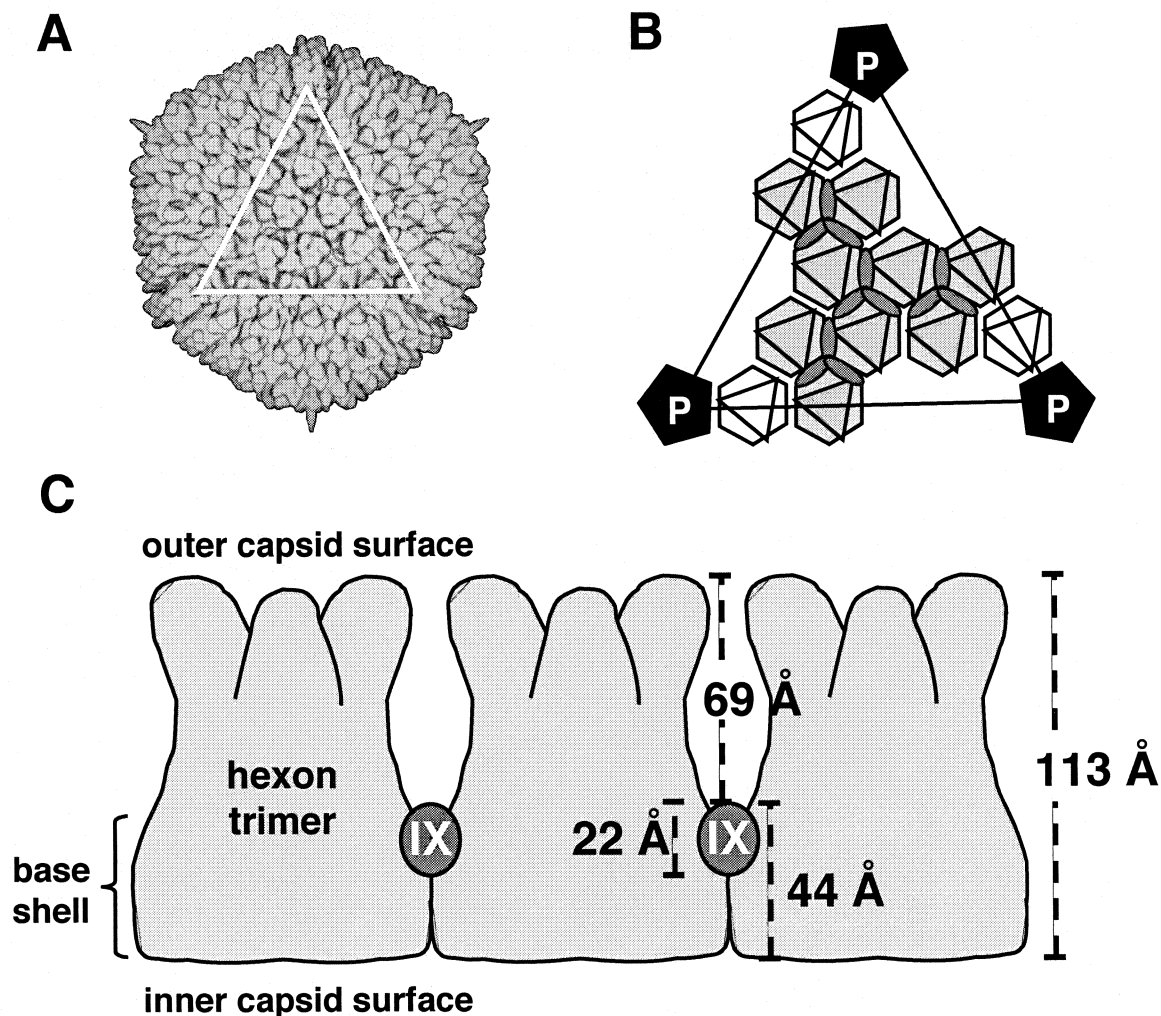


Fig 6.1 Structural organization and relationships between hexon trimers and protein IX. (A) Cryo-EM reconstruction of the Ad capsid, highlighting the central triangular facet. (B) Close up diagram of the twelve hexon trimers that comprise the facet. Three peripentonal hexons are drawn in white, with the GON hexons depicted in light grey. Four elongated trimers of IX, shown in dark grey, are present along the bases of these hexons, providing structural stability. (C) Side view of a cross-section of the GON hexons illustrating the spatial relationships. 22 Å thick protein IX is thought lie in deep cavities, along the bases of adjacent hexons, approximately 69 Å below the towers at the outer capsid surface.

Structurally, protein IX functions as a capsid cement and trimers of IX are thought to reside at the bottom of the four large cavities of each GON [53]. This arrangement of IX within the icosahedron results in 12 molecules per facet and 240 molecules of IX per

virion, in excellent agreement with the known stoichiometry of IX within the capsid, as calculated from [^{35}S] methionine labeling experiments [155]. Protein IX was indirectly visualized at this position by difference imaging between a cryo-EM reconstruction of purified GON's and an artificial GON, constructed by placing nine copies of a contour plot of the hexon trimer (derived from X-ray crystal structure coordinates) in the spatial orientation of the native GON. The difference image of this subtraction revealed electron density arranged as four elongated trimers present within each of the four large cavities of the GON and along the edges of the hexon trimers that surround them [53]. This density was assigned as protein IX based on several pieces of evidence. First, virions devoid of IX were shown to be thermolabile and ΔIX virions fail to dissociate into GON's as wild type virions do [29]. Second, IX has been shown to be associated with purified GON's [18]. Third, this spatial arrangement agrees perfectly with the known stoichiometry of IX and its apparent ability to form multimers [124, 159]. Lastly, the mass calculated from the difference image of the IX trimers was in close proximity to the actual molecular mass of protein IX; 16.6-18.9 kD vs. 14.3 kD [53].

Ad-IX-BAP displayed 71 ± 11 avidin-accessible biotins per capsid and was readily bound by avidin-functionalized resins for selective removal or purification of these biotinylated vectors. Given that the current models of adenoviral capsid structure [132] have protein IX placed along the bottom of hexon cavities approximately 69 Å below the outermost surface of the virion (Fig 6.1), it becomes questionable how the C-terminal BAP fusion and the associated biotin molecule could be accessible to avidin binding. One possibility was that the BAP domain was large enough and the linker sequence was long enough such that the biotin tags could reach outwards, above the tops

of the hexon trimers. However reports by others have described the production of vectors containing short peptide epitopes fused to the C-terminus of IX and in each case the epitope was accessible to antibody binding. Dmitriev et al. [46] described the encapsidation of a IX-Flag fusion that replaced the last ten amino acids of IX with the eight amino acid Flag epitope, resulting in the net loss of two residues, and even this modification resulted in effective display of accessible epitopes from the virion. Vellinga et al. [159] showed that the insertion of α -helical spacers between the C-terminus of IX and c-myc or RGD peptides resulted in better display of these peptides from the virion, in good agreement with the current model of a buried inaccessible protein IX. However even the fusion of peptides without any spacers resulted in accessible display from the virion as shown by negative stain immunoelectron microscopy. Also, the inclusion of spacers could conceivably improve accessibility of surface exposed epitopes by relieving steric hindrance imposed by the binding of large proteins like antibodies or avidin conjugates. Other studies focusing on the antigenicity of IX within the virion have demonstrated that IX is accessible to antibodies, enabling the immunoprecipitation of virions with IX antiserum [18, 49]. These observations prompted the question how the C-terminus of IX and any displayed ligands can be accessible to antibody/avidin binding if protein IX lies buried between hexon trimers well below the surface of the virion? In this chapter, cryo-electron microscopy (cryo-EM) and particle reconstruction of IX-modified vectors reveals that protein IX is localized between hexons of neighboring facets, rather than within the GON hexons central to each facet. Density present at this position is currently assigned as monomers of protein IIIa. This new data provides the

first direct evidence of IX localization within the capsid, suggesting that the IIIa density was previously misidentified and is actually attributable to four molecules of IX.

6.2 Materials and Methods

Sample Preparation. Wild type and IX-modified vectors were propagated and CsCl purified as previously described. All samples were equilibrated in PBS and adjusted to concentrations between 8×10^{11} VP/ml (Ad-IX-BAP) and 3×10^{12} VP/ml (Ad-IX-45-GFP, Ad Δ IX), as determined by OD₂₆₀. Low concentration preps were concentrated using Amicon Ultra-4 centrifugal filter devices, 100 kDa molecular weight cutoff. Approximately 3 μ l of each sample was applied to a holey-carbon grid, which was blotted and flash frozen in liquid propane using a vitrobot apparatus. Grids were stored under liquid N₂ until microscopic examination.

Cryo-Electron Microscopy and Particle Reconstruction. Cryo-EM analysis and particle reconstruction was performed by standard methods at the National Center for Macromolecular Imaging at Baylor College of Medicine. Several hundred individual particles of Ad-IX-BAP were individually boxed out and used for the reconstruction. Difference imaging (Fig 6.2) was done by subtracting the cryo-EM reconstruction density map of wild type Ad from that of Ad-IX-BAP and superimposing this difference (attributable to the BAP domain, shown in red) over the Ad-wt reconstruction.

6.3 Results and Discussion

To investigate these puzzling observations further the topology of the Ad capsid was closely analyzed by cryo-EM reconstruction. Reconstruction of the wild type capsid revealed that the cavities where IX is thought to reside are too small to physically accommodate the density of tetrameric avidin. Recent work has described the successful display of large proteins like EGFP and luciferase [81] from the C-terminus of IX, with little or no effect on capsid structure and stability or virion infectivity. Again, measurement of the hexon cavity dimensions showed that they are simply too small to contain these large additions and suggests that these domains must somehow be present on the outer surface of the capsid, above the tops of the hexon trimers.

To directly visualize how ligands might be displayed on the C-terminus of IX, cryo-EM analysis and particle reconstruction of Ad-IX-BAP was performed, with hopes that the 71 amino acid biotin acceptor, which folds into a compact β -sandwich structure [121], would have enough inherent electron density to be directly visualized within the framework of the icosahedron. Particle reconstruction and difference imaging from the wild type capsid reveals the presence of small irregular densities attributable to the extra density of the C-terminal BAP fusion (Fig 6.2A). Quite surprisingly, these small regions of density are present at an unexpected location of the icosahedral capsid. Rather than being above or within the large cavities of the GON, the extra density is present at locations on opposite and adjacent sides of the 2-fold axis of symmetry, positioned just along the outer edges of the GON (Fig 6.2C). Interestingly, the extra BAP density is located right above the pre-existing density currently assigned as protein IIIa (Fig 6.2B).

This assigned IIIa density is positioned between the borders of different facets, perhaps functioning to rivet the facets together (Fig 6.2C).

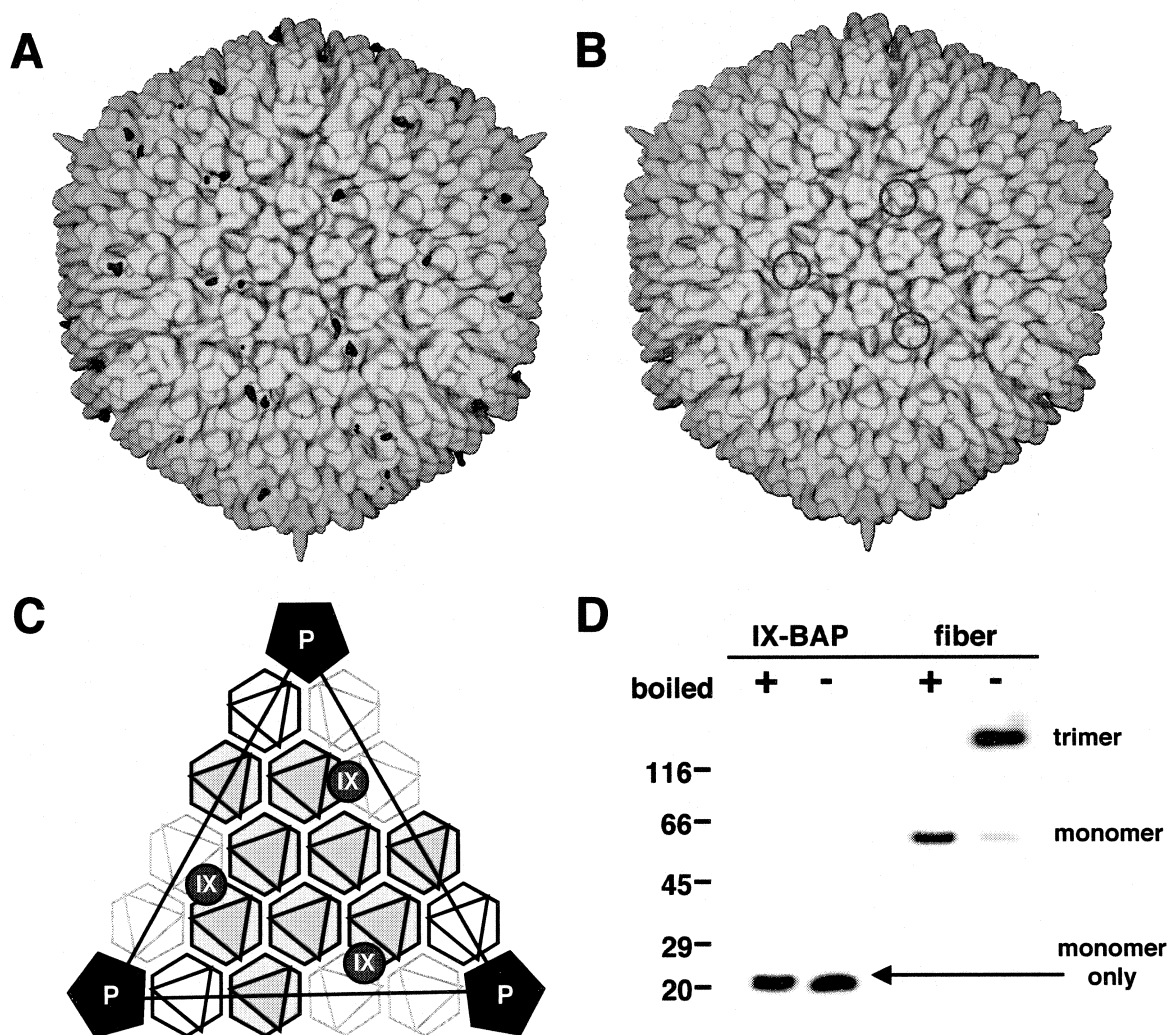


Fig 6.2 Cryo-EM reconstruction of Ad-IX-BAP. (A) Difference imaging reveals the presence of the C-terminal BAP fusion as small irregular densities (red) on the surface of the icosahedron. (B) Density currently assigned as protein IIIa (highlighted in red) lies directly underneath the BAP densities. (C) Diagram of the central facet showing the newly assigned position of protein IX. Four molecules of IX (red circles) are thought to reside at three symmetrical positions in each facet. Note that this newly assigned position lies on the outer edge of the GON (shaded in grey), bridging hexons of adjacent facets (outlined in light grey). (D) These groups are not believed to be true structural tetramers, as protein IX consistently runs as monomers on native polyacrylamide gels, in contrast to fiber, a trimeric protein.

To reinforce this unexpected observation, another IX-modified vector was constructed, which displays the much larger EGFP protein from the C-terminus of IX through a 45 Å α -helical spacer [159], to help alleviate any steric hindrance imposed by the EGFP tag during capsid assembly. This vector was produced by previously described methods [21] and displays EGFP on the capsid (Fig 5.5) with negligible effects on virion thermostability and infectivity (data not shown). The larger size of EGFP as compared to the BAP (26.9 kDa vs. 7.4 kDa) should result in much higher signal during image analysis, provided the 45 Å spacer does not provide too much flexibility. Ad-IX-45-EGFP virions have been analyzed by cryo-EM (Fig 6.3) and particle reconstruction is currently underway to determine if extra EGFP density again appears above the current IIIa density.

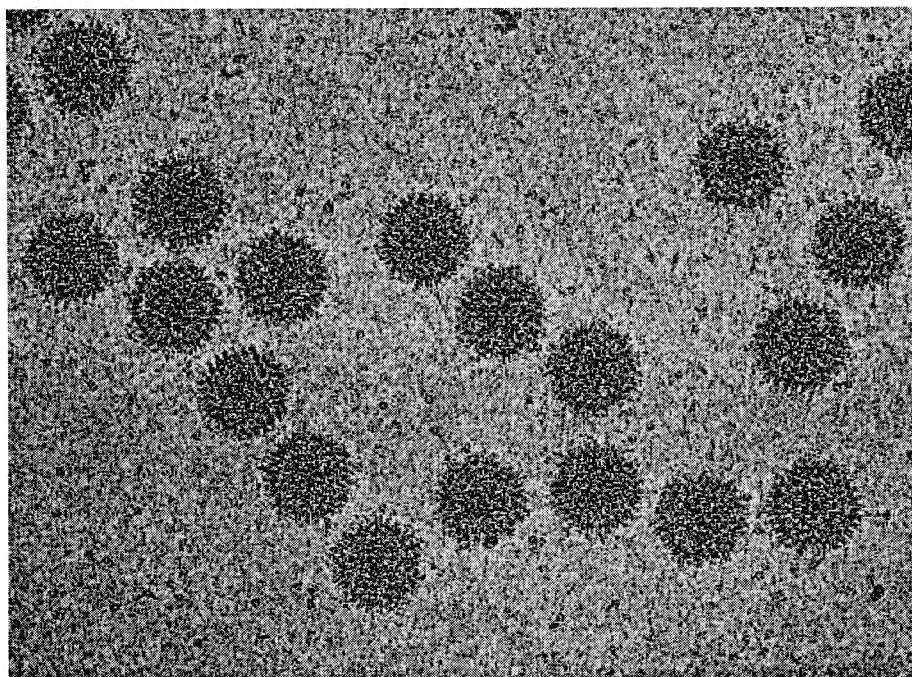


Fig 6.3 Cryo-electron micrograph of Ad-IX-45-EGFP particles embedded in vitreous ice. Contrast has been adjusted to allow visualization.

Review of the literature reveals that this density was originally assigned as dimers of the small 14.5 kDa protein VIII [143], another hexon associated protein that is thought to have a stoichiometry of 120 molecules per virion [155]. Shortly thereafter this density was reassigned as monomers of protein IIIa [145], which is thought to be present at 60 copies per virion [155]. The rationale for the reassignment from VIII to IIIa was never fully explained but the authors base the current assignment on comparisons of measured and predicted voxel sizes (volumes) and molecular masses. The measured volume of the density in question is 238 voxels, very close to the predicted volume of protein IIIa, which is 245 voxels, as based on molecular weight. This reasoning based on predicted volumes and known stoichiometry is rather indirect and could conceivably lead to erroneous conclusions.

The current IIIa density is reassigned as four molecules of IX based on the direct results of cryo-EM analysis of IX-modified virions. In this model, each facet contains three groups of four protein IX molecules, in agreement of the established stoichiometry of 240 copies of IX per virion. Interestingly, using the criteria for the original assignment as IIIa [145], the measured volume for this density of 238 voxels is close to the predicted volume of 220 voxels for four molecules of IX (4×55 voxels). Additionally the molecular mass of four molecules of protein IX (4×14.34 kDa = 57.36 kDa) is close to that of IIIa (63.53 kDa), so it becomes apparent how four molecules of IX might be mistaken for one molecule of IIIa.

The density is not described as a true “tetramer” of IX because recent work has shown that the C-terminal leucine zipper domain, responsible for the evident multimerization and associated transcriptional activities of IX [124], is not necessary for

the encapsidation of IX or its enhancement of virion thermostability [160]. These findings suggest that any apparent multimeric organization of IX within the icosahedral capsid may be a consequence of the inherent architecture and geometry imposed by the spatial arrangement of the hexon trimers and/or underlying minor capsid components, rather than a true multimeric state. Multimerization of protein IX has only been shown only by co-immunoprecipitation experiments of wild type IX and IX-epitope fusions [124, 159]. Attempts to directly visualize multimers of IX in non-denaturing polyacrylamide gels consistently fail while trimers of fiber, a true structural trimer, can be detected (Fig 6.2D). These experiments suggest that although IX may form weak multimers through its C-terminal leucine zipper domain, true structural dimers, trimers, or tetramers do not form inside or outside the context of the adenoviral capsid.

The new model for protein IX localization within the capsid makes sense in light of the direct visual data and conceptual arguments, but the reassignment of IX contradicts previous studies on capsid dissociation and the molecular composition of the GON. Why do virions devoid of IX fail to dissociate into GON structures? How can protein IX stabilize the GON from its current position in the capsid? The answer to these intriguing questions can only be revealed by more detailed structural and biochemical studies of the adenoviral capsid and its components.

A review of the previous studies on the composition of disrupted virions and GON's reveals many discrepancies, most likely due to different methods of disruption and different analytical techniques used in each experiment. Studies by [50] found that sequential dissociation of capsids by dialysis against Tris-maleate buffer followed by a series of ultracentrifugations and resuspensions in various buffers resulted in a fraction

enriched for the facet hexons as well as proteins IIIa, VI, VIII, IX, and X. This fraction should be similar in composition to the GON's because the GON comprises the central portion of each facet. Indeed, electron microscopy of this fraction showed rounded capsid-like particles lacking many of the pentons and peri-pentonal hexons [120]. When fractionated on a sucrose gradient to determine which proteins were physically associated with the facet hexons, only proteins VI and VIII were still bound to the hexons suggesting these minor capsid proteins have affinity for the hexons of each facet [50]. Additional analysis by using 10% pyridine disruption followed by sucrose density gradient centrifugation described the GON fraction as containing hexons together with proteins VI and IX, without any VIII. Later studies by [29] also analyzed the GON fraction resulting from disruption in 10% pyridine followed by sucrose density gradient centrifugation. The GON's isolated from these conditions were found to contain only hexon and IX without any protein VI. Similar results were obtained by [155] who isolated GON's by heat disruption in Tris-HCL with 0.5% sodium deoxycholate followed by glycerol density gradient centrifugation disruption. These conflicting results demonstrate that different methods of capsid disruption can cause profound differences in which protein components stay associated with hexons, leading to difficulties in the interpretation of which interactions are true in the context of pristine capsids.

The question then arises, if protein IX is not localized to the four large cavities within the GON structure, then what protein if any is? Difference imaging work by [53, 145] shows the presence of additional electron density at these regions. These structures may be other minor components, possibly VIII, which may act in concert with IX to stabilize the intact capsid and the GON structures. An older report [102] describes the

isolation of a thermolabile Ad5 mutant containing a modified protein VIII. The mutation resulted in a temperature sensitive phenotype and closer analysis revealed that the virions were in fact thermolabile as compared to a wild type adenovirus, similar to the phenotype of Δ IX virions [29]. Perhaps proteins VIII and IX work together to stabilize the GON's and facets through complex allosteric interactions, and a deficiency in either one of these minor capsid proteins renders the virion less stable and thermolabile.

Other recent studies also hint at the possibility of complex interactions between proteins VIII and IX. Analysis of empty capsids in preparations of column-purified adenoviruses [158] revealed that these particles were primarily composed of hexon, IIIa, and the precursor to VIII (pVIII). Interestingly these genome-free particles resembled Ad virions under the electron microscope but were rounder and appeared to lack the penton vertices. Another recent study [136] focused on the properties of helper-dependent adenoviral vectors that had small 12 kB genomes, about 1/3 the normal size. This group discovered that these particles, which appeared to bind enter cells properly, failed to escape the endosomes and deliver their genomes to the nucleus. Closer analysis of the composition and appearance of these particles demonstrated that they had high levels of precursors pVI, pVII, and pVIII, and appeared to be completely lacking IX. Visually these particles had abnormal morphology and were more permeable to uranyl acetate than normal virions. These two recent studies seem to indicate that when immature pVIII is present (perhaps due to the lack of or small genomes) protein IX does not properly incorporate into the capsid. This implies an interaction between the hexons, mature VIII, and IX and suggests that these minor capsid proteins may work together to organize and stabilize the icosahedral hexon facets.

6.4 Conclusions

Cryo-EM reconstruction of protein IX-modified capsids represents the first direct visual evidence for the localization of this small protein within the context of the large adenoviral icosahedron. These results contradict all previous biochemical and structural reports on the location of IX within the GON structures of the capsid and show that protein IX has been previously mistaken for protein IIIa. At this new position IX is more surface exposed and may function to confer capsid stability by bridging hexons between the interlocking facets. The fact that Δ IX virions cannot package large genomes into functional particles [133] and that non-functional virions with unusually small genomes fail to incorporate IX [136] implies that the interactions of protein IX with other capsomers both during and after encapsidation are much more complicated than previously thought. The new assignment of IX raises many questions about the molecular architecture of the adenoviral capsid and the organization of the minor components therein. Clearly this work highlights the need for new biochemical and structural analysis of the adenoviral icosahedron.

Chapter VII

Conclusions and Future Directions

This work describes the construction, characterization and avidin-based applications of genetically engineered, metabolically biotinylated vectors. Fusion of the biotin acceptor peptide from *P. shermanii* transcarboxylase to the C-termini of fiber and protein IX, or insertion within the HVR5 loop of hexon results in genetically modified vectors that are metabolically biotinylated during propagation in 293 cells. These vectors retain their infectivity and transduction capabilities and display covalently attached biotin molecules on their surface. The magnitude and position of biotinylation is dependent on the stoichiometry and location of the modified capsomeres within the icosahedral virion. These vectors readily bind avidin and streptavidin functionalized resins, enabling the enhancement of transduction through physical force, as well as the avidin-based purification and enrichment of vector from crude cell lysate.

The principal goal of this work was investigation into the use of these vectors as platforms for adenoviral vector targeting. Attachment of cell targeting ligands to the capsid surface was mediated through tetrameric avidin and the inherently strong interaction it has with biotin. Vector transduction was redirected through a wide variety of receptor-ligand pairs by using avidin to bridge biotinylated ligands to the biotinylated capsid surface. Metabolically biotinylated vectors therefore represent a versatile platform

for the incorporation of a broad range of targeting ligands into the Ad capsid. Complex ligands that cannot be genetically engineered into the virion like monoclonal antibodies, secreted proteins, growth factors, natural toxins, even carbohydrates and nucleic acids, can readily be displayed from the Ad capsid with this system.

Direct comparison of ligand-mediated transduction through the different capsid proteins reveals that although biotin display is possible through the IX and hexon capsomeres, transduction is only efficiently redirected through the fiber protein. Fiber has evolved as the natural cell binding protein of the Ad capsid and inefficient transduction results from the redirection of binding and uptake through other capsid components. This work represents the first direct comparison of targeting between different capsomeres and suggests that future efforts should be focused on modification of the fiber protein.

Protein IX and hexon may serve as useful locales for the attachment of other functional domains like GFP for particle tracking, immunomodulatory domains to repress host innate immune responses, or fusogenic peptides and nuclear localization signals to enhance intracellular trafficking of vector particles. Although large relatively high affinity protein ligands (CTx-B, antibodies) appear to fail when displayed from IX and hexon, lower affinity peptide ligands, isolated through selection of phage peptide display libraries [9], may work when displayed at high copy number from IX or hexon. Indeed, previous work showing enhancement of transduction through IX and hexon used small lower affinity peptides like poly-(lysine) and RGD-peptides to mediate transduction [46, 159, 163].

Although the exact mechanisms behind the inability of IX and hexon to support ligand-targeted transduction have not been determined, one general working hypothesis suggests that the underlying differences between fiber and the other capsomeres during virion uptake and trafficking might be the cause. It is well established that fiber releases from incoming virions at early time points. Data presented herein suggests that IX remains capsid associated with the hexons, failing to release from the virions. Receptor binding through IX or hexon may therefore trap the virions on their bound receptors, leading to improper trafficking and inefficient transduction.

The ultimate goal of creating truly targeted vectors will require the ablation of natural tropism as well as the addition of new targeting ligands. Recently, several studies have demonstrated that the fiber is a major determinant for both hemagglutination properties as well as in vivo tropism and that ablation of the CAR and HS-GAG binding interactions of the knob and shaft domains, combined with the knockout of the penton base-integrin interactions can result in significant alteration of in vivo tropism [108] [140, 141]. These de-targeted vectors might serve as good platforms for the introduction of new targeted tropism through the addition of specific cell binding ligands

In accordance with these observations, new versions of the Ad-fiber-BAP vector have been designed (Fig 7.1). Complete removal of the fiber protein would be ideal for de-targeting, but deletion of fiber has been shown to result in unstable virions [165]. The recently reported X-ray crystal structure of the penton base bound to the N-terminal portion of the fiber has provided valuable insight into the nature of the fiber-penton base interaction [184]. Penton base, with no fiber bound adopts a different conformation than when it is in complex with the N-terminal fiber tail. Fiberless virions may be inherently

unstable because their penton vertices are not in the proper conformation, as when fiber is present.

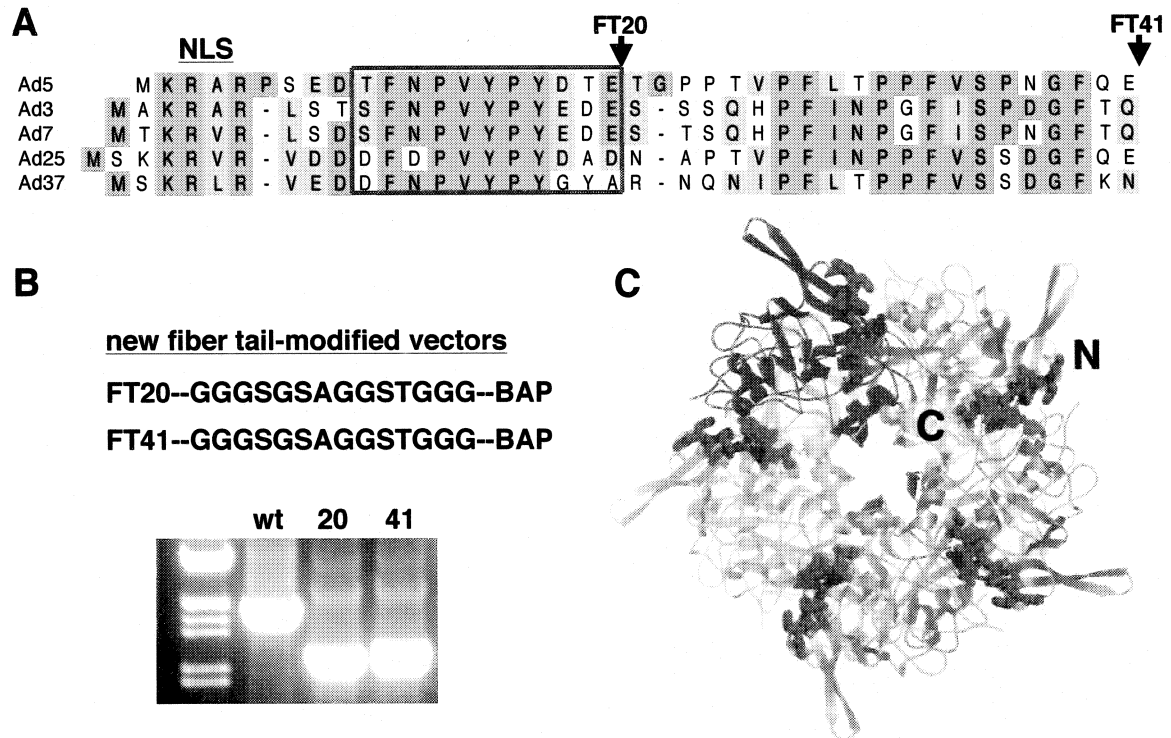


Fig 7.1 Design of Ad-FT-BAP vectors. (A) Sequence alignment of the N-terminal fiber tails from several Ad serotypes showing the high degree of sequence homology. The position of the nuclear localization signal (NLS) residues 20 and 41 are marked. (B) Design of the FT-BAP fusions and PCR conformation of their replacement of the native fiber sequence within the pAd genomes. (C) Structure of the penton base-FT peptide complex. The peptides in red correspond to the region marked in red in (A). Orientation is looking down on the vertex, taken from [184].

The new BAP-modified vectors have been designed with this information in mind. The two vectors, Ad-FT20-BAP and Ad-FT41-BAP, consist of different lengths of the N-terminal fiber tail (FT) peptide (20 and 41 amino acids, respectively) fused to the 70 residue BAP, with a flexible linker sequence in between (Fig 7.1B). The FT peptide might possibly allow five of these BAP fusion molecules to dock into each penton base (Fig 7.1C), thereby avoiding the unstable conformation seen when fiber is

absent. The FT peptide also naturally includes the NLS, needed to facilitate nuclear import of these molecules for encapsidation in the nucleus (Fig 7.1A). The mechanisms of fiber release during endocytic uptake are not known, but perhaps if conformational changes in penton base are involved, then the FT-BAP fusions might be released as natural fibers, thereby avoiding the problems observed with ligand targeting through IX and hexon. If this design works, it may represent a substantially de-targeted biotinylated vector, upon which targeting ligands could be added through the avidin-biotin interaction. Currently the vector genomes have been constructed through Red recombination, resulting in the replacement of the native fiber sequences (shaft and knob) within the pAd-dsRed genomes with the FT-BAP fusion sequences. PCR with primers flanking the fiber ORF (Fig 7.1B) and sequencing have confirmed the modifications. These vectors are currently in the early stages of amplification in the 633 cell line, an E1 and fiber-complementing cell line for the production of fiber-deleted Ad vectors [166].

The basic biology of adenovirus and its vectors, from their beautiful seemingly simple icosahedral design to their pharmacological behavior in vivo, is very complex. A more comprehensive knowledge and understanding of this biology must be achieved before the successful development of safer, more effective vectors, targeted to the site of disease. Ultimately, rational engineering of the capsid, together with advances in Ad vector genome design, incorporating modified transposon elements and targeted integration capabilities, for the stable long term expression of therapeutic genes in human tissues [73, 150, 180], will yield a new generation of Ad vectors for the safe and effective gene therapy of hereditary and acquired disease.

References

1. Akalu, A., H. Liebermann, U. Bauer, H. Granzow, and W. Seidel. 1999. The subgenus-specific C-terminal region of protein IX is located on the surface of the adenovirus capsid. *J Virol* 73:6182.
2. Alemany, R., K. Suzuki, and D. T. Curiel. 2000. Blood clearance rates of adenovirus type 5 in mice. *J Gen Virol* 81:2605-2609.
3. Amalfitano, A. 1999. Next-generation adenoviral vectors: new and improved. *Gene Ther* 6:1643-1645.
4. Anderson, C. W. 1990. The proteinase polypeptide of adenovirus serotype 2 virions. *Virology* 177:259-272.
5. Athappilly, F. K., R. Murali, J. J. Rux, Z. Cai, and R. M. Burnett. 1994. The refined crystal structure of hexon, the major coat protein of adenovirus type 2, at 2.9 Å resolution. *J Mol Biol* 242:430-455.
6. Bailey, C. J., R. G. Crystal, and P. L. Leopold. 2003. Association of adenovirus with the microtubule organizing center. *J Virol* 77:13275-13287.
7. Barnett, B. G., C. J. Crews, and J. T. Douglas. 2002. Targeted adenoviral vectors. *Biochim Biophys Acta* 1575:1-14.
8. Barry, M. A., S. K. Campos, D. Ghosh, K. E. Adams, H. Mok, G. T. Mercier, and M. B. Parrott. 2003. Biotinylated gene therapy vectors. *Exp Opin Biol Ther* 3:926-940.
9. Barry, M. A., W. J. Dower, and S. A. Johnston. 1996. Toward cell-targeting gene therapy vectors: Selection of cell-binding peptides from random peptide-presenting phage libraries. *Nat Med* 2:299-305.
10. Belousova, N., N. Korokhov, V. Krendelshchikova, V. Simoneko, G. Mikheeva, P. L. Triozzi, W. A. Aldrich, P. T. Banerjee, S. D. Gillies, D. T. Curiel, and V. Krasnykh. 2003. Genetically targeted adenovirus vector directed to CD40-expressing cells. *J Virol* 77:11367-11377.
11. Belousova, N., V. Krendelchtkhikova, D. T. Curiel, and V. Krasnykh. 2002. Modulation of adenovirus vector tropism via incorporation of polypeptide ligands into the fiber protein. *J Virol* 76:8621-8631.

12. Beltz, G. A., and S. J. Flint. 1979. Inhibition of HeLa cell protein synthesis during adenovirus infection: Restriction of cellular messenger RNA sequences to the nucleus. *J Mol Biol* 131:353-373.
13. Benson, S. D., J. K. H. Bamford, D. H. Bamford, and R. M. Burnett. 1999. Viral evolution revealed by bacteriophage PRD1 and adenovirus coat protein structures. *Cell* 98:825-833.
14. Bergelson, J. M., J. A. Cunningham, G. Droguett, E. A. Kurt-Jones, A. Krithivas, J. S. Hong, M. S. Horwitz, R. L. Crowell, and R. W. Finberg. 1997. Isolation of a common receptor for Coxsackie B viruses and adenoviruses 2 and 5. *Science* 275:1320-1323.
15. Berk, A. J. 1986. Adenovirus promoters and E1A transactivation. *Annu Rev Genet* 20:45-79.
16. Berkner, K. L., and P. A. Sharp. 1983. Generation of adenovirus by transfection of plasmids. *Nucleic Acids Res* 11:6003-6020.
17. Bogusiewicz, A., N. I. Mock, and D. Mock. 2004. Instability of the biotin-protein bond in human plasma. *Anal Biochem* 327:156-161.
18. Boulanger, P., P. Lemay, G. E. Blair, and W. C. Russell. 1979. Characterization of adenovirus protein IX. *J Gen Virol* 44:783-800.
19. Brown, J. C., M. Westphal, B. T. Burlingham, U. Winterhoff, and W. Doerfler. 1975. Structure and composition of the adenovirus type 2 core. *J Virol* 16:366-387.
20. Brown, T. L., H. E. Lemay, and B. E. Bursten. 1995. *Chemistry: The central science*. Prentice Hall, New York, NY.
21. Campos, S. K., and M. A. Barry. 2004. Rapid construction of capsid-modified adenoviral vectors through bacteriophage λ Red recombination. *Hum Gene Ther* 15:1125-1130.
22. Campos, S. K., M. B. Parrott, and M. A. Barry. 2004. Avidin-based targeting and purification of a protein IX-modified, metabolically biotinylated adenoviral vector. *Mol Ther* 9:942-954.
23. Caravokyri, C., and K. N. Leppard. 1995. Constitutive episomal expression of polypeptide IX (pIX) in a 293-based cell line complements the deficiency of pIX mutant adenovirus type 5. *J Virol* 69:6627-6633.
24. Cepko, C. L., and P. A. Sharp. 1982. Assembly of adenovirus major capsid protein is mediated by a nonvirion protein. *Cell* 31:407-415.

25. Chapman-Smith, A., and J. E. Cronan, Jr. 1999. Molecular biology of biotin attachment to proteins. *J Nutr* 129:477S-484S.
26. Chartier, C., E. Degryse, M. Gantzer, A. Dieterle, A. Pavirani, and M. Mehtali. 1996. Efficient generation of recombinant adenovirus vectors by homologous recombination in *Escherichia coli*. *J Virol* 70:4805-4810.
27. Chatterjee, P. K., M. E. Vayda, and S. J. Flint. 1985. Interactions among the three adenovirus core proteins. *J Virol* 55:379-386.
28. Chiu, C. Y., P. Mathias, G. R. Nemerow, and P. L. Stewart. 1999. Structure of adenovirus complexed with its internalization receptor, alphavbeta5 integrin. *J Virol* 73:6759-68.
29. Colby, W. W., and T. E. Shenk. 1981. Adenovirus type 5 virions can be assembled in vivo in the absence of detectable polypeptide IX. *J Virol* 39:977-980.
30. Corden, J., M. Engelking, and G. Pearson. 1976. Chromatin-like organization of the adenovirus chromosome. *Proc Natl Acad Sci USA* 73:401-404.
31. Court, D. L., J. A. Sawitzke, and L. C. Thomason. 2002. Genetic engineering using homologous recombination. *Annu Rev Genet* 36:361-388.
32. Crompton, J., C. I. A. Toogood, N. Wallis, and R. T. Hay. 1994. Expression of a foreign epitope on the surface of the adenovirus hexon. *J Gen Virol* 75:133-139.
33. Cronan, J. E., Jr. 1990. Biotination of proteins in vivo. A post-translational modification to label, purify, and study proteins. *J Biol Chem* 265:10327-33.
34. Crouzet, J., L. Naudin, C. Orsini, E. Vigne, L. Ferrero, A. Le Roux, P. Benoit, M. Latta, C. Torrent, D. Branelle, P. Deneffe, J. F. Mayaux, M. Perricaudet, and P. Yeh. 1997. Recombinatorial construction in *Escherichia coli* of infectious adenoviral genomes. *Proc Natl Acad Sci USA* 94:1414-1419.
35. Croyle, M. A., N. Chirmule, Y. Zhang, and J. M. Wilson. 2002. PEGylation of E1-deleted adenovirus vectors allows significant gene expression on readministration to liver. *Hum Gene Ther* 13:1887-1900.
36. Crystal, R. G. 1995. Transfer of genes to humans: Early lessons and obstacles to success. *Science* 270:404-410.
37. D'Halluin, J. C., M. Milleville, P. Boulanger, and G. R. Martin. 1978. Temperature-sensitive mutant of adenovirus type 2 blocked in virion assembly: Accumulation of light intermediate particles. *J Virol* 26:344-356.

38. Danthinne, X., and M. J. Imperiale. 2000. Production of first generation adenoviral vectors: a review. *Gene Ther* 7:1707-1714.
39. Datsenko, K. A., and B. L. Wanner. 2000. One-step inactivation of chromosomal genes in *Escherichia coli* K-12 using PCR products. *Proc Natl Acad Sci USA* 97:6640-6645.
40. Davis, A. R., K. Meyers, and J. M. Wilson. 1998. High Throughput method for creating and screening recombinant adenoviruses. *Gene Ther* 5:1148-1152.
41. Davis, M. E. 2002. Non-viral gene delivery systems. *Curr Opin Biotechnol* 13:128-131.
42. Davison, A. J., M. Benko, and B. Barrach. 2003. Genetic content and evolution of adenoviruses. *J Gen Virol* 84.
43. Dechecchi, M. C., P. Melotti, A. Bonizzato, M. Santacatterina, M. Chilosi, and G. Cabrini. 2001. Heparan sulfate glycosaminoglycans are receptors sufficient to mediate the initial binding of adenovirus types 2 and 5. *J Virol* 75:8772-8780.
44. DeJong, R. N., P. C. Van der Vliet, and A. B. Brenkman. 2003. Adenovirus DNA replication: protein priming, jumping back and the role of the DNA binding protein DBP. *Curr Top Microbiol Immunol* 272:187-211.
45. Dmitriev, I., V. Krasnykh, C. R. Miller, M. Wang, G. Kashenteva, N. Mikheeva, N. Belousova, and D. T. Curiel. 1998. An adenovirus vector with genetically modified fibers demonstrates expanded tropism via utilization of a coxsackievirus and adenovirus receptor-independent mechanism. *J Virol* 72:9706-9713.
46. Dmitriev, I. P., E. A. Kashentseva, and D. T. Curiel. 2002. Engineering of adenovirus vectors containing heterologous peptide sequences in the C terminus of capsid protein IX. *J Virol* 76:6893-6899.
47. Edvardsson, B., E. Everitt, H. Jornvall, and L. Prage. 1976. Intermediates in adenovirus assembly. *J Virol* 19:533-547.
48. Evans, R. K., D. K. Nawrocki, L. A. Isopi, D. M. Williams, D. R. Casimiro, S. Chin, M. Chen, D. M. Zhu, J. W. Shiver, and D. B. Volkin. 2004. Development of stable liquid formulations for adenovirus-based vaccines. *J Pharm Sci* 93:2458-2475.
49. Everitt, E., L. Lutter, and L. Philipson. 1975. Structural proteins of adenoviruses. XII. Location and neighbor relationship of proteins of adenovirion type 2 as revealed by enzymatic iodination, immunoprecipitation, and chemical cross-linking. *Virology* 67:197-208.

50. Everitt, E., B. Sundquist, U. Pettersson, and L. Philipson. 1973. Structural proteins of adenoviruses. X. Isolation and topography of low molecular weight antigens from the virion of adenovirus type 2. *Virology* 52:130-147.
51. Fessler, S. P., and C. S. Young. 1999. The role of the L4 33K gene in adenovirus infection. *Virology* 263:507-516.
52. Fisher, K. D., Y. Stallwood, N. K. Green, K. Ulbrich, V. Mautner, and L. W. Seymour. 2001. Polymer-coated adenovirus permits efficient retargeting and evades neutralising antibodies. *Gene Ther* 8:341-348.
53. Furcinitti, P. S., J. van Oostrum, and R. M. Burnett. 1989. Adenovirus polypeptide IX revealed as capsid cement by difference images from electron microscopy and crystallography. *EMBO J* 8:3563-3570.
54. Gaggar, A., D. M. Shayakhmetov, and A. Lieber. 2003. CD46 is a cellular receptor for group B adenoviruses. *Nat Med* 9:1408-1412.
55. Ghosh-Choudhury, G., Y. Haj-Ahmad, and F. L. Graham. 1987. Protein IX, a minor component of the human adenovirus capsid, is essential for the packaging of full length genomes. *EMBO J* 6:1733-1739.
56. Graham, F. L., J. Smiley, W. C. Russell, and R. Nairn. 1977. Characteristics of a human cell line transformed by DNA from adenovirus type 5. *J Gen Virol* 36:59-72.
57. Greber, U. F. 1998. Virus assembly and disassembly: The adenovirus cysteine protease as a trigger factor. *Rev Med Virol* 8:213-222.
58. Greber, U. F., M. Suomalainen, R. P. Stidwill, K. Boucke, M. W. Ebersold, and A. Helenius. 1997. The role of the nuclear pore complex in adenovirus DNA entry. *EMBO J* 16:6998-6007.
59. Greber, U. F., M. Willetts, P. Webster, and A. Helenius. 1993. Stepwise dismantling of adenovirus 2 during entry into cells. *Cell* 75:477-486.
60. Green, N. M. 1975. Avidin. *Adv Prot Chem* 29:85-133.
61. Gustin, K. E., and M. J. Imperiale. 1998. Encapsidation of viral DNA requires the adenovirus L1 52/55-kilodalton protein. *J Virol* 70:6463-6467.
62. Hacein-Bey-Abina, S., C. von Kalle, M. Schmidt, F. Le Deist, N. Wulffrat, E. McIntyre, I. Radford, J. L. Villeval, C. C. Fraser, M. Cavazzana-Calvo, and A. Fischer. 2003. A serious adverse event after successful gene therapy for X-linked severe combined immunodeficiency. *N Engl J Med* 348:255-256.

63. Halbert, D. N., J. R. Cutt, and T. E. Shenk. 1985. Adenovirus early region 4 encodes functions required for efficient DNA replication, late gene expression, and host cell shutoff. *J Virol* 56:250-257.
64. Hardy, S., M. Kitamura, T. Harris-Stansil, Y. Dai, and M. L. Phipps. 1997. Construction of adenovirus vectors through Cre-lox recombination. *J Virol* 71:1842-1849.
65. Havenga, M. J., A. A. Lemckert, O. J. Ophorst, M. van Meijer, W. T. Germeraad, J. Grimbergen, M. A. van den Doel, R. Vogels, J. van Deutekom, A. A. Janson, J. D. de Bruijn, F. Uytdehaag, P. H. Quax, T. Logtenberg, M. Mehtali, and A. Bout. 2002. Exploiting the natural diversity of adenovirus tropism for therapy and prevention of disease. *J Virol* 76:4612-4620.
66. He, T. C., S. Zhou, L. da Costa, J. Yu, K. W. Kinzler, and B. Vogelstein. 1998. A simplified system for generating recombinant adenoviruses. *Proc Natl Acad Sci USA* 95:2509-2514.
67. Hong, S. S., M. K. Magnusson, P. Henning, L. Lindholm, and P. A. Boulanger. 2003. Adenovirus stripping: a versatile method to generate adenovirus vectors with new cell target specificity. *Mol Ther* 7:692-699.
68. Horne, R. W., S. Brenner, A. P. Walterson, and P. Wildy. 1959. The icosahedral form of an adenovirus. *J Mol Biol* 1:84-86.
69. Horwitz, M. S. 2001. Adenoviruses, vol. 2. Lippincott Williams & Wilkins, Philadelphia, PA.
70. Howitt, J., C. W. Anderson, and P. Freimuth. 2003. Adenovirus interaction with its cellular receptor CAR. *Curr Top Microbiol Immunol* 272:331-364.
71. Imelli, N., O. Meier, K. Boucke, S. Hemmi, and U. F. Greber. 2004. Cholesterol is required for endocytosis and endosomal escape of adenovirus type 2. *J Virol* 78:3089-3098.
72. Imler, J. L., C. Chartier, A. Dieterle, D. Dreyer, M. Mehtali, and A. Pavirani. 1995. An efficient procedure to select and recover recombinant adenovirus vectors. *Gene Ther* 2:263-268.
73. Izsvak, Z., and Z. Ivics. 2004. Sleeping Beauty transposition: Biology and applications for molecular therapy. *Mol Ther* 9:147-156.
74. Karimova, G., J. Pidoux, A. Ullmann, and D. Ladant. 1998. A bacterial two-hybrid system based on a reconstituted signal transduction pathway. *Proc Natl Acad Sci USA* 95:5752-5756.

75. Kelkar, S. A., K. K. Pfister, R. G. Crystal, and P. L. Leopold. 2004. Cytoplasmic dynein mediates adenovirus binding to microtubules. *J Virol* 78:10122-10132.
76. Kirby, I., E. Davison, A. J. Beavil, C. Soh, T. J. Wickham, P. W. Roelvink, I. Kovesdi, B. J. Sutton, and G. Santis. 2000. Identification of contact residues and definition of the CAR-binding site of adenovirus type 5 fiber protein. *J Virol* 74:2804-2813.
77. Kirkeby, S., D. Moe, T. C. Bog-Hansen, and C. J. F. van Noorden. 1993. Biotin carboxylases in mitochondria and the cytosol from skeletal and cardiac muscle as detected by avidin binding. *Histochemistry* 100:415-421.
78. Krasnykh, V., N. Belousova, N. Korokhov, G. Mikheeva, and D. T. Curiel. 2001. Genetic targeting of an adenovirus vector via replacement of the fiber protein with the phage T4 fibritin. *J Virol* 75:4176-4183.
79. Krasnykh, V., I. Dmitriev, G. Mikheeva, C. R. Miller, N. Belousova, and D. T. Curiel. 1998. Characterization of an adenovirus vector containing a heterologous peptide epitope in the HI loop of the fiber knob. *J Virol* 72:1844-1852.
80. Lanciotti, J., A. Song, J. Doukas, B. Sosnowski, G. Pierce, R. Gregory, S. C. Wadsworth, and C. O'Riordan. 2003. Targeting adenoviral vectors using heterofunctional polyethylene glycol FGF2 conjugates. *Mol Ther* 8:99-107.
81. Le, L. P., I. P. Dmitriev, J. G. Davydova, M. Yamamoto, and D. T. Curiel. 2004. Genetic labeling of adenovirus with luciferase on pIX for vector detection. *Mol Ther* 9:297-298.
82. Leon-Del-Rio, A., D. Leclerc, B. Akerman, N. Wakamatsu, and R. A. Gravel. 1995. Isolation of a cDNA encoding human holocarboxylase synthetase by functional complementation of a biotin auxotroph of *Escherichia coli*. *Proc Natl Acad Sci USA* 92:4626-4630.
83. Li, E., S. Brown, D. Stupack, X. Puente, D. A. Cheresh, and G. L. Nemerow. 1998. Integrin $\alpha_v\beta_1$ is an adenovirus coreceptor. *J Virol* 75:5405-5409.
84. Logan, J., and T. E. Shenk. 1984. Adenovirus tripartate leader sequence enhances translation of mRNAs late after infection. *Proc Natl Acad Sci USA* 81:3655-3659.
85. Lozier, J. N., M. E. Metzger, R. E. Donahue, and R. A. Morgan. 1999. Adenovirus-mediated expression of human coagulation factor IX in the rhesus macaque is associated with dose-limiting toxicity. *Blood* 94:3968-3975.

86. Magnusson, M. K., S. S. Hong, P. Henning, P. Boulanger, and L. Lindholm. 2002. Genetic retargeting of adenovirus vectors: Functionality of targeting ligands and their influence on virus viability. *J Gene Med* 4:356-370.
87. Mangel, W. F., M. L. Baniecki, and W. J. McGrath. 2003. Specific interactions of the adenovirus proteinase with the viral DNA, an 11-amino acid viral peptide, and the cellular protein actin. *Cell Mol Life Sci* 60:2347-2355.
88. Marshall, E. 1999. Gene therapy death prompts review of adenovirus vector. *Science* 286:2244-2245.
89. Martin-Fernandez, M., S. V. Longshaw, I. Kirby, G. Santis, M. J. Tobin, D. T. Clarke, and G. R. Jones. 2004. Adenovirus type-5 entry and disassembly followed in living cells by FRET, fluorescence anisotropy, and FLIM. *Biophys J* 87:1316-1327.
90. Mathews, M. B. 1980. Binding of adenovirus VA RNA to mRNA: A possible role for splicing? *Nature* 285:575-577.
91. Matthews, D. A., and W. C. Russell. 1998. Adenovirus core protein V is delivered by the invading virus to the nucleus of the infected cell and later in infection is associated with nucleoli. *J Gen Virol* 79:1671-1675.
92. McConnell, M. J., and M. J. Imperiale. 2004. Biology of adenovirus and its use as a vector for gene therapy. *Hum Gene Ther* 15:1022-1023.
93. Meier, O., K. Boucke, S. Vig, S. Keller, R. P. Stidwill, S. Hemmi, and U. F. Greber. 2002. Adenovirus triggers macropinocytosis and endosomal leakage together with its clathrin mediated uptake. *J Cell Biol* 158.
94. Meier, O., and U. F. Greber. 2004. Adenovirus endocytosis. *J Gene Med* 6:S152-163.
95. Mellman, I. 1992. The importance of being acid: The role of acidification in intracellular membrane traffic. *J Exp Biol* 172:39-45.
96. Mercier, G. T., J. A. Campbell, J. D. Chappell, T. Stehle, T. S. Dermody, and M. A. Barry. 2004. A chimeric adenovirus vector encoding reovirus attachment protein $\sigma 1$ targets cells expressing junctional adhesion molecule 1. *Proc Natl Acad Sci USA* 101:6188-6193.
97. Mitraki, A., S. Miller, and M. J. Van Raaij. 2002. Conformation and folding of novel beta-structural elements in viral fiber proteins: The triple beta-spiral and triple-beta helix. *J Struc Biol* 137:236-247.

98. Mizuguchi, H., and T. Hayakawa. 2004. Targeted adenovirus vectors. *Hum Gene Ther* 15:1034-1044.
99. Mok, H., D. J. Palmer, P. Ng, and M. A. Barry. 2005. Evaluation of polyethylene glycol modification of first-generation and helper-dependent adenoviral vectors to reduce innate immune responses. *Mol Ther* 11:66-79.
100. Murphy, K. C. 1998. Use of bacteriophage lambda recombination functions to promote gene replacement in *Escherichia coli*. *J Bacteriol* 180:2063-2071.
101. Muruve, D. A. 2004. The innate immune response to adenovirus vectors. *Hum Gene Ther* 15:1157-1166.
102. Muruve, D. A., M. J. Cotter, A. K. Zaiss, L. R. White, Q. Liu, T. Chan, S. A. Clark, P. J. Ross, R. A. Meulenbrock, G. M. Maelandsmo, and R. J. Parks. 2004. Helper-dependent adenovirus vectors elicit intact innate but attenuated adaptive host immune responses in vivo. *J Virol* 78:5966-5972.
103. Nakano, M. Y., K. Boucke, M. Suomalainen, R. P. Stidwill, and U. F. Greber. 2000. The first step of adenovirus type 2 disassembly occurs at the cell surface, independently of endocytosis and escape to the cytosol. *J Virol* 74:7085-7095.
104. Narang, M. A., R. Dumas, L. M. Ayer, and R. A. Gravel. 2004. Reduced histone biotinylation in multiple carboxylase deficiency: A nuclear role for holocarboxylase synthetase. *Hum Mol Genet* 13:15-23.
105. Nevins, J. R., and J. E. Darnell. 1978. Groups of adenovirus type 2 mRNAs derived from a large primary transcript: Probable nuclear origin and possible common 3' ends. *J Virol* 25:811-823.
106. Newcomb, W. W., J. W. Boring, and J. C. Brown. 1984. Ion etching of human adenovirus 2: Structure of the core. *J Virol* 51:52-56.
107. Nicklin, S. A., S. J. White, S. J. Watkins, R. E. Hawkins, and A. H. Baker. 2000. Selective targeting of gene transfer to vascular endothelial cells by use of peptides isolated by phage display. *Circulation* 102:231-237.
108. Nicol, C. G., D. Graham, W. H. Miller, S. J. White, S. T.A.G., S. A. Nicklin, S. C. Stevenson, and A. H. Baker. 2004. Effect of adenovirus serotype 5 fiber and penton modifications on in vivo tropism in rats. *Mol Ther* 10:344-354.
109. O'Malley, R. P., T. M. Mariano, J. Siekierka, and M. B. Mathews. 1986. A mechanism for the control of protein synthesis by adenovirus VA RNAI. *Cell* 44:391-400.

110. Ornelles, D. A., and T. E. Shenk. 1991. Localization of the adenovirus early region 1B 55-kilodalton protein during lytic infection: Association with nuclear viral inclusions requires the early region 4 34-kilodalton protein. *J Virol* 65:424-429.
111. Palmer, D. J., and P. Ng. 2005. Helper-dependent adenoviral vectors for gene therapy. *Hum Gene Ther* 1:1-16.
112. Pandori, M., D. Hobson, and T. Sano. 2002. Adenovirus-microbead conjugates possess enhanced infectivity: A new strategy for localized gene delivery. *Virology* 299:204-212.
113. Parks, R. J. 2005. Adenovirus protein IX: A new look at an old protein. *Mol Ther* 11:19-25.
114. Parrott, M. B., K. E. Adams, G. T. Mercier, H. Mok, S. K. Campos, and M. A. Barry. 2003. Metabolically Biotinylated Adenovirus for Cell-targeting, Ligand Screening, and Vector Purification. *Mol Ther* 8:689-702.
115. Parrott, M. B., and M. A. Barry. 2000. Metabolic biotinylation of recombinant proteins in mammalian cells and in mice. *Mol Ther* 1:96-104.
116. Parrott, M. B., and M. A. Barry. 2001. Metabolic biotinylation of secreted and cell surface proteins from mammalian cells. *Biochem Biophys Res Comm* 281:993-1000.
117. Pasqualini, R., and E. Ruoslahti. 1996. Organ targeting in vivo using phage display peptide libraries. *Nature* 380:364-366.
118. Pilder, S., M. Moore, J. Logan, and T. E. Shenk. 1986. The adenovirus E1B-55K transforming polypeptide modulates transport or cytoplasmic stabilization of viral and host cell mRNAs. *Mol Cell Biol* 6:470-476.
119. Poteete, A. R. 2001. What makes the bacteriophage λ Red system useful for genetic engineering: molecular mechanism and biological function. *FEMS* 201:9-14.
120. Prage, L., U. Pettersson, S. Hoglund, K. Lonberg-Holm, and L. Philipson. 1970. Structural proteins of adenoviruses. IV. Sequential degradation of the adenovirus type 2 virion. *Virology* 42:341-358.
121. Reddy, D. V., B. C. Shenoy, P. R. Carey, and F. D. Sönnichsen. 2000. High resolution structure of the 1.3S subunit of transcarboxylase from *Propionibacterium shermanii*. *Biochemistry* 39:2509-2516.

122. Richards, F. 1990. Reflections: The avidin-biotin system. *Methods Enzymol* 184:3-5.
123. Romanczuk, H., C. Galer, J. Zabner, G. Barsomian, S. C. Wadsworth, and C. O'Riordan. 1999. Modification of an adenoviral vector with biologically selected peptides: A novel strategy for gene delivery to cells of choice. *Hum Gene Ther* 10:2615-2626.
124. Rosa-Calatrava, M., L. Grave, F. Puvion-Dutilleul, B. Chatton, and C. Keding. 2001. Functional analysis of adenovirus protein IX identifies domains involved in capsid stability, transcriptional activity, and nuclear reorganization. *J Virol* 75:7131-7141.
125. Rosa-Calatrava, M., F. Puvion-Dutilleul, and P. Lutz. 2003. Adenovirus protein IX sequesters host-cell promyelocytic leukaemia protein and contributes to efficient viral proliferation. *EMBO Rep* 4:969-975.
126. Rowe, W. P., R. J. Huebner, L. K. Gillmore, R. H. Parrott, and T. G. Ward. 1953. Isolation of a cytopathic agent from human adenoids undergoing spontaneous degeneration in tissue culture. *Proc Soc Exp Biol Med* 84:570-573.
127. Roy-Chowdhury, J., and M. Horwitz. 2002. Evolution of adenoviruses as gene therapy vectors. *Mol Ther* 5:340-344.
128. Rux, J. J., and R. M. Burnett. 2004. Adenovirus Structure. *Hum Gene Ther* 15:1167-1176.
129. Rux, J. J., and R. M. Burnett. 2000. Type-specific epitope locations revealed by X-ray crystallographic study of adenovirus type 5 hexon. *Mol Ther* 1:18-30.
130. Salone, B., Y. Martina, S. Piersanti, E. Cundari, G. Cherubini, L. Franqueville, C. M. Failla, P. Boulanger, and I. Saggio. 2003. Integrin $\alpha_3\beta_1$ is an alternate cellular receptor for adenovirus serotype 5. *J Virol* 77:13448-13454.
131. Samols, D., C. G. Thornton, V. L. Murtif, G. K. Kumar, F. C. Haase, and H. G. Wood. 1988. Evolutionary conservation among biotin enzymes. *J Biol Chem* 263:6461-6464.
132. San Martin, C., and R. M. Burnett. 2003. Structural studies on adenoviruses. *Curr Top Microbiol Immunol* 272:57-94.
133. Sargent, K. L., P. Ng, C. Eveleigh, F. L. Graham, and R. J. Parks. 2004. Development of a size-restricted pIX-deleted helper virus for amplification of helper-dependent adenovirus vectors. *Gene Ther* 11:504-511.

134. Sarnow, P., Y. S. Ho, J. Williams, and A. J. Levine. 1982. Adenovirus E1b-58kd tumor antigen and SV40 large tumor antigen are physically associated with the same 54 kd cellular protein in transformed cells. *Cell* 28:387-394.
135. Schhaak, J., S. Langer, and X. Guo. 1996. Efficient selection of recombinant adenoviruses by vectors that express β -galactosidase. *J Virol* 69:3920-3923.
136. Shayakhmetov, D. M., Z. Y. Li, A. Gaggar, H. Gharwan, V. Ternovoi, V. Sandig, and A. Lieber. 2004. Genome size and structure determine efficiency of postinternalization steps and gene transfer of capsid-modified adenovirus vectors in a cell-type-specific manner. *J Virol* 78:10009-10022.
137. Shenk, T. E. 2001. *Adenoviridae: The Viruses and Their Replication*, Fourth Edition ed, vol. 2. Lippincott Williams & Wilkins, Philadelphia, PA.
138. Short, J. J., A. V. Pereboev, Y. Kawakami, C. Vasu, M. J. Holterman, and D. T. Curiel. 2004. Adenovirus serotype 3 utilizes CD80 (B7.1) and CD86 (B7.2) as cellular attachment receptors. *Virology* 322:349-359.
139. Sirena, D., B. Lilienfeld, M. Eisenhut, S. Kalin, K. Boucke, R. R. Beerli, L. Vogt, C. Reudl, M. F. Bachmann, U. F. Greber, and S. Hemmi. 2004. The human membrane cofactor CD46 is a receptor for species B adenovirus serotype 3. *J Virol* 78:4454-4462.
140. Smith, T. A. G., N. Idamakanti, H. Kylefjord, M. L. Rollence, L. King, M. Kaloss, M. Kaleko, and S. C. Stevenson. 2002. *In vivo* hepatic adenoviral gene delivery occurs independently of the Coxsackievirus-adenovirus receptor. *Mol Ther* 5:770-779.
141. Smith, T. A. G., N. Idamakanti, M. L. Rollence, J. Marshall-Neff, J. Kim, K. Mulgrew, G. R. Nemerow, M. Kaleko, and S. C. Stevenson. 2003. Adenovirus serotype 5 fiber shaft influences *in vivo* gene transfer in mice. *Hum Gene Ther* 14:777-787.
142. Solorzano-Vargas, S. R., D. Pacheco-Alvarez, and A. Leon-Del-Rio. 2002. Holocarboxylase synthetase is an obligate participant in biotin-mediated regulation of its own expression and of biotin-dependent carboxylase mRNA levels in human cells. *Proc Natl Acad Sci USA* 99:5325-5330.
143. Stewart, P. L., R. M. Burnett, M. Cyrklaff, and S. D. Fuller. 1991. Image reconstruction reveals the complex molecular organization of adenovirus. *Cell* 67:145-154.
144. Stewart, P. L., C. Y. Chiu, S. Huang, T. Muir, Y. Zhao, B. Chait, P. Mathias, and G. R. Nemerow. 1997. Cryo-EM visualization of an exposed RGD epitope on adenovirus that escapes antibody neutralization. *EMBO J* 16:1189-98.

145. Stewart, P. L., S. D. Fuller, and R. M. Burnett. 1993. Difference imaging of adenovirus: bridging the resolution gap between X-ray crystallography and electron microscopy. *EMBO J* 12:2589-2599.
146. Sundararajan, R., A. Cuconati, D. Nelson, and E. White. 2001. Tumor necrosis factor- α induces Bax-Bak interaction and apoptosis, which is inhibited by adenovirus E1B 19K. *J Biol Chem* 276:45120-45127.
147. Tao, N., G. P. Gao, M. Parr, J. Johnston, T. Baradet, J. M. Wilson, J. Barsoum, and S. E. Fawell. 2001. Sequestration of adenoviral vector by Kupffer cells leads to a nonlinear dose response of transduction of liver. *Mol Ther* 3:28-35.
148. Templeton, N. S., and D. D. Lasic. 2000. *Gene therapy: Therapeutic mechanisms and strategies*. Dekker, New York, NY.
149. Thomas, C. E., A. Ehrhardt, and M. A. Kay. 2003. Progress and problems with the use of viral vectors for gene therapy. *Nat Rev Genet* 4:346-358.
150. Thyagarajan, B., E. C. Olivares, R. P. Hollis, D. S. Ginsburg, and M. P. Calos. 2001. Site-specific genomic integration in mammalian cells mediated by phage ϕ C31 integrase. *Mol Cell Biol* 21:3926-3924.
151. Toietta, G., V. P. Mane, W. S. Norona, M. J. Finegold, P. Ng, A. F. McDonagh, A. L. Beaudet, and B. Lee. 2005. Lifelong elimination of hyperbilirubenemia in the Gunn rat with a single injection of helper-dependent adenoviral vector. *Proc Natl Acad Sci USA* 102:3930-3935.
152. Trotman, L. C., N. Mosberger, M. Fornerod, R. P. Stidwill, and U. F. Greber. 2001. Import of adenovirus DNA involves the nuclear pore complex receptor CAN/Nup214 and histone H1. *Nat Cell Biol* 3:1092-1100.
153. Valentine, R. C., and H. G. Pereira. 1965. Antigens and the structure of the adenovirus. *J Mol Biol* 13:13-20.
154. Vales, L. D., and J. E. Darnell. 1989. Promoter occlusion prevents transcription of adenovirus polypeptide IX mRNA until after DNA replication. *Genes Dev* 3:49-59.
155. van Oostrum, J., and R. M. Burnett. 1985. Molecular composition of the adenovirus type 2 virion. *J Virol* 56:439-448.
156. van Raaij, M. J., A. Mitraki, G. Lavigne, and S. Cusack. 1999. A triple β -spiral in the adenovirus fibre shaft reveals a new structural motif for a fibrous protein. *Nature* 401:935-938.

157. Varghese, R., Y. Mikyias, P. L. Stewart, and R. Ralston. 2004. Postentry neutralization of adenovirus type 5 by an antihexon antibody. *J Virol* 78:12320-12332.
158. Vellekamp, G., F. W. Porter, S. Sutjipto, C. Cutler, L. Bondoc, Y. H. Liu, D. Wylie, S. Cannon-Carlson, J. T. Tang, A. Frei, M. Voloch, and S. Zhuang. 2001. Empty capsids in column-purified recombinant adenovirus preparations. *Hum Gene Ther* 12:1923-1936.
159. Vellinga, J., M. J. Rabelink, S. J. Cramer, D. J. van den Wollenberg, H. Van der Meulen, K. N. Leppard, F. J. Fallaux, and R. C. Hoeben. 2004. Spacers increase the accessibility of peptide ligands linked to the carboxyl terminus of adenovirus minor capsid protein IX. *J Virol* 78:3470-3479.
160. Vellinga, J., D. J. M. van den Wollenberg, S. van der Heijdt, M. J. Rabelink, and R. C. Hoeben. 2005. The coiled-coil domain of the adenovirus type 5 protein IX is dispensible for capsid incorporation and thermostability. *J Virol* 79:3206-3210.
161. Verma, I. M., and N. Somia. 1997. Gene therapy-promises, problems and prospects. *Nature* 389:239-242.
162. Verma, I. M., and M. D. Weitzman. 2005. Gene Therapy: Twenty-first century medicine. *Annu Rev Biochem* 74:711-738.
163. Vigne, E., I. Mahfouz, J. F. Dedieu, A. Brie, M. Perricaudet, and P. Yeh. 1999. RGD inclusion in the hexon monomer provides adenovirus type 5-based vectors with a fiber knob-independent pathway for infection. *J Virol* 73:5156-5161.
164. Volpers, C., and S. Kochanek. 2004. Adenoviral vectors for gene transfer and therapy. *J Gen Virol* 6:S164-S171.
165. Von Seggern, D. J., C. Y. Chiu, S. K. Fleck, P. L. Stewart, and G. R. Nemerow. 1999. A helper-independent adenovirus vector with E1, E3, and fiber deleted: Structure and infectivity of fiberless particles. *J Virol* 73:1601-1608.
166. Von Seggern, D. J., S. Huang, S. K. Fleck, S. C. Stevenson, and G. R. Nemerow. 2000. Adenovirus vector pseudotyping in fiber-expressing cell lines: improved transduction of Epstein-Barr virus-transformed B cells. *J Virol* 74:354-364.
167. Weber, J. M. 1976. Genetic analysis of adenovirus type 2. III. Temperature sensitivity of processing of viral proteins. *J Virol* 17:462-471.
168. Wickham, T. J., P. Mathias, D. A. Cheresch, and G. L. Nemerow. 1993. Integrins $\alpha_v\beta_3$ and $\alpha_v\beta_5$ promote adenovirus internalization but not adenovirus attachment. *Cell* 73:309-319.

169. Wickham, T. J., P. W. Roelvink, D. E. Brough, and I. Kovesdi. 1996. Adenovirus targeted to heparan-containing receptors increases its gene delivery efficiency to multiple cell types. *Nat Biotechnol* 14.
170. Wickham, T. J., D. M. Segal, P. W. Roelvink, M. E. Carrion, A. Lizonova, G. M. Lee, and I. Kovesdi. 1997. Targeted adenovirus gene transfer to endothelial and smooth muscle cells by using bispecific antibodies. *J Virol* 70:6831-6838.
171. Wickham, T. J., E. Tzeng, L. L. Shears II, P. W. Roelvink, Y. Li, G. M. Lee, D. E. Brough, A. Lizonova, and I. Kovesdi. 1997. Increased in vitro and in vivo gene transfer by adenovirus vectors containing chimeric fiber proteins. *J Virol* 71:8221-8229.
172. Widera, A., F. Norouziyan, and W. C. Shen. 2003. Mechanisms of TfR-mediated transcytosis and sorting in epithelial cells and applications toward drug delivery. *Adv Drug Deliv Rev* 55:1439-1466.
173. Wiethoff, C. M., H. Wodrich, L. Gerace, and G. L. Nemerow. 2005. Adenovirus protein VI mediates membrane disruption following capsid disassembly. *J Virol* 79:1992-2000.
174. Wilchek, M., and E. A. Bayer. 1999. Foreward and introduction to the book (strept)avidin-biotin system. *Biomol Eng* 16:1-4.
175. Wisnivesky, J. P., P. L. Leopold, and R. G. Crystal. 1999. Specific binding of the adenovirus capsid to the nuclear envelope. *Hum Gene Ther* 10:2187-2195.
176. Wodrich, H., T. Guan, G. Cingolani, D. Von Seggern, G. Nemerow, and L. Gerace. 2003. Switch from capsid protein import to adenovirus assembly by cleavage of nuclear transport signals. *EMBO J* 22:6245-6255.
177. Work, L. M., S. A. Nicklin, N. J. Brain, K. L. Dishart, D. J. Von Seggern, M. Hallek, H. Buning, and A. H. Baker. 2004. Development of efficient viral vectors selective for vascular smooth muscle cells. *Mol Ther* 9:198-208.
178. Wu, E., L. Pache, D. J. Von Seggern, T. M. Mullen, Y. Mikiyas, P. L. Stewart, and G. R. Nemerow. 2003. Flexibility of the adenovirus fiber is required for efficient receptor interaction. *J Virol* 77:7225-35.
179. Xia, D., L. J. Henry, R. D. Gerard, and J. Deisenhofer. 1994. Crystal structure of the receptor binding domain of adenovirus type 5 at 1.7Å resolution. *Structure* 2:1259-1270.
180. Yant, S. R., A. Ehrhardt, J. G. Mikkelsen, L. Meuse, T. Pham, and M. A. Kay. 2002. Transposition from a gutless adeno-transposon vector stabilizes transgene expression in vivo. *Nat Biotechnol* 20:999-1005.

181. Yeuh, A., and R. J. Schneider. 1996. Selective translation initiation by ribosome jumping in adenovirus-infected and heat-shocked cells. *Genes Dev* 10:1557-1567.
182. Zhang, W., J. A. Low, J. B. Christensen, and M. J. Imperiale. 2001. Role for the adenovirus IVa2 protein in packaging of viral DNA. *J Virol* 75:10446-10454.
183. Ziff, E., and N. Fraser. 1978. adenovirus type 2 late mRNAs: structural evidence for 3'-coterminial sequences. *J Virol* 25:897-906.
184. Zubieta, C., G. Schoehn, J. Chroboczek, and S. Cusack. 2005. The structure of the human adenovirus 2 penton. *Mol Cell* 17:121-135.